UNIVERSIDADE DE SÃO PAULO

FACULDADE DE CIÊNCIAS FARMACÊUTICAS

Programa de Pós-Graduação: Tecnologia Bioquímico-Farmacêutica
Área de Concentração: Tecnologia Químico-Farmacêutica

Efeitos da PEGuilação sítio-dirigida na termoestabilidade da L-aparaginase

Jheniffer Rabelo Cunha

Dissertação para obtenção do título de Mestre em Ciências Farmacêuticas, no Programa de Tecnologia Bioquímica-Farmacêutica.

Orientadora: Profa. Dra. Carlota de Oliveira Rangel Yagui

São Paulo

2021

UNIVERSIDADE DE SÃO PAULO

FACULDADE DE CIÊNCIAS FARMACÊUTICAS

Programa de Pós-Graduação: Tecnologia Bioquímico-Farmacêutica
Área de Concentração: Tecnologia Químico-Farmacêutica

Efeitos da PEGuilação sítio-dirigida na termoestabilidade da L-aparaginase

Jheniffer Rabelo Cunha

Versão Original

Dissertação para obtenção do título de Mestre em Ciências Farmacêuticas, no Programa de Tecnologia Bioquímica-Farmacêutica.

Orientadora: Profa. Dra. Carlota de Oliveira Rangel Yagui

São Paulo

2021

Jheniffer Rabelo Cunha

Efeitos da PEGuilação sítio-dirigida na termoestabilidade da L-asparaginase

Comissão Julgadora da dissertação para obtenção do título de Mestre em Ciências Farmacêuticas:

Orientadora/Presidente: Profa. Dra. Carlota de Oliveira Rangel Yagui

---

1° Examinador

2° Examinador

3° Examinador

São Paulo, ____ de_____ de 2021.

Ficha Catalográfica elaborada eletronicamente pelo autor, utilizando o programa desenvolvido pela Seção Técnica de Informática do ICMC/USP e adaptado para a Divisão de Biblioteca e Documentação do Conjunto das Químicas da USP

Bibliotecária responsável pela orientação de catalogação da publicação:
Marlene Aparecida Vieira - CRB - 8/5562

Cunha, Jheniffer

C972e Efeitos da PEGuilação sítio-dirigida na termoestabilidade da L-asparaginase / JhenifferCunha. - São Paulo, 2021.

115 p.

Dissertação (mestrado) - Faculdade de Ciências Farmacêuticas da Universidade de São Paulo.

Departamento de Tecnologia Bioquímico-Farmacêutica.

Orientador: Rangel-Yagui, Carlota

1. Termoestabilidade. 2. L-asparaginase. 3. Termo-inativação. 4. Bioconjugação. 5. PEGuilação. I. T. II. Rangel-Yagui, Carlota, orientador.

“Não sei, só sei que foi assim”

Ariano Suassuna (Em: O Auto da Compadecida)

Acknowledgements

I would like to thank my father for all the inspiration to pursue my dreams and my mother for giving me the persistence to never give up. Without the development of imagination and reason, I probably would not have pursued a scientific career. Therefore, thank you so much for raising me this way.

Dear Professor Carlota, thank you so much for opening Nanobio's doors for me. I am also grateful that you have always kept an open communication with me so that we could talk as pairs.

To my lab team (Nanobio and Labiotec), I reserve the sincerest gratitude. The endless discussions and support will always remain in my heart with great affection. In special, Karin and João. Without you, my project would've been a lot harder.

To all of my friends and specially, my non-blood brothers Luís and Brenno, I thank you for all the emotional support, for not letting me give up. Not even once.

Tiago, thank you for opening your home to me, for your friendship and companionship. Thaís, thank you for all the cake of sadness and happiness that we share. You are very important in my life.

To Pitica, all my love for maintaining my sanity and giving me countless funny pictures.

Jhéssica, Jhonattan, and Stéffany, I hope I have opened the way for you. That it is possible to come from so little to go further each day more. And that our persistence pays off someday. I love you. This work is dedicated to you.

To my dear Anderson, thank you for your support in all my steps. From technical assistance to affective support. Thank you, my love.

And yet, thank you to the Rio Azul Temple, which opened the doors for me right at the beginning of my São Paulo journey. To the priestesses Milene, Tati, and Priscila, all my affection for not letting my spiritual side fade. To all the entities that embraced me and gave me the necessary strength, Laroiê!

Also, thanks to the funding agencies (CAPES and FAPESP) that allowed this work to be carried out.

RESUMO

CUNHA, J.R. **Efeitos da PEGuilação sítio-dirigida na termoestabilidade da L-asparaginase.** 2021. 115f. Dissertação (Mestrado) – Faculdade de Ciências Farmacêuticas, Universidade de São Paulo, São Paulo, 2021.

A enzima L-asparaginase (ASNase) é amplamente usada como medicamento para tratamento da leucemia linfoblástica aguda, bem como na indústria de alimentos para evitar a formação de acrilamida em alimentos cozidos e fritos. No presente trabalho, ASNase foi covalentemente ligada ao polímero poli(etilenoglicol) (PEG) de diferentes massas moleculares (ASNase-PEG-5, ASNase-PEG- 10, ASNase-PEG-20, and ASNase-PEG-40) na região *N*-terminal (monoPEGuilação) a fim de se estudar os efeitos da PEGuilação na termoestabilidade da enzima. As formas PEGuiladas e nativa foram analisadas em relação à termodinâmica e termoestabilidade a partir de atividade enzimática. A ASNase (nativa e PEGuilada) apresentou atividade máxima a 40 °C e a desnaturação ocorreu por cinética de primeira ordem. Com base nesses resultados, a energia de ativação para desnaturação (E^*_d) foi estimada e maiores valores foram observados para as formas PEGuiladas em comparação à enzima nativa, destacando-se a ASNase-PEG10 com aumento de 4.24 vezes (48.85 kJ.mol^{-1}) em comparação com a forma nativa in (11.52 kJ.mol^{-1}). As enzimas foram avaliadas por sua atividade residual ao longo do tempo em diferentes temperaturas de armazenamento (4 e 37 °C) e os conjugados PEGuilados mostraram-se mais estáveis após os 21 dias de ensaio. Parâmetros termodinâmicos como entalpia ($\Delta H^{\ddagger}$), entropia ($\Delta S^{\ddagger}$) e energia livre de Gibbs ($\Delta G^{\ddagger}$) de desnaturação irreversível foram analisados. Valores maiores – e positivos – da energia livre de Gibbs foram encontrados para os conjugados PEGuilados (61.21 a 63.45 kJ·mol^{-1}), indicando que o processo de desnaturação não ocorreu de forma espontânea. A entalpia também foi maior para os conjugados PEGuilados (18.84 a 46.08 kJ·mol^{-1}), demonstrando o efeito protetivo da PEGuilação. Já para a entropia, os valores negativos foram mais elevados para a ASNase nativa (-0.149 J/mol·K), apontando que o processo de desnaturação aumentou a aleatoriedade e agregação do sistema, o que foi confirmado pelo dicroísmo circular. Dessa forma, a PEGuilação revelou o seu potencial de aumento de termoestabilidade para a ASNase.

Palavras-chave: PEGuilação *N*-terminal, termoestabilidade, termodinâmica, enzimas, bioconjugação, termo-inativação.

ABSTRACT

CUNHA, J.R. **Effects of site-directed PEGylation on L-asparaginase thermostability.** 2021. 115p. Dissertação (Mestrado) – Faculdade de Ciências Farmacêuticas, Universidade de São Paulo, São Paulo, 2021.

The enzyme L-asparaginase (ASNase) is broadly applied as a drug to treat acute lymphoblastic leukemia, as well as in the food industry to avoid acrylamide formation in baked and fried food. In the present work, ASNase was covalently attached to polyethylene glycol (PEG) of different molecular weights (ASNase-PEG-5, ASNase-PEG-10, ASNase-PEG-20, and ASNase-PEG-40) at the *N*-terminal portion (monoPEGylation). Native and PEGylated forms were analyzed regarding thermodynamics and thermostability based on enzyme activity measurements. ASNase (native and PEGylated) presented maximum activity at 40 °C and denaturation followed a first-order kinetics. Based on these results, the activation energy for denaturation (E^*_d) was estimated and higher values were observed for PEGylated forms compared to the native ASNase, highlighting the ASNase-PEG10 with a 4.24-fold increase (48.85 kJ.mol^{-1}) in comparison to the native form (11.52 kJ.mol^{-1}). The enzymes were evaluated by residual activity over time (21 days) under different storage temperatures (4 and 37 °C) and the PEGylated conjugates remained stable after the 21 days. Thermodynamic parameters like enthalpy ($\Delta H^{\ddagger}$), entropy ($\Delta S^{\ddagger}$) and Gibbs free energy ($\Delta G^{\ddagger}$) of ASNase (native and PEGylated) irreversible denaturation were also investigated. Higher – and positive – values of Gibbs free energy were found for the PEGylated conjugates (61.21 a 63.45 kJ·mol^{-1}), indicating that the process of denaturation was not spontaneous. Enthalpy also was higher for PEGylated conjugates (18.84 a 46.08 kJ·mol^{-1}), demonstrating the protective role of PEGylation. As for entropy, the negative values were more elevated for native ASNase (-0.149 J/mol·K), pointing out that the denaturation process enhanced the randomness and aggregation of the system, which was observed by circular dichroism. Thus, PEGylation proved its potential to increase ASNase thermostability.

Keywords: *N*-terminal PEGylation, enzyme thermostability, thermodynamics, enzymes, bioconjugation, thermo-inactivation.

List of Figures

List of Tables

List of Abbreviations

Asn	Asparagine
ATRP	Atom Transfer Polymerization
BCA	Bicinchoninic Acid
BSA	Bovine Serum Albumin
CD	Circular Dichroism
CHMP	Committee for Medicinal Products for Human Use
CTSB	Cathepsin B
Cyt-c	Cytochrome c
EMA	European Medicines Agency
E^*	Activation Energy from the catalyzed reaction
E^*_d	Activation Energy for Denaturation
FDA	Food and Drug Administration
FPLC	Fast Protein Liquid Chromatography
GDH	Glutamate Dehydrogenase
k_d	First-order denaturation constant
K_m	Michaelis constant
Lys	Lysine
MM	Molecular Marker
mPEG-NHS	methoxy-poly (ethylene glycol) carboxymethyl *N*-hydroxysuccinimidyl ester
MW	Molecular Weight
Native-PAGE	Native Polyacrylamide Gel Electrophoresis
NHS	*N*-succinimidyl ester
PEG	poly(ethylene glycol)

PSA	Ammonium Persulphate
RAFT	Radical Addition-Fragmentation Chain Transfer
r*Sso*Pox	recombinant *Sulfolobus solfataricus* paraoxonase
SCID	Severe Combined Immunodeficiency Disease
SDS-PAGE	Polyacrylamide Gel Electrophoresis
SE	Standard Errors
SEC	Size Exclusion Chromatography
$t_{1/2}$	half-life
TEMED	Tetramethylethylenediamine
T_m	Melting Temperature
T_{opt}	Optimum Temperature
V*max*	Maximum Value
β-NADH	β-nicotinamide adenine nucleotide
$\Delta G^{\ddagger}$	Gibbs free energy
$\Delta H°_U$	Standard enthalpy variation of the unfolded enzyme
$\Delta H^{\ddagger}$	Enthalpy
$\Delta S^{\ddagger}$	Entropy

SUMMARY

1. INTRODUCTION

Due to patent protection and the high market Therapies based on biological medicines were a revolutionary innovation in the pharmaceutical industry due to the success obtained in meeting previously unmet medical needs of diseases such as hemophilia, diabetes, arthritis, and diseases of the immune system. price of biological products, the companies that own innovative molecules have generated considerable revenues. An increase of 6.9% in the protein therapeutics market is expected from 2018 to 2025 (an estimative to reach at least $17,813 million) (Jaiswal and Shinde, 2018). In 2017, twelve new biological drugs were approved by the Food and Drug Administration (FDA), one referring to a new treatment by gene therapy (La Torre, De and Albericio, 2018). Figure 1 illustrates the increase in biological drugs over the years.

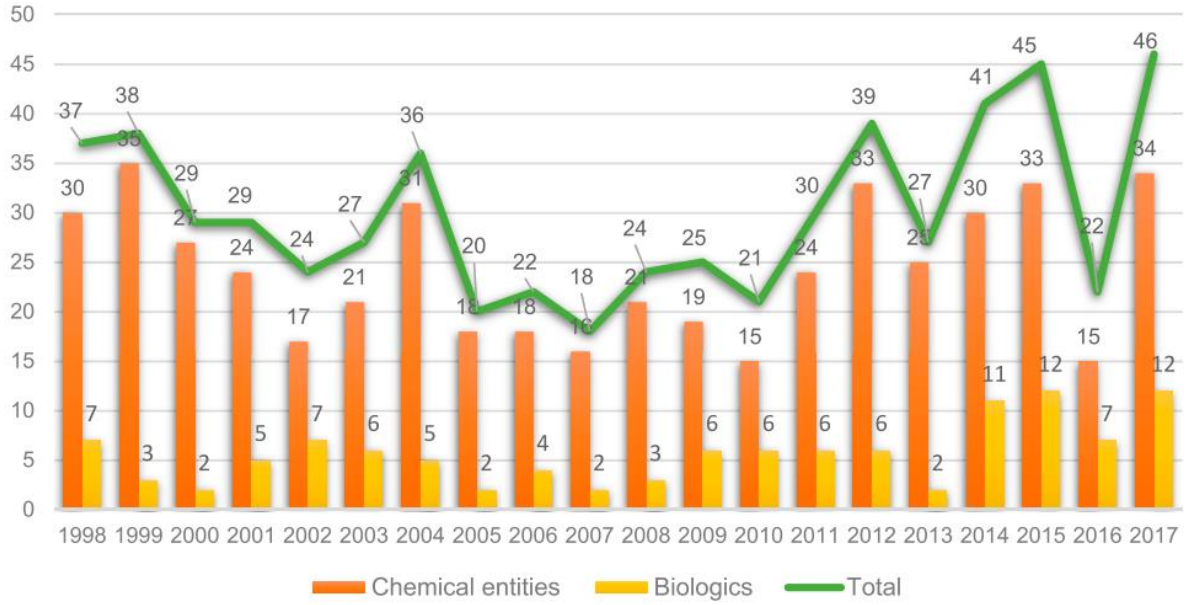

Figure 1. Chemical and biological drugs approved over two decades (La Torre, De and Albericio, 2018).

Despite the large advantages attributed to the biological drugs, a few caveats can be enumerated, such as the low plasma half-life and immunogenicity. The low half-life renders to frequent administration and consequently, impairs treatment adherence due to the discomfort

of the dosing interval (Santos, et al., 2018). As for immunogenicity, the main concerns are the production of anti-drug antibodies that can reduce clinical efficacy by neutralizing biological activity, hypersensitivity, and anaphylactic reactions (Barbosa, 2011; Barbosa et al., 2012).

Another concern regarding biological products available on the pharmaceutical market is the "patent cliff", an economic burden for industry financing. It is a market phenomenon evident for traditional drugs (small molecule drugs) and which is also approaching biological drugs. This term refers to an abrupt drop in sales for a group of "blockbuster" products as the end of patent protection approaches. This drop in sales may impact the main players in the biological medicine industry negatively or positively, depending on the marketing strategies adopted (Calo-Fernández and Martínez-Hurtado, 2012).

Aligning both the economic need to remain competitive in the market and the demand to solve intrinsic problems of biological drugs, we have a new generation of biological products, the "follow-on" biologics, which include biosimilars and biobetters (Santos et al., 2018). Biosimilars are biological products with the same molecular profile of reference products and sufficient evidence that there are no significant clinical differences (Satterwhite, 2013) compared to the reference product. Despite of the similarity, there are some limitations concerning the information on the clinical efficacy and safety of biosimilars and usually, regulatory agencies do not preclude interchangeability. However, even after almost 30 years of approval of the first biosimilar in Europe, there have been no differences in terms of safety to date (Ingrasciotta et al., 2018).

Biobetters, on the other hand, are other class of "follow-on" biologics containing changes in the originating molecular profile, such as bioconjugation, with the specific purpose of increasing therapeutic efficacy, thus introducing a superior product to the market (Satterwhite, 2013). In the context of the next generation of biological drugs, biobetters

represent an opportunity for innovation with reduced risks, since the mechanism of action of the originating molecule is already known. Bioconjugation comprises natural and non-natural modifications to protein surfaces. Natural modifications such as glycosylation (addition of sugar to a molecule), phosphorylation (addition of a phosphate to a molecule), and acetylation (addition of an acetate group to a molecule) are intended to improve the pharmacokinetics of biological drugs or change the folded state of the protein, adding new characteristics and dynamics to the molecule. As for non-natural modifications, strategies such as atom transfer polymerization (ATRP), radical addition-fragmentation chain transfer (RAFT), and PEGylation are common techniques involving the addition of a polymer to the side chain of one or more amino acid residues at the protein surface.

One of the most used techniques of bioconjugation to produce biological drugs, including biobetters, consists of the covalent attachment of poly(ethylene glycol) (PEG) chains. This technique allows the improvement of pharmacokinetic profiles of biological drugs (Pfister and Morbidelli, 2014; Wu et al., 2017). For instance, Neulasta® (a PEGylated version of Neupogen®) and Aranesp®, (PEGylated version of Epogen®) are examples of biobetters presenting longer half-lives than their originating drug (Strohl, 2015).

Biological drugs also face problems related to transport and stock (Silva et al., 2018). In this regard, it is essential to ascertain the differences in temperature, pH, and humidity to which they are submitted until they reach their delivery point. In addition to the pharmacokinetics benefits of PEGylation, it is widely recognized that this strategy commonly increases the thermostability of protein drugs (Mora, White and DeWall, 2020). However, there is not a consensus on the real advantage – or disadvantage – of coupling PEG to molecules and, which criteria of PEGylation are considered to enhance thermostability is still a matter of debate (Matthews, 2013; Turecek et al., 2016). Therefore, important factors should be investigated to correlate with thermostability, such as temperature, degree of PEGylation, and coupling

chemistry (Turecek et al., 2016). In order to explore the thermostability, thermodynamic and kinetic parameters should be considered. The difference between the parameters of the unfolded and folded state of the protein – i.e. half-life ($t_{1/2}$), first-order denaturation constant (k_d), enthalpy ($\Delta H^{\ddagger}$), entropy ($\Delta S^{\ddagger}$), and Gibbs free energy ($\Delta G^{\ddagger}$) – indicates the profile of structural conformation under different temperatures (França, 2018). These parameters address the real improvement in thermostability attributed to PEGylation. In this dissertation, we evaluated the thermodynamic and kinetic parameters of *N*-terminal site-directed PEGylated L-asparaginase and correlated to thermostability. We investigated PEGylation with PEG of different molecular weights (PEGs of 5, 10, 20, and 40 kDa) to determine whether it would interfere on the degree of thermostability conferred to the enzyme.

1 LITERATURE REVIEW

Amongst non-natural modifications, PEGylation is one of the most used strategies to develop biological drugs. It refers to the covalent attachment of poly(ethylene glycol) (PEG) to the protein surface (Veronese and Pasut, 2005). PEGs are commonly used as excipients in the industry due to their characteristics, they are uncharged molecules presenting flexibility, solubility, and biocompatibility (Ekladious, Colson and Grinstaff, 2019; Pelegri-O'day and Maynard, 2016). The PEG polymer is hydrophilic and, therefore, its hydrodynamic volume is higher than that of a globular protein of the same molecular mass, due to the number of hydrogen bonds between the polymer oxygen atoms and water molecules (Kolate et al., 2014; Pasut and Veronese, 2012). The solubility of PEG in both organic and aqueous solvents (Torbica, 2015) is an important characteristic to enhance the solubility of the molecule conjugated.

Abuchowski and collaborators (1977) published the first study of PEGylation, which describes the random conjugation of PEG molecules to lysine residues in catalase (from the bovine liver) resulting in a PEG-catalase solution with low immunogenicity, resistance to proteases, increased stability, and enhanced half-life. Considering the assets brought by PEGylation, the technique became over the years a suitable tool to modify nanoparticles (drug delivery) or drugs such as proteins, peptides, oligonucleotides, small molecules, and aptamers (Ekladious, Colson and Grinstaff, 2019).

PEGylation technique was consolidated for industrial applications over the '90s when FDA approved the first PEGylated protein, Adagen®. This biological drug corresponds to the PEGylated adenosine deaminase, used as enzyme replacement therapy in patients with severe combined immunodeficiency disease (SCID). The first generation of PEGylation is non-specific, yielding products with high polydispersity in terms of the number of PEG molecules attached and low control of the conjugation sites. Commonly known as random PEGylation,

this conjugation occurs frequently in lysine residues. Lysine is one of the most abundant amino acids in proteins, comprising up to 10% of total amino acids in proteins (Roberts, Bentley and Harris, 2002). Hence, there is a lack of batch-to-batch control over the PEGylation sites. In order to solve the caveats of random conjugation, site-specific PEGylation methods were developed, known as the second generation of PEGylation (Pasut and Veronese, 2012). Control over the conjugation site is important for regulatory agencies' approval since the requisitions for approval are becoming more stringent with increasing knowledge of the technique.

According to the FDA, 27 molecules were PEGylated and marketed, and 23 correspond to biological medicines (Table 1). However, most of the reactions described for these biotherapeutics correspond to random PEGylation.

Table 1. FDA approved PEGylated drugs. (Biochempeg, 2020)

Entry	Drug	Company	PEGylated entity	Indications	Average MW of PEGs	Approved Year
Macromolecular Drugs						
1	Esperoct	Novo Nordisk	recombinant antihemophilic factor	hemophilia A	40 kDa	2019
2	Ziextenzo	Sandoz	G-CSF	infection during chemotherapy	20 kDa	2019
3	Udenyca	Coherus Biosciences	G-CSF	infection during chemotherapy	20 kDa	2018
4	Palynziq	BioMarin Pharmaceutical	recombinant phenylalanine ammonia lyase	phenylketonuria	~ 9 x 20 kDa	2018
5	Revcovi	Leadiant Bioscience	recombinant adenosine deaminase	ADA-SCID	80 kDa	2018
6	Fulphila	Mylan GmbH	G-CSF	infection during chemotherapy	20 kDa	2018

Table 1. (cont.) FDA approved PEGylated drugs. (Biochempeg, 2020)

Entry	Drug	Company	PEGylated entity	Indications	Average MW of PEGs	Approved Year
7	Asparlas	Servier Pharma	L-asparaginase	leukemia	31-39 x 5 kDa	2018
8	Jivi	Bayer Healthcare	recombinant antihemophilic factor	hemophilia A	2 x 30 kDa	2017
9	Rebinyn	Novo Nordisk	recombinant coagulation factor lX	hemophilia B	40 kDa	2017
10	Adynovate	Baxalta	recombinant antihemophilic factor	hemophilia A	≥1 x 20 kDa	2015
11	Plegridy	Biogen	peginterferon beta-1a	multiple sclerosis	20 kDa	2014
12	Omontys	Takeda	erythropoietin	anemia	2 X 20 kDa	2012
13	Sylatron	Merck	peginterferon-alfa-2b	melanoma	12 kDa	2011
14	Krystexxa	Horizon Pharma	recombinant uricase protein	gout	40 X 10 kDa	2010
15	Cimzia	UCB	antitumor necrosis factor	rheumatoid arthritis	40 kDa	2008
16	Mircera	Roche	erythropoietin	anemia	30 kDa	2007
17	Macugen	Pfizer	aptamer	macular degeneration	2 x 20 kDa	2004
18	Somavert	Pfizer	human growth hormone	acromegaly	4-6 x 5 kDa	2003
19	Neulasta	Amgen	G-CSF	infection during chemotherapy	20 kDa	2002
20	Pegasys	Roche	peginterferon-alfa-2a	hepatitis B and C	40 kDa	2002
21	Pegintron	Schering	peginterferon-alfa-2b	hepatitis C, melanoma	12 kDa	2001
22	Oncaspar	Enzon	asparaginase	leukemia	69-82 x 5 kDa	1994
23	Adagen	Enzon	adenosine deaminase	ADA-SCIO	11-17 x 5 kDa	1990
Small Molecule Drugs						
24	Movantik	AstraZeneca	naloxone	constipation	339 Da	2014
25	Asclera	Chemische Fabrik Kreussler	dodecyl alcohol	varicose veins	400 Da	2010
Nanoparticles						
26	Doxil	Schering	liposomal	ovarian cancer, multiple myeloma	2 kDa	1995

Drugs containing multiple units of PEGs are indicated (number of units) x (MW of each PEG unit). G-CSF: growth colony-stimulating factor.

ADA-SCIO: adenosine deaminase severe combined immune deficiency.

1.1. Advantages of PEGylation

PEGylation was applied to improve several commercialized biological drugs conferring advantages such as (i) increased hydrodynamic volume, which slows down the renal clearance and prolong *in vivo* half-life (Mishra, Nayak and Dey, 2016), (ii) reduced immunogenicity of the molecule conjugated to PEG, less exposure of the immunogenic epitopes of the molecule; (iii) protection against *in vivo* degradation (proteases and endocytosis); and (iv) improved water solubility (Fee, 2007; Turecek et al., 2016). These benefits are usually achieved without significant conformational changes (Pasut and Veronese, 2012; Santos et al., 2021).

1.1.1. Renal clearance

Bioproducts with a low molecular weight (until 50-70 kDa) are more likely to pass through the renal glomerular filter. Therefore, PEGylation holds the ability to decrease kidney filtration and improve circulation time, since it increases the drug molecular weight (Akbarzadehlaleh et al., 2016). In addition to the molecular weight, PEGylation also increases the hydrodynamic volume, reducing the glomerular sieving coefficient (Fee, 2007). In the case of proteins with larger molecular weight, the effect of PEGylation is observed mostly by the increased serum half-life and prolonged elimination half-life (Lu and Zhang, 2018). For instance, the PEGylated version of the enzyme L-asparaginase (~137 kDa) is an antileukemic drug commercialized as Oncaspar® with a 17.85-fold increase in the half-life compared to the non-modified molecule (Graham, 2003). Despite the elevated prices of Pegaspargase in comparison to the unmodified enzyme, the conjugation represents cost savings for the patients due to the lower frequency of doses and hospital assistance contrasted with the non-modified L-asparaginase (Hu et al., 2019). As for smaller biomolecules like interferon-α2a (~19 kDa), PEGylation at lysine at the α-amino group and ε-amino group with *N*-hydroxysuccinimide 40 kDa branched PEG represented a significant decrease in the renal excretion of the bioproduct

(Bailon et al., 2001; Monfardini et al., 1995). Pegasys®, the PEGylated interferon-α2a, is used for the treatment of hepatitis C and compared to the native protein, presents a 70-fold increase in serum half-life and 50-fold increase of residence in serum plasma. The advantages of PEGylation to interferon-α2a also included enhanced thermostability, protection against proteases, and improved pH stability relative to the native protein (Bailon et al., 2001). The *in vitro* activity of Pegasys® is 7% of the native protein, but the advantages in pharmacokinetics brought by PEGylation compensate the loss of activity (Bailon et al., 2001; Gefen et al., 2013).

1.1.2. Reduced immunogenicity and Protection Against Proteases

The reduced immunogenicity is also associated with the extended half-life of the conjugated molecules (Mishra, Nayak and Dey, 2016). As long as the immune system is not recognizing the PEGylated molecule, it could stay longer in the organism. In terms of architecture, branched-PEGs usually result in a more efficient shielding and, therefore, a smaller number of PEG molecules is needed (Lu and Zhang, 2018).

In addition to lowering the immunogenic response, PEGylation promotes protection against proteases and aggregation (Pandey et al., 2013). Meneguetti et al. (2019) studied the antileukemic protein L-asparaginase (~137 kDa) PEGylated with mPEG-NHS of 10 kDa at the *N*-terminal site and showed that site-directed PEGylation protected against proteases like asparaginyl endopeptidase (AEP) and cathepsin B (CTSB) *in vitro*. Parikh and collaborators (2015) demonstrated the potential of PEGylation of recombinant SsoPox (rSsoPox) (~35 kDa), an enzyme that acts as a therapeutic agent for the prophylaxis of organophosphate compounds poisoning in humans. The PEGylation at the *N*-terminal site with mPEG-propionaldehyde (5 kDa) enhanced resistance to degradation by trypsin.

1.2. Drawbacks of PEGylation

Despite the advantages of PEGylation, it has some drawbacks such as: (i) decreased activity due to steric shielding during the target-protein process of recognition (Pasut and Veronese, 2012; Zhang et al., 2016), (ii) polydispersity, (iii) cytoplasmic vacuolization and (iv) PEG may present immunogenicity (Zhang et al., 2016). These drawbacks are mainly associated with the first generation of PEGylation. Random PEGylation may cause steric shielding or disrupt the tertiary structure of the protein (Giorgi, Agusti and Lederkremer, 2014). Nonetheless, site-directed PEGylation tends to lower these effects since fewer PEGs molecules are attached and at specific sites, lowering polydispersity and interfering less in the protein activity. In other words, site-directed PEGylation yields products with higher homogeneity and less activity loss (Verhoef et al., 2014).

As for the cytoplasmic vacuolation, it occurs mainly in phagocytes and is not correlated to changes in organ function under toxicological studies (Ivens et al., 2015). It is suggested an alternative for these problems by controlling the size of PEG attached to the molecules, using polymers of lower molecular weight (Zhang, Liu and Wan, 2014).

Immunogenicity caused by PEG is still a matter of debate, there are no validated protocols to predict immunogenicity in PEGylated biomolecules (Schellekens, Hennink and Brinks, 2013). Notwithstanding, a pre-clinical screening of anti-PEG antibodies is included in the Food and Drug Administration (FDA) guidelines for PEGylated biological drugs (Verhoef et al., 2014). The number of papers concerning the immunogenic potential and antigenicity of this polymer is growing over the years and building important data. Unmodified biological drugs are usually associated with higher immunogenicity and frequent dose administration than PEGylated drugs (Fu and Sakamoto, 2007; Wu et al., 2017; Xu et al., 2018). Wróblewska and Jędrychowski (2002) PEGylated cow whey protein with different concentrations of PEG 8000 and investigated the formation of anti-PEG antibodies in humans by immunoassays

(competitive and indirect ELISA). The systems containing higher concentrations of PEGs presented a significant decrease in immunoreactivity, corresponding to 0.05% of the immunoreactivity of raw milk. However, further studies are needed to comprehend the effect in a larger number of volunteers.

In another work, L-asparaginase (Oncaspar®) and uricase (Pegloticase®) demonstrated to result in anti-PEG antibodies development (Armstrong et al., 2007; Ganson et al., 2005; Ivens et al., 2015). PEG-uricase induced anti-PEG antibodies (both IgM and IgG) in 38% of patients and PEG-ASNase resulted in 32% of anti-PEG antibodies (mainly IgM) in treated patients (Armstrong et al., 2007; Ganson et al., 2005). The presence of PEGs in other compounds such as cosmetics, food, and drugs may have contributed to the hypersensitivity reactions of the conjugated drugs in the first application. Nonetheless, these drugs have proved useful and are currently in use. Additionally, most of the tests on anti-PEG antibodies refer to molecules randomly conjugated to PEG. Nyborg et al. (2016) presented studies of site-specific PEGylation of uricase, that indicated lower effects of immunogenicity. Consequently, despite the immune response generated by random PEGylation, comparative research of immunogenicity of drugs associated with PEGs demonstrated that site-directed PEGylation is an available technique in continuous advance.

Towards the efforts to decrease immunogenicity, studies of derivatives of less immunogenic PEGs such as branched PEGs (Zhang, Liu and Wan, 2014) and hydroxy-PEGs (Saifer et al., 2014; Schellekens, Hennink and Brinks, 2013) are important to explore this unpredictable issue. With the aid of computational techniques, the specific sites at the protein for PEG attachment can be investigated (Sousa et al., 2018). These tests are important to predict the stability and activity of the PEGylated protein.

Another alternative to minimize the effects of low activity refers to cleavable PEGylation (Figure 2). Accordingly, the conjugation is based on a cleavable linkage that, at a certain kinetic rate will result in PEG release by hydrolysis or reduction *in vivo* (Veronese and Pasut, 2008; Yadav and Dewangan, 2020).

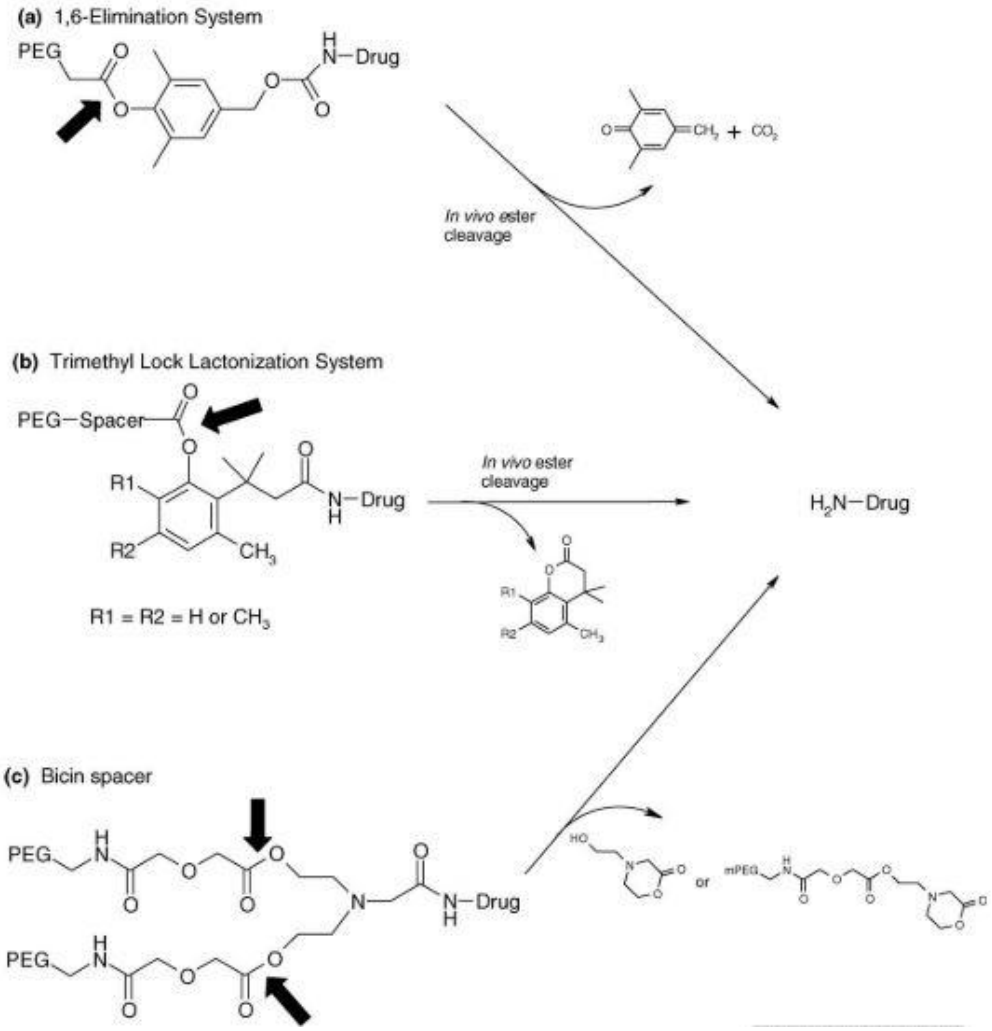

Figure 2. Examples of releasable PEGylated drugs action scheme. The black arrows indicate the ester linkage that causes the cleavage point after hydrolysis (Veronese and Pasut, 2008).

More studies are needed for a better knowledge of PEGylation and PEG effects in the body, however new and specific methods to quantitatively analyze the biodistribution and immunogenicity of PEG are needed (Zhang et al., 2020).

1.3. Strategies for Site-Specific PEGylation

In experimental planning of site-specific PEGylation, some parameters must be taken into consideration, such as PEG chemical structure and molecular mass (Figure 3), the sterical shielding, and the reactivity of the biomolecule and polymer (Ginn et al., 2014; Pasut and Veronese, 2012). In order to improve pharmacokinetics and pharmacodynamics, it is vital to analyze the protein to be associated with PEG, for controlling the number of molecules of PEG and the site of conjugation. Therefore, for each protein the PEGylation conditions could be different, indicating the need for individual studies (Pfister and Morbidelli, 2014).

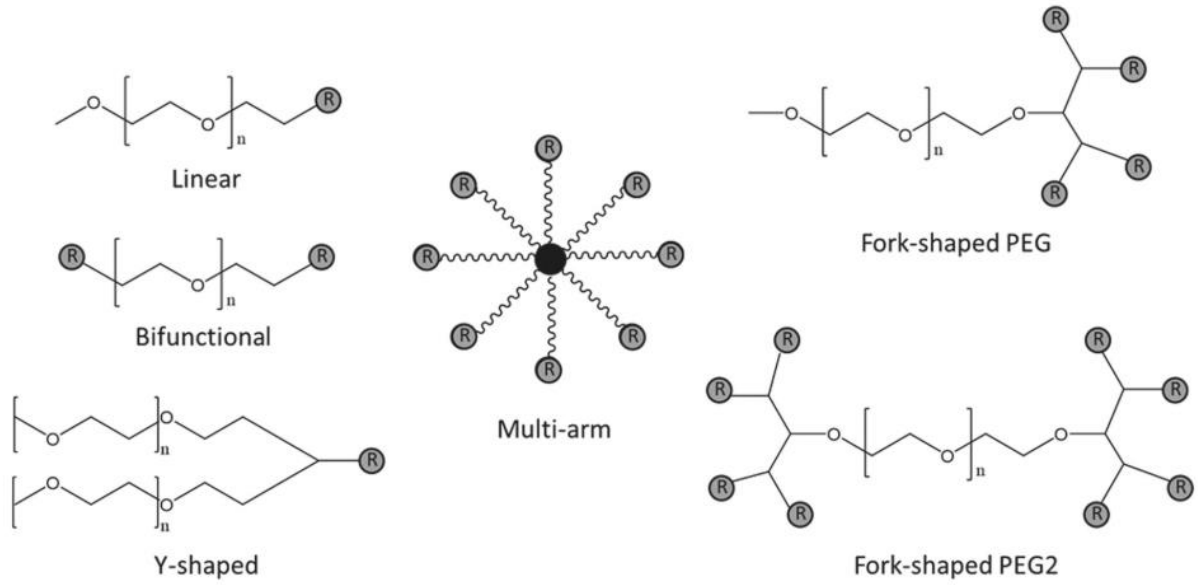

Figure 3. Types of PEG structure used for PEGylation reaction (Santos et al., 2018).

For protein PEGylation, usually one of the ends of the reactive PEG acts as a selective ligand to specific residues at the surface of the protein, while the other end is methylated to avoid reactivity and remains exposed to the solution (Zhang et al., 2012). Due to the presence of one methyl ether group at the end of the linear chain, mPEG avoids cross-linking and polymerization of the molecule (Zalipsky, 1995a; b). In addition, the methyl ether group at the end of the linear chain also protects from oxidation or degradation in the solution (Hermanson,

2013). More recently, branched PEG molecules are also used for protein PEGylation. Polymers with more than one reactive end such as fork-shaped and multi-arm PEGs are interesting for small molecule drugs.

PEGylation reactions have evolved from random conjugation to site-directed, resulting in more homogeneous and potentially effective conjugates (Ginn et al., 2014; Pasut and Veronese, 2012). In this sense, different types of PEGylation are possible, which depend on the site of conjugation at the protein and the reactive end of PEG, as shown in Figure 4.

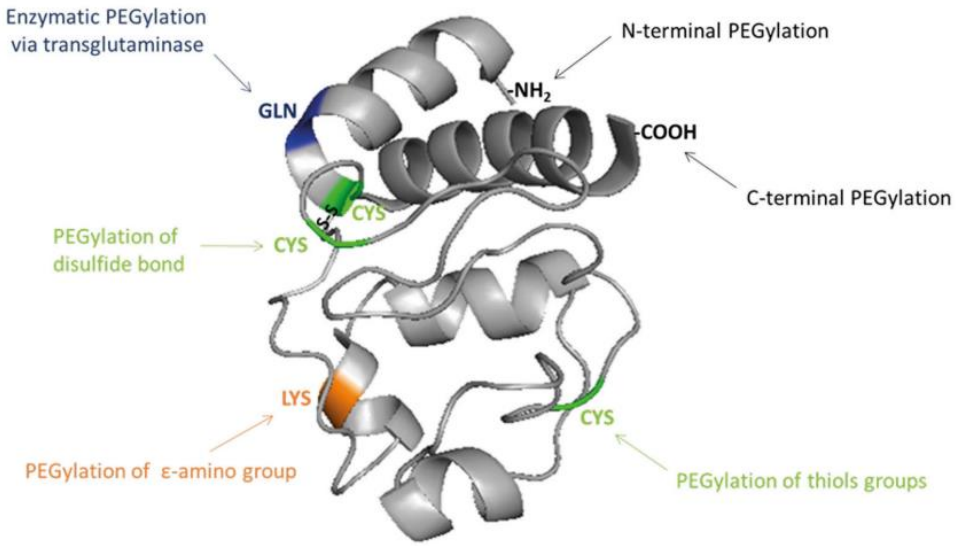

Figure 4. Possible PEG binding sites to protein (Santos et al., 2018).

1.3.1. PEGylation in ε-amino group

This is one of the most studied types of PEGylation and is divided into two segments: random (lysine and *N*-terminal residues) and site-directed (*N*-terminal). Originally, random PEGylation was the only approach to develop PEGylated molecules. The popularity involving the ε-amino group is due to the large number of lysines in proteins, which facilitates molecules of PEGs to be attached (Figure 5). Nonetheless, this method lacks specificity (PEG molecules

can be conjugated to all the lysines in the molecule) and therefore polydispersity, low reproducibility, and sterical hindrance.

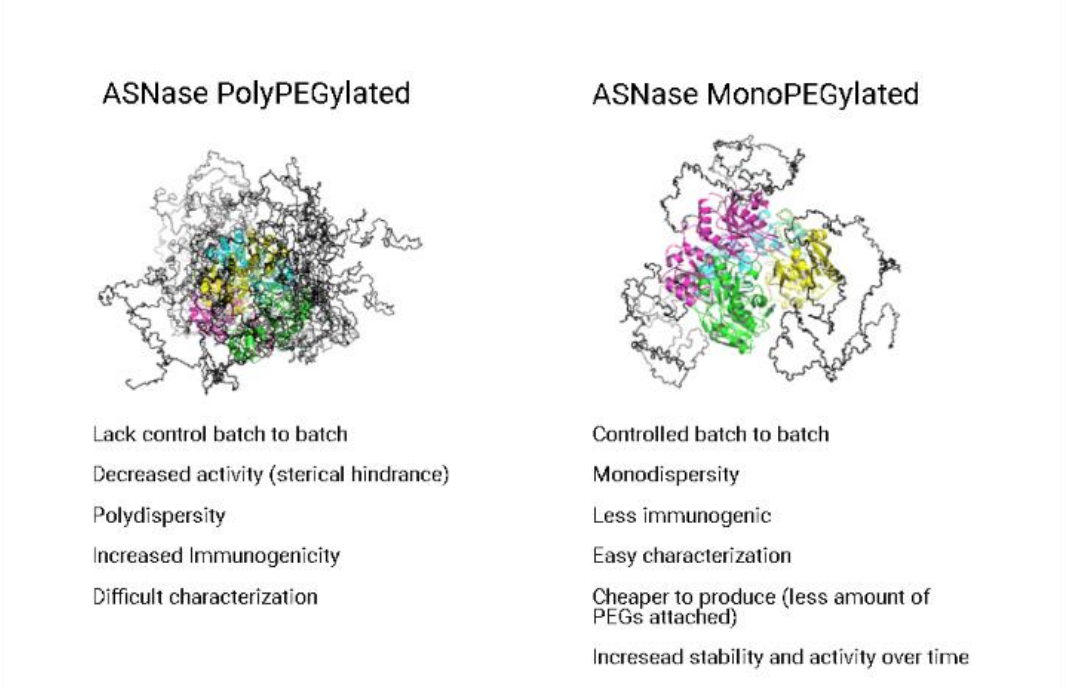

Figure 5. Differences of number of PEGs on site-directed PEGylation and random PEGylation (Created with Biorender).

Grafting mPEG chains in amine residues via amide linkage is achieved by using ester derivatives of the polymer. Succinimidyl esters are a well-known option owing to their stability in physiological conditions (Hermanson, 2013). *N*-succinimidyl ester (NHS), for example, confers ease of preparation and optimized reactivity towards amine nucleophiles under mild conditions (Yamasaki et al., 1990; Zalipsky, 1995a). The mPEG-NHS reacts with unprotonated primary amines and yields a covalent bond (amide linkage), releasing the NHS group as a byproduct (Roberts, Bentley and Harris, 2002).

The *N*-terminal strategy was developed to improve aspects aforementioned of random PEGylation in lysine residues. This reaction involves the conjugation of a molecule of PEG to the *N*-terminal of the protein, controlled by the difference in pKa for the different amino groups in proteins: α-amino (*N*-terminal) is approximately 7.6 and the ε-amino (lysine) is

approximately 10.5 (Turecek et al., 2016). The *N*-terminal PEGylation occurs by an acylation reaction, yielding stable amide linkage in a range of pH of 7-9 (Figure 6). In this range of pH, lysine residues are protonated, avoiding conjugation since the pH determines the nucleophilicity of nucleophiles (for instance, the amine residues). The nucleophilic attack takes place when the operating pH is close to or higher than the pKa value of the amine group of the amino acid to be conjugated so that it is predominantly deprotonated. Despite the specificity of the reaction, undesired byproducts such poly-PEGylated proteins are still formed but at much lower extension.

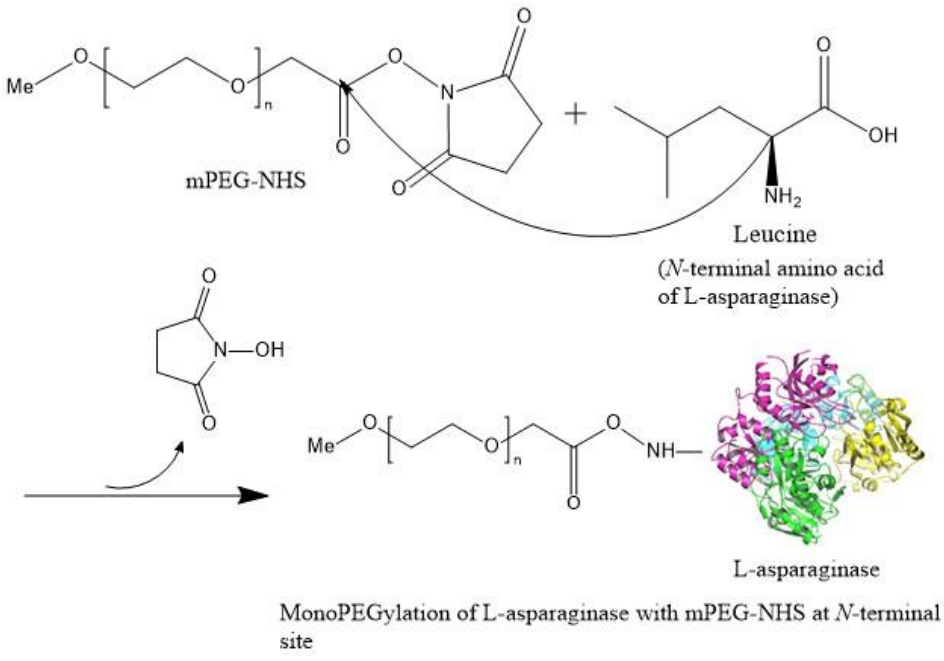

Figure 6. N-terminal PEGylation reaction using methoxy-poly (ethylene glycol) carboxymethyl N-hydroxysuccinimidyl ester (mPEG-NHS) at the N-terminal site of L-asparaginase (PDB: 3ECA) (Created with ChemDraw).

1.3.2. PEGylation in thiol groups

This site-directed reaction depends on a free cysteine in the molecule to be attached to a maleimide-PEG (Ramirez-Paz et al., 2018). Owing to the reduced number of free cysteines in proteins compared to lysines, this strategy is considered very specific since it allows a higher control of selectivity. Usually, it results in conjugates with less PEG attached allowing the enzymatic activity to be maintained. However, cysteines are mainly present in disulfide bridges, thus free cysteines occur less frequently in nature (Gupta et al., 2019; Santos et al., 2018; Turecek et al., 2016). In these cases, it is possible to introduce a cysteine in the molecule by mutagenesis. CIMZIA is a biological drug produced by this type of PEGylation (Figure 7). It is derived from a monoclonal antibody (TNF-α) associated with a maleimide-PEG (Dozier and Distefano, 2015).

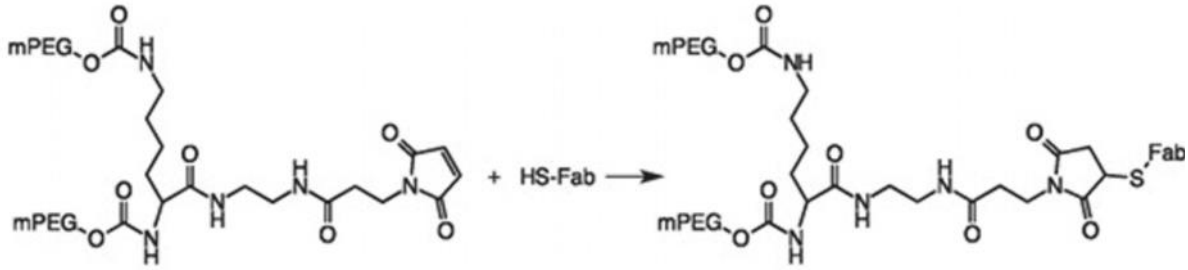

Figure 7. Schematic PEGylation of the biological drug Cimzia® (Turecek et al., 2016)

1.3.3. PEGylation in disulfide bridges

Proposed by Brocchini et al., (2006), the coupling occurs with a PEG-bis-thiol by an alkylation reaction. This process may form a bridge of three carbons, after reducing a disulfide bridge. The reduction allows the structure of the protein to open up, and then the cysteine residues of the protein react with PEG (Figure 8). This reaction is not common due to the low

frequency of disulfide bridges in proteins and the difficulty to access these sites (usually located in hydrophobic regions). Therefore, the reaction in disulfide bridges is highly specific.

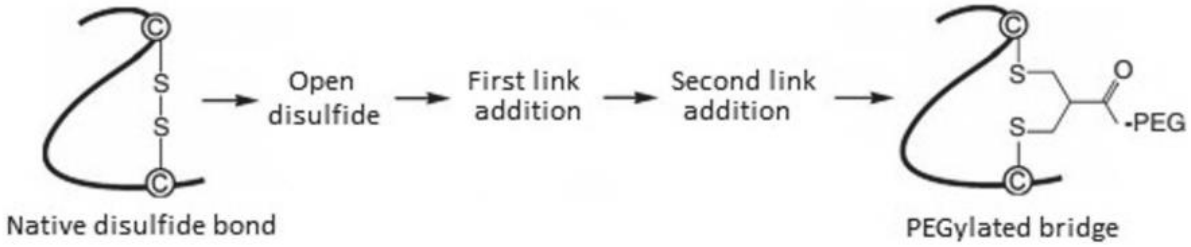

Figure 8. Representation of PEGylation reaction by disulfide bridge (Santos et al., 2018).

1.3.4. Enzymatic PEGylation

Unlike the previous methods, which require cysteine residues, the enzymatic reaction takes place in glutamine residues (Silva Freitas, Mero and Pasut, 2013). A transglutaminase (TGase) catalyzed acyl transfer reaction occurs between glutamine residues and an amino-derivative PEG (Fontana et al., 2008; Sato, 2002). Like PEGylation in cysteine, enzymatic PEGylation preserves the bioactivity of the protein (Duarte et al., 2020), which is an interesting advantage compared to other reactions where the bioactivity decreases (Sato, 2002). PEGylation through TGase demonstrated its high potential at a bench scale, but further studies are needed to establish a basis for industrial processes (Figure 9).

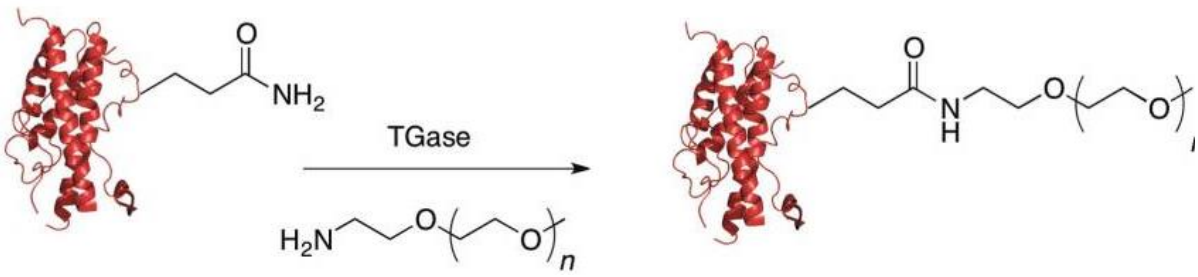

Figure 9. Enzymatic PEGylation with transglutaminase (Dozier and Distefano, 2015).

To remove impurities of PEGylated proteins (excess of activated PEG, impurities of low molecular mass) as well as poly-PEGylated species, a purification process must be developed (Fee, 2007). In general, the purification involves chromatography, especially size exclusion and ion-exchange chromatography due to the differences in mass and charge of PEGylated and non-PEGylated molecules (Fee and Alstine, Van, 2011).

1.3.5. Thermostability of PEGylated Proteins

For several years, studies concerning the benefits of PEGylation were related to immunogenicity and half-life. Some studies concluded that PEGylation could be improved by selecting the site of the conjugation of PEG to the proteins. These studies led to other questions, such as the effect of the conjugation site in bioactivity, immunogenicity, kidney clearance, etc. Nonetheless, few investigations have been carried out on the thermostability of PEGylated proteins.

Thermostability is a relevant factor due to its importance for industrial application and drug cold chain management. During storage and transportation, protein drugs may unfold and lose activity due to long exposure to temperature variations (França, 2018). Knowledge of the thermodynamics and kinetics parameters of the protein can be very helpful to reduce thermoinactivation (Silva et al., 2018). Prior studies have demonstrated that PEGylation could improve (Monfardini et al., 1995; Rodríguez-Martínez et al., 2008; Santos et al., 2019), reduce (García-Arellano et al., 2002a; Plesner et al., 2011) or have no effect on a protein thermostability (Natalello et al., 2012; Popp et al., 2011). In this aspect, studies correlating thermoinactivation over time with temperature are well-known to anticipate the thermostability of a protein (Lawrence et al., 2014; Silva et al., 2018). Thermoinactivation can be quantified by estimating thermodynamic constants (enthalpy, entropy, Gibbs free energy) during denaturation and at the optimal temperature to characterize this process (spontaneity, order degree, etc.).

Parikh et al. (2015) described the effect of the thermostability of site-directed PEGylated recombinant *Sulfolobus solfataricus* paraoxonase (r*Sso*Pox). *N*-terminal PEGylation occurred with a mPEG-propionaldehyde (5 kDa) resulting in a monoPEGylated r*Sso*Pox, enhancing protection against proteases and thermostability. PEGylated and non-PEGylated r*Sso*Pox were exposed to 90 °C for 30 minutes and after measuring the residual activity, rSsoPox presented 100% of activity, but monoPEGylated rSsoPox presented higher activity (around 160%, compared to the unmodified protein).

Under the light of the possibility of different sites of the same protein incur in unknown effects, Matthews (2013) investigated PEGylation of the human protein Pin 1 (domain WW) at different sites. To perform the conjugation, he modified the WW domain at certain residues (19, 18, 14, 17, 30, 16, 26, and 23) to the amino acid asparagine (Asn) for bioconjugation. He observed that the site of the conjugation of PEGs is relevant to increase/decrease/or preserve thermostability. PEGylation at positions 14 and 30 had no impact on thermostability. As for 18 and 23, PEGylation seemed to decrease the thermostability of the WW domain. The positions 19 and 16 (present on the reverse turn of WW) indicated higher thermostability compared to the other positions and PEG was found to be positioned back toward the surface of the protein.

Santos and coworkers (2019) performed a site-directed PEGylation of cytochrome c (Cyt-c) and evaluated the potential to bring thermostability to this protein (Cyt-c–PEG-4 and Cyt-c–PEG-8). The authors correlated the number of PEG chains attached to the protein to improved thermostability, Cyt-c–PEG-8 presented the highest thermostability ($\Delta G^{\ddagger}$ 106.55 at 95 °C) compared to the native protein ($\Delta G^{\ddagger}$ 104.98 at 95 °C) and Cyt-c–PEG-4 ($\Delta G^{\ddagger}$ 105.17 at 95 °C). Regarding the denaturation energy ($\Delta H^{\ddagger}$), Cyt-c-PEG-4 represented a larger amount of energy for denaturation (69.57 kJ/mol at 95 °C), compared to the native (47.45 kJ/mol at 95 °C) and Cyt-c-PEG-8 (60.30 kJ/mol at 95 °C). Therefore, PEGylation was successful to enhance the thermostability of Cytochrome c.

1.4. L-asparaginase (EC 3.5.1.1)

L-asparaginase was discovered by Kidd (1953). He observed that guinea pig serum was inhibiting the formation of a certain lymphoma. Years later, Broome (1961) identified L-asparaginase as the antileukemic inhibitor of lymphoma in guinea pig serum, observed by Kidd. L-asparaginase (ASNase) catalyzes the hydrolysis of asparagine in the bloodstream into L-aspartate and ammonia (Figure 10) and is used in the treatment of Acute Lymphoblastic Leukemia (ALL), reducing neoplastic cells dependent on asparagine in the bloodstream (Brumano et al., 2019; Cachumba et al., 2016). L-asparaginase is also related to the treatment of breast cancer metastasis (Knott et al., 2018). In addition to its therapeutic applications, ASNase is used in the food industry to avoid acrylamide formation from sugars and amino acids when some products are exposed to high temperature processes (Cachumba et al., 2016).

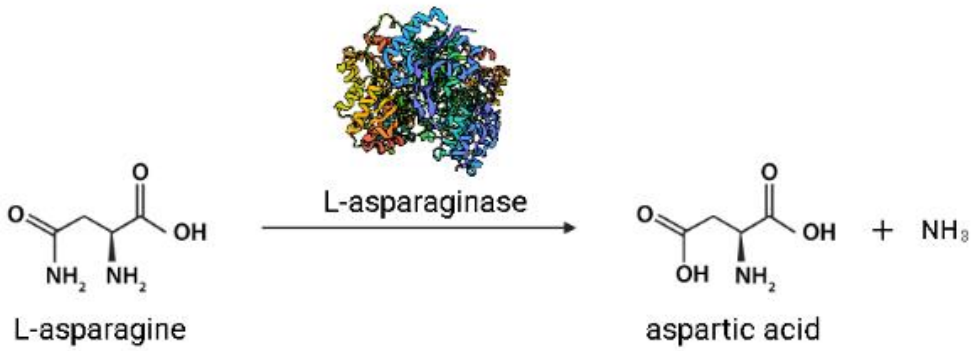

Figure 10. Hydrolysis reaction of asparagine catalyzed by L-asparaginase (Created with Biorender).

The enzyme is a tetramer (~137 kDa), constituted by 1304 amino acid residues (326 amino acids at each monomer) and a disulfide bond located at the surface of the protein, close to the *N*-terminal site. The active sites of the molecule are in fissures formed by each *N*-terminal domain that binds to the C-terminal portion, linking dimers. Between the dimers, we find 22 lysines and the active sites; however only the tetrameric form is active (Cerofolini et al., 2019;

Swain et al., 1993). Commercial ASNase for therapeutic purposes is produced by *Escherichia coli* (first choice) and *Dickeia chrysanthemi*. A PEGylated version of *E. coli* ASNase, Oncaspar® (pegaspargase) is also available; it contains 69 to 82 molecules of mPEG-NHS 5 kDa randomly connected to lysine residues in the enzyme (Sigma-Tau, 1994). Recently, a new PEGylated L-asparaginase was released, Asparlas® (calaspargase pegol-mkln). Compared to Oncaspar®, Asparlas® is administered no more frequently than 21 days (Oncaspar® is administered until 14 days), due to a more stable succinimidyl carbamate linker (Lew, 2020). Despite the modification on the linker chemistry, there are no significant differences between Oncaspar® and Asparlas® in terms of toxicity (Angiolillo et al., 2014; Lew, 2020).

Our research group (Meneguetti et al., 2019) already studied the site-specific *N*-terminal PEGylation of ASNase and determined the best reaction conditions. In the same work, it is also shown *in vitro* that *N*-terminal PEGylation with 10 kDa PEG preserves activity, reduces protein degradation by proteases, and increases stability overtime at 4 ^{o}C. Given that the thermostability of proteins is hard to predict and dependent on several factors abovementioned, we aimed to study the effect of site-directed PEGylation of ASNase with increasing PEG sizes on protein thermostability.

3 OBJECTIVES

Considering the importance of PEGylation as a strategy to improve the pharmacokinetics of therapeutic proteins, the objective of this work was to study the effect of PEGylation with different molecular weight PEGs on ASNase thermostability. To reach this goal, the following specific objects were defined:

- Study the *N*-terminal PEGylation of ASNase with different PEG molecular weights (5, 10, 20, and 40 kDa);
- Purify the PEGylated ASNases, separating the monoPEGylated and native proteins;
- Study the thermostability of PEGylated and native ASNase;
- Determine the thermodynamics parameters of PEGylated and native ASNase under denaturation, as well as specific activity and stability over time;
- Evaluate the kinetics profile of PEGylated and native ASNase;
- Study the conformational structure of PEGylated and native ASNase by circular dichroism.

4 MATERIAL AND METHODS

4.1. Material

L-asparaginase (ASNase, ≥ 96% purity) was obtained from ProSpec® Tany (Ness-Ziona, Central District, Israel). Hydroxylammonium chloride (99% purity) was purchased from Sigma-Aldrich/Merck (Darmstadt, Germany). The methoxy-polyethylene-glycol-carboxymethyl *N*-hydroxysuccinimidyl ester of 5, 10, 20, and 40 kDa (mPEG-NHS) was from Nanocs® (New York, USA). For the PEGylation reaction and purification step, buffer solutions PBS (Synth, Brazil), Tris-HCl (Synth, Brazil), and Bis-Tris-HCl (Sigma, USA) were prepared with purified water obtained through a Milli-Q plus 185 water purification system (Millipore/Merck, Darmstadt, Germany). Glutamate dehydrogenase (GDH), α-ketoglutarate, and β-nicotinamide adenine nucleotide were purchased from Sigma-Aldrich/Merck (Darmstadt, Germany). All other reagents were of analytical grade.

4.2. L-asparaginase PEGylation reaction

With the aid of the H++ software, (Anandakrishnan, Aguilar and Onufriev, 2012) the protonation state and p*K*a values of each amino acid of ASNase were estimated. Briefly, ASNase (1 $mg \cdot mL^{-1}$) was dissolved in 100 mM PBS buffer (pH 7.5) and mixed with mPEG-NHS (5, 10, 20, or 40 kDa) at room temperature for 30 minutes under magnetic stirring at 400 rpm, with a molar ratio of PEG:ASNase 25:1. The reaction was stopped with 1 M hydroxylamine 1:10 (v/v), due to its reactive amine group that rapidly reacts with reactive PEG molecules and it also cleaves unspecific esters linkage between PEG and protein (Meneguetti et al., 2019).

4.3. Purification of L-asparaginase PEGylated conjugates

4.3.1. Ultrafiltration

After PEGylation, the reaction media containing native and PEGylated ASNase was diafiltrated using an Amicon-Ultra 50 mL with a cut-off of 30 kDa cellulose membrane. Firstly, the sample was washed with purified water at least five times its own volume and centrifuged at 800 g for six minutes. Subsequently, the sample was diafiltrated with Bis-Tris-HCl 20 mM (pH 7.0) at the same aforementioned conditions. This procedure was important to remove the cleaved portion of the polymer (NHS and non-conjugated PEG) and change the buffer, preparing the sample for the next step of chromatography.

4.3.2. Ion Exchange Chromatography

Protein purification for all PEG-ASNase conjugates (5, 10, 20, and 40 kDa) was carried out using a strong anionic column Resource Q 6 mL (GE Healthcare Life Science, Marlborough, USA) on a Fast Protein Liquid Chromatography Equipment (FPLC) GE Healthcare Äkta Start. The equilibration buffer was 20 mM Bis-Tris-HCl, pH 7.0 and the elution buffer 20 mM Bis-Tris-HCl with 1 M NaCl pH 7.0. The protein elution profile was observed spectrophotometrically at 280 nm in a running protocol consisting of 12 column volumes in a linear gradient up to 17% of elution buffer at a flow rate of 2 $mL \cdot min^{-1}$. Fractions of 1 mL were selected for protein concentration determination by BCA Protein Assay Kit (Sigma, Darmstadt, Germany) and Native-PAGE to estimate the degree of PEGylation.

4.4. Native Electrophoresis

Native Polyacrylamide gel electrophoresis (PAGE) was adapted according to Arndt et al. (2012) and Laemmli, 1970. Separating gel was prepared with 6% of acrylamide/bis-acrylamide, 522 mM of Tris-HCl (pH 8.8), 0.09% (w/v) of ammonium persulphate (PSA) and

0.19% (v/v) of tetramethylethylenediamine (TEMED). The packing gel was prepared with 5% of acrylamide/bis-acrylamide, 116 mM of Tris-HCl (pH 6.8), 0.14% (w/v) of PSA and 0.1% (v/v) of TEMED. For the running gel, a mix of 20 μL of protein solution was added to 5 μL of sample solution (2x) containing glycerol and the dye bromophenol blue. The running buffer was Tris-Glycine 1 x (pH 8.3) and the run was performed at 120 mV at room temperature (22 to 25 °C). Finally, samples were stained with Coomassie Brilliant Blue (Coomassie Brilliant Blue R-250, CBB) (Blum, Beier and Gross, 1987).

4.5. Electrophoresis under denaturing conditions

Polyacrylamide Gel Electrophoresis under denaturing conditions (SDS-PAGE) was performed according to Laemmli, 1970. Separating gel was prepared with 12% of acrylamide/bis-acrylamide, 522 mM of Tris-HCl (pH 8.8), 0.09% (w/v) of ammonium persulphate (PSA), 0.19% (v/v) of tetramethylethylenediamine (TEMED), and 0.1% (w/v) of sodium dodecyl sulfate (SDS). The packing gel was prepared with 5% of acrylamide/bis-acrylamide, 116 mM of Tris-HCl (pH 6.8), 0.14% (w/v) of PSA, 0.1% (v/v) of TEMED, and 0.1% (w/v) of SDS. For the running gel, a mix of 20 μL of protein solution was added to 5 μL of sample solution (2x) containing glycerol and the dye bromophenol blue. The running buffer was Tris-Glycine 1 x (pH 8.3) and the run was performed at 120 mV at room temperature (22 to 25 °C). Finally, samples were stained with Coomassie Brilliant Blue.

4.6. Determination of L-asparaginase concentration

Protein concentration was determined by the bicinchoninic acid (BCA) method (Merck-Sigma, Daemstadt, Germany). This protocol is based on the reduction of Cu^{+2} to Cu^{+1} by proteins in alkaline media. Bicinchoninic acid is highly specific to the Cu^{+1}, resulting in a purple

solution analyzed spectrophotometrically at 562 nm (Sigma-Aldrich, [s.d.]). The protocol was performed as described by the manufacturer; samples were incubated for 30 minutes at 37 °C and the absorbance measured at 562 nm in the Spectramax Plus 384 (Molecular Devices). The total protein concentration was obtained by interpolating the absorbance values in a calibration curve based on bovine serum albumin (BSA) at concentrations from 200 to 1000 $\mu g \cdot mL^{-1}$.

4.7. Enzymatic activity of L-asparaginase and PEGylated conjugates

ASNase activity (from native and conjugated forms) was determined by Nessler, based on the supplier's protocol adapted to microplates (Sigma-Aldrich/Merck, Darmstadt, Germany). Accordingly, enzyme activity is a function of ammonia released by L-asparagine hydrolysis catalyzed by ASNase, which can be quantified spectrophotometrically based on a standard curve using ammonium sulfate at different concentrations. Briefly, 14 μL of the enzyme solution were added to 137 μL of 50 mM Tris-HCl buffer (pH 8.8), 14 μL of 189 mM L-asparagine, and 123 μL of deionized water. The reaction was incubated at 37 ºC for 30 minutes and stopped with 14 μL of 1.5 M of trichloroacetic acid. Subsequently, samples were analyzed in a spectrophotometer at 436 nm. One L-asparaginase unit was defined as the amount of enzyme that catalyzes the formation of 1 μmol of ammonia per minute at 37 ºC.

4.8. Kinetic analysis

The reactions catalyzed by enzymes are saturable and the rate of catalysis does not indicate a linear response to the increase in the substrate. If the initial reaction rate is measured on a scale of substrate concentration (denoted [S]), the reaction rate (v) increases with the addition of [S]. However, as [S] increases, the enzyme becomes saturated and the reaction rate reaches the maximum value (V_{max}). For the determination of Michaelis constant (K_m) and

Vmax, we used a glutamate dehydrogenase (GDH) coupled assay, which measures the oxidation of the nicotinamide and reduced adenine nucleotide (β-NADH) to β-NAD^+ by GDH. GDH oxidizes one molecule of β-NADH for the synthesis of each glutamate molecule from one molecule of α-ketoglutarate and one molecule of ammonia. In the coupled assay, the ammonia molecule is derived from the hydrolysis of asparagine by L-asparaginase (Balcão et al., 2001).

The assay was performed as Rodrigues (2016) adaptation to the protocol suggested by Balcão et al. (2001), in 96 microwell plates. Briefly, each well received final concentrations of 400 mU GDH (diluted in 50 mM of PBS, pH 7.4; 50% of glycerol), 1 mM α-ketoglutarate, and 131 µM β-NADH, L-asparagine at different concentrations (0.047, 0.094, 0.188, 0.375, 0.5, 0.75, 1.0 and 1.25 mM), and 15 nm of the enzyme samples. All tests were performed in 50 mM Tris-HCl pH 8.0 buffer, in triplicate. The oxidation of β-NADH was monitored in real time on a plate spectrophotometer Spectra Max M2 – Molecular Devices) at 340 nm for 15 minutes. The molar extinction coefficient was calculated and determined as 6.1 $\mu M^{-1} \cdot cm^{-1}$. For each sample, spontaneous deamination of L-asparagine was discounted using a control containing all components of the reaction, except for the enzyme ASNase. The blank was performed with all components except β-NADH. The kinetic analysis was performed using GraphPad Prism 8.4 (La Jolla, California/USA).

4.9. Circular Dichroism

Circular Dichroism (CD) spectra of ASNase and its PEGylated forms were acquired in a Jasco J-815 Spectropolarimeter (Jasco, Tokyo, Japan). The final spectra were the average of six scans, following subtraction of the spectrum of the buffer 20 mM Tris-HCl pH 7,0 obtained under the same conditions. CD spectra were obtained in the far-UV range (190-260 nm) to investigate enzymes' secondary structure content. Measurements were performed at 30 ºC both

before and after heating and cooling processes to investigate secondary structure changes due to the temperature variation and the refolding possibility. Samples were placed in 5.00 mm optical length quartz cells with concentrations of approximately 0.4 µM. Spectra intensities (θ, mdeg) were converted to residual molar ellipticity ([θ], $deg.cm^2.dmol^{-1}$) based on Equation 8:

$$[\theta] = \theta/(10 * C * l * n) \quad \text{(Eq. 8)}$$

where C is the protein concentration in mol/L, "l" is the optical length in cm and "n" is the estimated number of residues in the protein.

Thermal stability studies of ASNase and its modified counterparts were performed at varying temperature from 30 °C to 90 °C, at a rate of 1 °C/minute, and back from 90 °C to 30 °C to study unfolding and refolding processes, respectively. Samples were placed in a 5.00 mm optical length quartz cell and the intensities of ellipticity at 222 nm (θ_{222}, mdeg) were registered throughout the experiment. A Hill-type equation was adjusted to the experimental data to determine the melting temperature of the enzymes as follow:

$$\text{Ellipticity} = \text{Ellipticity}_{30^oC} + (\text{Ellipticity}_{90^oC} - \text{Ellipticity}_{30^oC}) \times T^n / (T_{Melting}^n + T^n) \quad \text{(Eq. 9)}$$

where Ellipticity and T are the *y* and *x* variables, respectively, $\text{Ellipticity}_{30^oC}$ and $\text{Ellipticity}_{90^oC}$ are the values of ellipticity measured at 30 ^oC and 90 ^oC, $T_{Melting}$ the melting temperature and n the cooperativity coefficient.

4.10. Determination of long-term PEGylated ASNase stability over different temperatures

Samples of PEG-ASNase and free ASNase were maintained at 4 ˚C and 37 °C for 21 days to verify activity over storage time by quantifying protein residual enzymatic activity (4.7

section). Measurements were done in triplicate and a non-linear regression fit was applied using GraphPad Prism 5.

4.11. Determination of L-asparaginases thermodynamic parameters

The general phenomenon of thermal inactivation of enzymes can be described by an enzyme unfolding equilibrium (equilibrium constant, K_U), followed by an irreversible step, leading to its denaturation (first-order rate constant k_d) as proposed by Volkin and Klibanov (1989):

$$E \overset{K_U}{\leftrightarrow} E' \overset{k_d}{\rightarrow} E_d \quad \text{(Eq.1)}$$

where E corresponds to the active enzyme, E' to the unfolded enzyme, k_d the first-order rate constant, and E_d to the denatured enzyme (inactive). At temperatures below the optimum temperature ($T < T_{opt}$), the equilibrium tends to the left side predominating the native or folded form, and the rate constant of the enzyme-catalyzed reaction (k_0) is described by the Arrhenius model. On the other hand, when $T > T_{opt}$, the equilibrium tends to the right side, predominating the unfolded form (Converti et al., 2002). This equilibrium model can be described as it follows:

$$k_0 = \frac{A}{B} \exp\left(\frac{\left(\Delta H_U^O - E^*\right)}{RT}\right) \quad \text{(Eq. 2)}$$

where E^* is the activation energy from the catalyzed reaction, k_0 is the initial specific rate of protein hydrolysis, R is the universal ideal gas constant, A and B the Arrhenius factor, and an additional pre-exponential factor, and $\Delta H°_U$ the standard enthalpy variation of the unfolded enzyme.

In spite of the difficulty to achieve real values for k_0, the parameters E^* and $\Delta H°_U$ can be estimated according to the Arrhenius equation and Eq. (2), respectively, and the dependence

of enzymatic activity on the initial instants ($\ln v_0$) from reciprocal temperature ($1/T$). The irreversible thermal inactivation (denaturation) process can be described by:

$$v_d = k_d E \qquad \text{(Eq. 3)}$$

where v_d is the rate of enzyme denaturation, k_d the first-order reaction rate constant, and E represents the concentration of the enzyme active form after the time (t). Defining the activity coefficient as a ratio of E and the enzyme concentration before exposition to different temperatures ($\Psi = E_d/E$), k_d was estimated at each temperature from the angular coefficient of the straight line of $\ln\Psi$ as a function of time ($1/T$). According to Melikoglu (2013), the entropy of activation can be calculated using the enthalpy and free energy of activation, represented by the Equations (4) to (6):

$$\Delta H_d^* = E_d^* - RT \qquad \text{(Eq. 4)}$$

$$\Delta G_d^* = -RT \ln\left[\frac{k_d h}{k_B T}\right] \qquad \text{(Eq. 5)}$$

$$\Delta S_d^* = \frac{\Delta H_d^* - \Delta G_d^*}{T} \qquad \text{(Eq. 6)}$$

where h and k_B are Planck (6.626×10^{-34} J·s) and Boltzmann (1.381×10^{-23} J·K^{-1}) constants, respectively. Also, to estimate the influence of temperature on the denaturation process, we calculated half-life ($t_{1/2}$) as described by Gohel and Singh (2013) according to Equation 7:

$$t_{1/2} = \frac{\ln 2}{k_d} \qquad \text{(Eq. 7)}$$

Measurements were done in triplicate and a non-linear regression fit was applied using GraphPad Prism 5.

4.12. Statistical analysis

The results obtained from tests carried out in repetitions (triplicates) were expressed as means ± standard error (SE) using the GraphPad Prism 5 program. When possible, we applied a two-way ANOVA (analysis of variance) for the data obtained. Finally, to indicate differences between the groups, we conducted a Dunnett's *pos-hoc* test. The level of significance considered in all tests was $p<0.05$.

5 RESULTS AND DISCUSSION

5.1. PEGylation reaction and purification of PEGylated L-asparaginase

ASNase was successfully PEGylated with different PEG molecular weights, similar to previous studies (Meneguetti et al., 2019; Santos et al., 2019; Torres-Obreque et al., 2019). According to the software H^{++}, ASNase presents a p*K*a of 7.24 in the *N*-terminal; a p*K*a higher than 12 at arginine (Arg) residues and approximately 10 for lysine (Lys) residues. Therefore, the conjugation was directed by the pH of the solution. Initially, SDS-PAGE was used to analyze the reaction of PEGylation (Figure 11). Nonetheless, the technique was not suitable to represent all degrees of PEGylation (ASNase-40 did not present band and ASNase-20 was not well distinguished). The inefficiency of representation of SDS-PAGE is mainly observed for higher MWs of PEGs; for lower MWs (10 and 5 kDa), the technique was representative. The reaction media of PEGylation contains free NHS, free PEGs, free ASNase, and PEGylated ASNase, thus the migration of higher MWs is more complicated to observe by SDS-PAGE. According to Zheng (2007), PEG might interact with SDS and interfere with the electrophoretic mobility in the gel. SDS-PAGE led to bands smeared or broadened and an alternative to characterize the PEGylated molecules was to execute the protocol under nondenatured conditions.

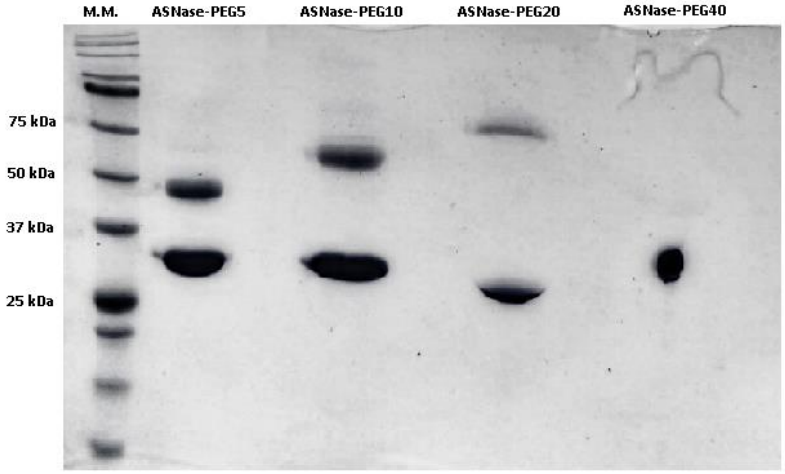

Figure 11. SDS-PAGE of PEGylation reaction of different molecular weights. Molecular Marker (M.M.) Precision Plus Protein™ Standards (Bio Rad).

Therefore, Native-PAGE was used to demonstrate the reaction of PEGylation (Figure 12). PEGylation bands were observed for all PEG MWs; however, the position did not properly correspond to the PEG size increase. This was not expected since PEG is a linear flexible polymer and its electrophoretic mobility is different from that of a globular protein. We can also see that some degree of polydispersity took place since lighter bands corresponding to larger molecules are present in most of the cases. Unfortunately, the PEGylation with 40 kDa PEG did not present a clear result in the gel due to its larger molecular weight. However, purification of ASNase-PEG40 clearly shows a separation of the monoPEGylated fraction and native ASNase.

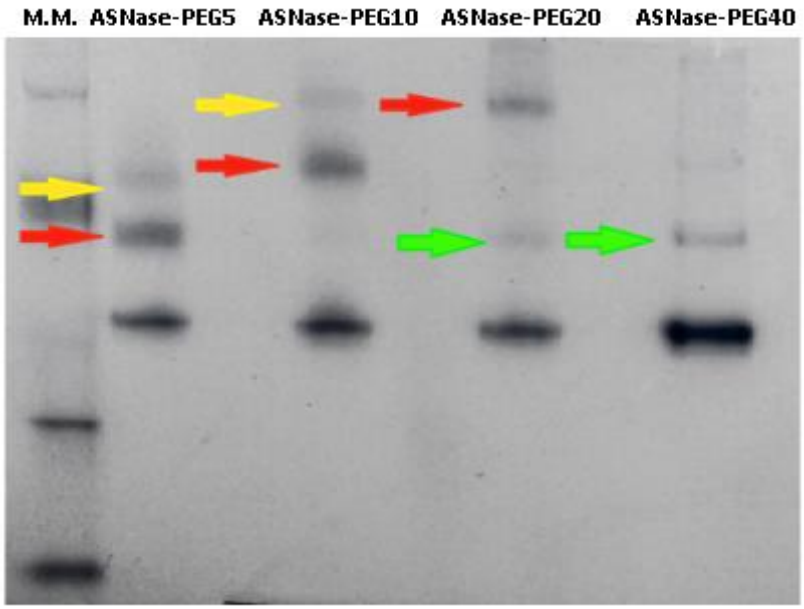

Figure 12. Native electrophoresis of the PEGylation reaction media using PEGs of different molecular weight. M.M. Molecular Marker (NativeMark™ Unstained Protein Standard, Life Technologies). PolyPEGylation was demonstrated by the yellow arrows (ASNase-PEG5 and ASNase-PEG10). MonoPEGylation was indicated by the red arrows. The green arrows show that in the reaction of PEGylation, a monomer of ASNase could have been PEGylated, commonly observed for higher MWs.

Reaction media were purified by size exclusion chromatography (SEC) to evaluate the separation between polyPEGylated, monoPEGylated, and native ASNase. As depicted in Figure 13, one peak was obtained for protein species, referring to both ASNase and PEG-ASNase. Therefore, the purification parameters were adjusted to obtain separated peaks. Based on Torres-Obreque (2017), the system flow was lowered from 0.7 $mL \cdot min^{-1}$ to 0.1 $mL \cdot min^{-1}$, however, no improvement was observed in peak resolution. According to Guttman (2012), for an efficient separation by SEC, the difference between the molecular weight of the modified and the native molecule should be at least three times. ASNase is a 137 kDa protein and therefore, even monoPEGylation with 40 kDa PEG (one chain at each one of the four monomers) increases by 2.2 times and MW = 297 kDa. In contrast, Santos et al. (2019) and Silva Freitas et al. (2013) showed that PEGylated Cytochrome c (19 kDa) and hGH (22 kDa), respectively, were successfully separated from the non-PEGylated molecules by SEC, due to their low molecular weight. This indicates that the effectiveness of separation by SEC depends

greatly on the molecular sizes of the molecules studied (Fee and Alstine, Van, 2011). Therefore, the strategy to purify the conjugated and non-conjugated proteins was changed.

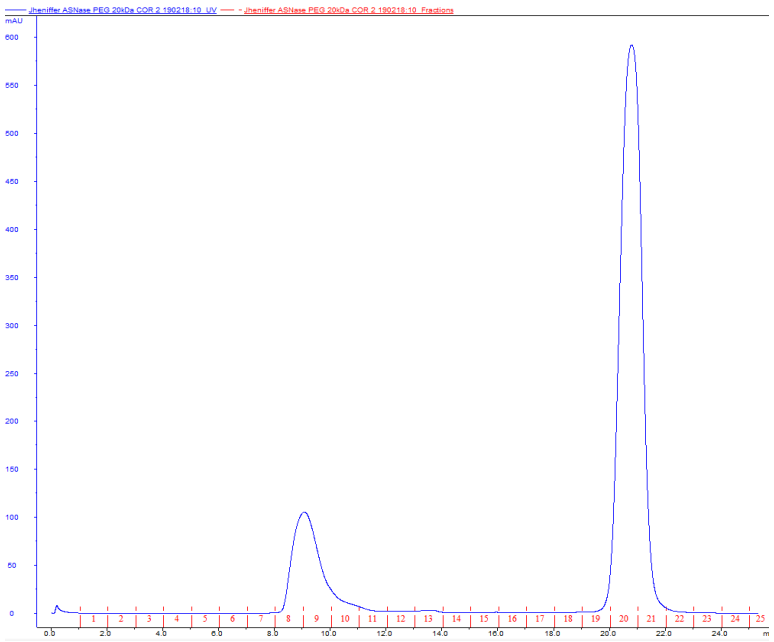

Figure 13. Purification of ASNase-PEG10 with Superdex 200 Increase 10/300 GL. The first peak is an overlap of conjugated ASNase (PEG20) with a native ASNase. The second peak is attributed to the byproduct NHS.

Considering the changes in the charge properties caused by PEGylation, *i.e*. i) the neutralization of a single charge with each PEG group conjugated, thus altering the isoelectric point (pI), ii) the shielding of surface charges (weakening the electrostatic interactions), and iii) PEGs may form hydrogen bonds to raise p*K*a values, modifying the charge of the conjugated molecule (Delgado, Malmsten and Alstine, Van, 1997), ion exchange chromatography (IEC) was used to purify PEG-ASNases. Initially, we selected the HiTrap® DEAE Fast Flow column (5mL) (GE Healthcare) and investigated system flow, buffer ionic strength, and concentration of the samples. Yet, the column (weak anionic) was not adequate to separate the molecules with different degrees of PEGylation and peaks were not clear (Figure 14). Hence, we decided to use a strong anionic column, Resource™ Q (GE Healthcare).

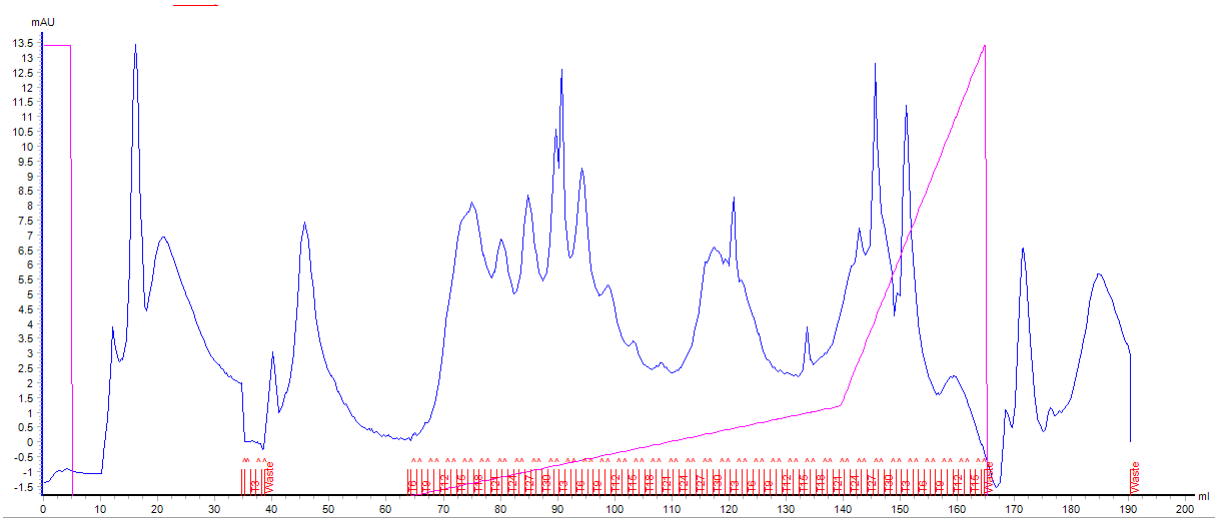

Figure 14. Chromatogram of the purification of L-asparaginase conjugated with mPEG-NHS (10 kDa) by HiTrap® DEAE FF column. The peaks of free NHS, ASNase, ASNase-PEG10 (mono or poly) are indistinguishable.

Chromatograms from ionic exchange purification with the strong anionic column (Resource Q – GE Healthcare) resulted in the separation of all forms present in the PEGylation reaction media: monoPEGylated (*N*-terminal), polyPEGylated ASNase, and the remaining native form. Typical chromatograms corresponding to ASNase-PEG of all MWs are presented in Figures 15 to 18. With the aid of the Unicorn™ 5 Software, the areas of the peaks were measured and PEGylation reaction yields calculated. The sum of the results for all PEGs of different MWs is presented in Table 2. The yields in monoPEGylated enzymes in most cases varied from 45 to 52% and were similar to previously published results (Meneguetti et al., 2019). For the 40 kDa reactive PEG, yields were lower (29%) probably because of the sterical hindrance. For all modifications, there was also an initial peak that did not present a band in the gel. We assume that it could be NHS from free PEGs, because its structure gives a signal at 280 nm, as also observed by Nguyen (2016).

Samples from the chromatographic fractions corresponding to monoPEGylated ASNase were submitted to Native-PAGE and single bands were obtained.

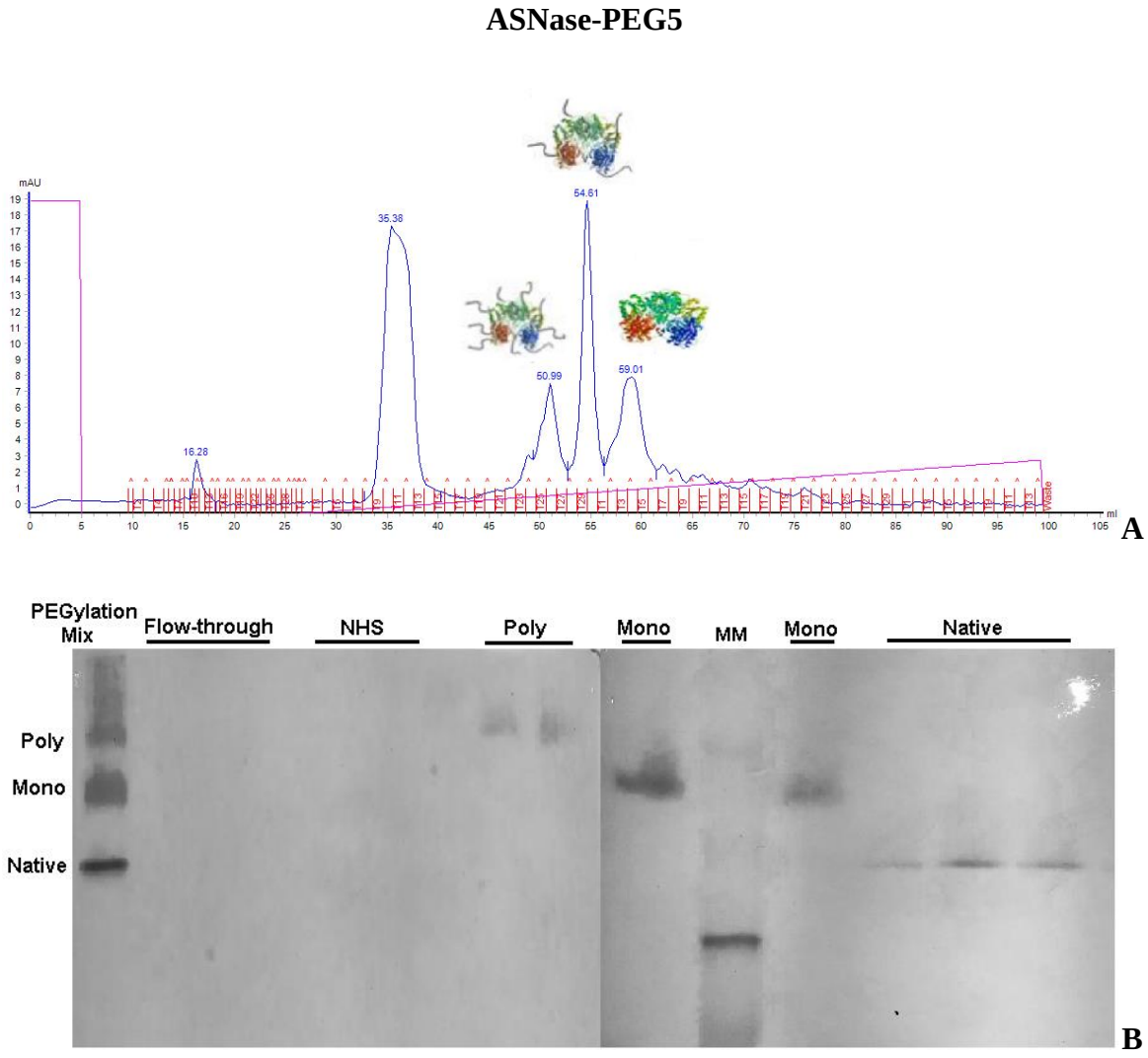

Figure 15. (A) Chromatogram of the purification of L-asparaginase conjugated with mPEG-NHS (5 kDa). The first peak corresponds to free NHS and the others to the polyPEGylated, monoPEGylated and native form, as illustrated in the figure. **(B)** Native electrophoresis (6% acrylamide gel) of the main peaks of the chromatogram depicted at (A), representing polyPEGylated, monoPEGylated and native forms of L-asparaginase PEGylated with 5 kDa PEG. M.M. Molecular Marker (NativeMark™ Unstained Protein Standard, Life Technologies).

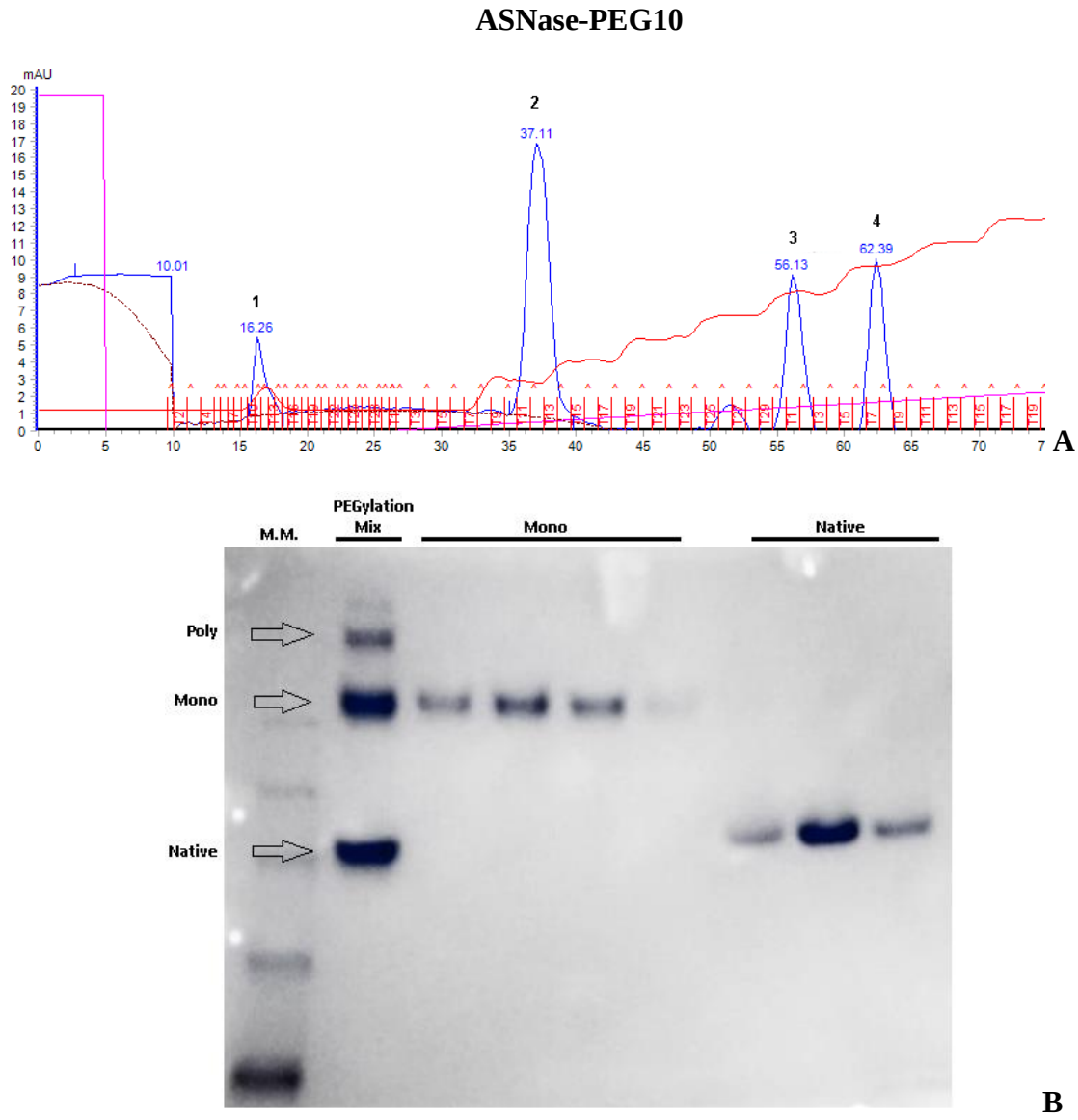

Figure 16. (A) Chromatogram of the purification of L-asparaginase conjugated with mPEG-NHS (10 kDa). The first peak corresponds to flow through, the second, to free NHS and the others to the (3) monoPEGylated and (4) native form. **(B)** Native-PAGE 6% from the purification above, showing the third (3) peak, the monoPEGylated L-asparaginase and the fourth (4) peak, the native ASNase. M.M. Molecular Marker (NativeMark™ Unstained Protein Standard, Life Technologies).

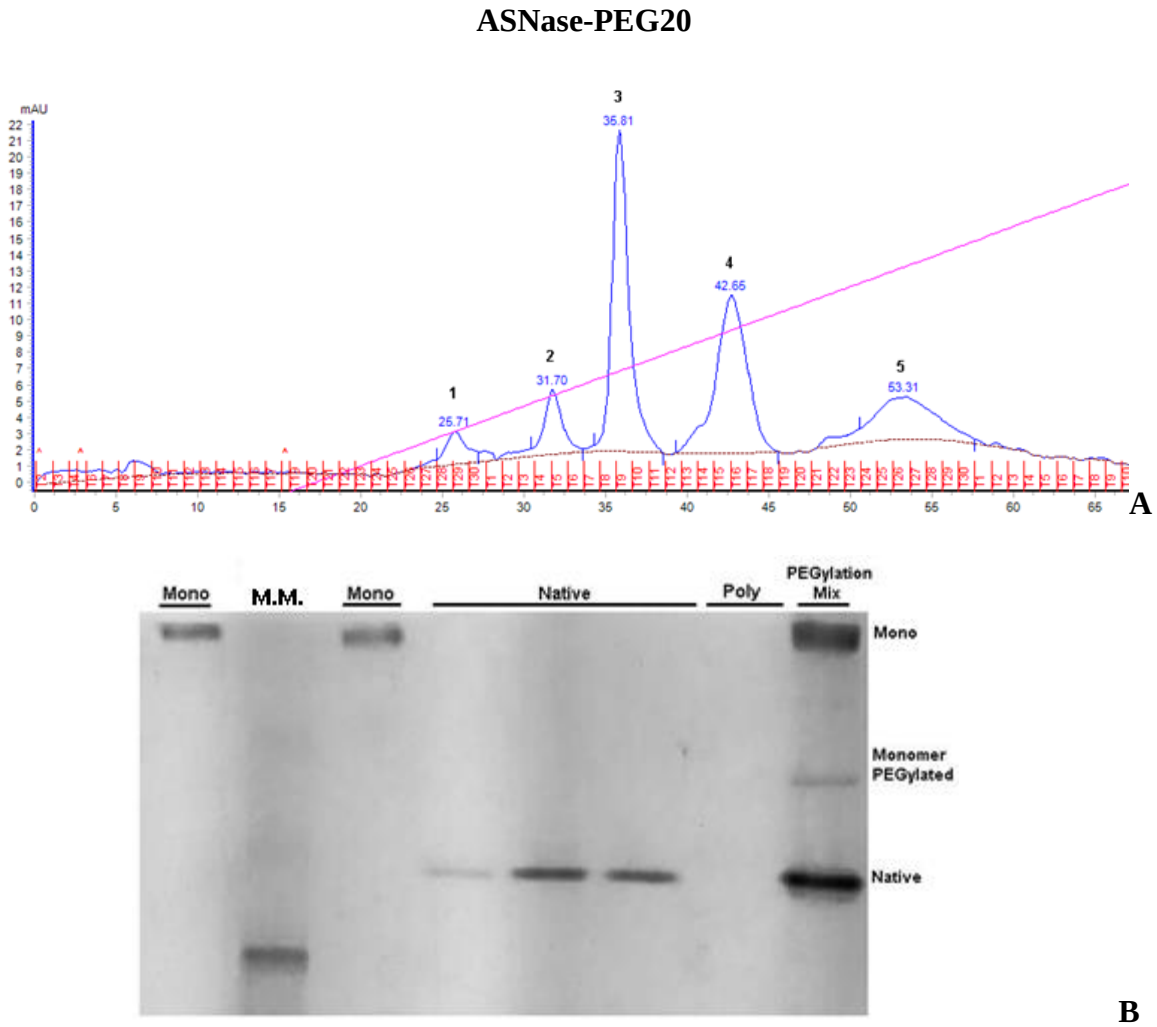

Figure 17. (A) Chromatogram of the purification of L-asparaginase conjugated with mPEG-NHS (20 kDa). The first peak corresponds to free NHS. The second (2) might be the polyPEGylated, the other peaks, (3) monoPEGylated and (4) native form. **(B)** Native electrophoresis (6% acrylamide gel) of the main peaks of the chromatogram presented in (A), representing polyPEGylated, monoPEGylated and native forms of L-asparaginase PEGylated with 20 kDa PEG. The polyPEGylated form was unable to be observed in this purification gel. M.M. Molecular Marker (NativeMark™ Unstained Protein Standard, Life Technologies).

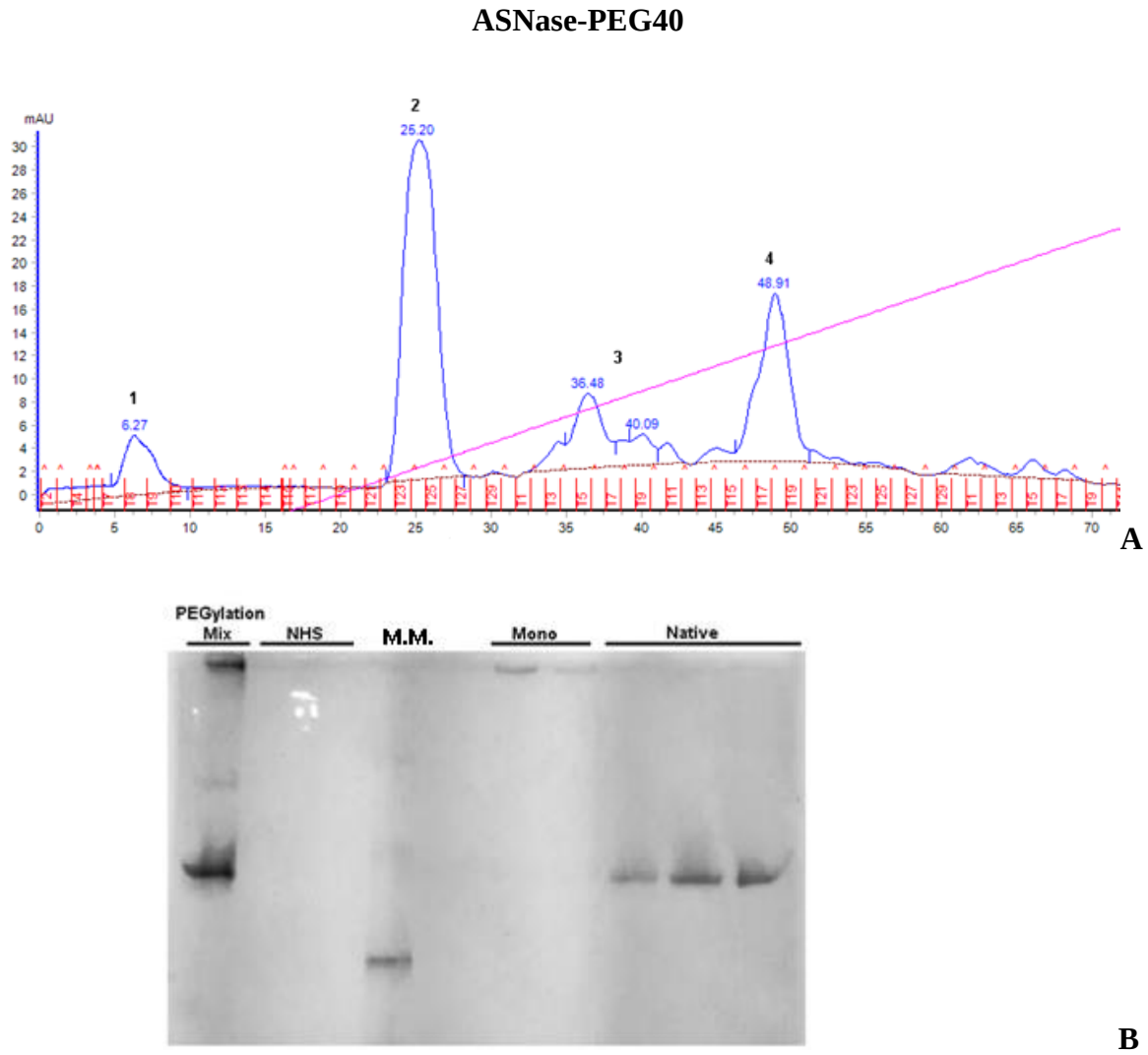

Figure 18. (A) Chromatogram of the purification of L-asparaginase conjugated with mPEG-NHS (40 kDa). The first peak (1) corresponds to flow through, second peak (2) to free NHS. The third (3) the monoPEGylated and (4) native form. **(B)** Native electrophoresis (6% acrylamide gel) of the main peaks of the chromatogram presented in (A), the monoPEGylated and native forms of L-asparaginase PEGylated with 40 kDa PEG. M.M. Molecular Marker (NativeMark™ Unstained Protein Standard, Life Technologies).

Table 2. Summary of reaction yield (%) of L-asparaginase PEGylated with different molecular weight PEGs (5, 10, 20 and 40 kDa).

Sample		Retention time (mL)	Peak Area (mL*mAU)	Yield (%)
Asnase-PEG5	PolyPEGylated	50.99	10.69	23
	MonoPEGylated	54.61	21.4	45
	Unreacted ASNase	59.01	15.29	32
Asnase-PEG10	MonoPEGylated	56.12	16.29	48
	Unreacted ASNase	62.39	17.62	52
ASNase-PEG20	MonoPEGylated	35.08	24.1	52
	Unreacted ASNase	42.65	21.92	48
ASNase-PEG40	MonoPEGylated	36.48	14.13	29
	Unreacted ASNase	40.09	34	71

5.2. Determination of PEGylated and native L-asparaginase specific activity

The specific activity of all ASNase variants was determined based on the activity of L-asparaginase at different concentrations ($U \cdot mL^{-1}$) and using a linear regression fit of the units (U) present as a function of protein concentration (mg) (Figure 19). The summary of the results is presented in Table 3.

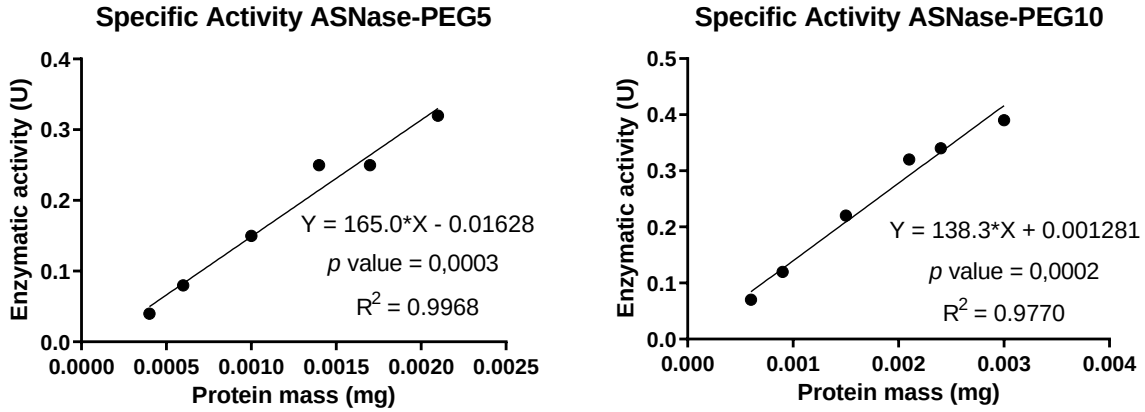

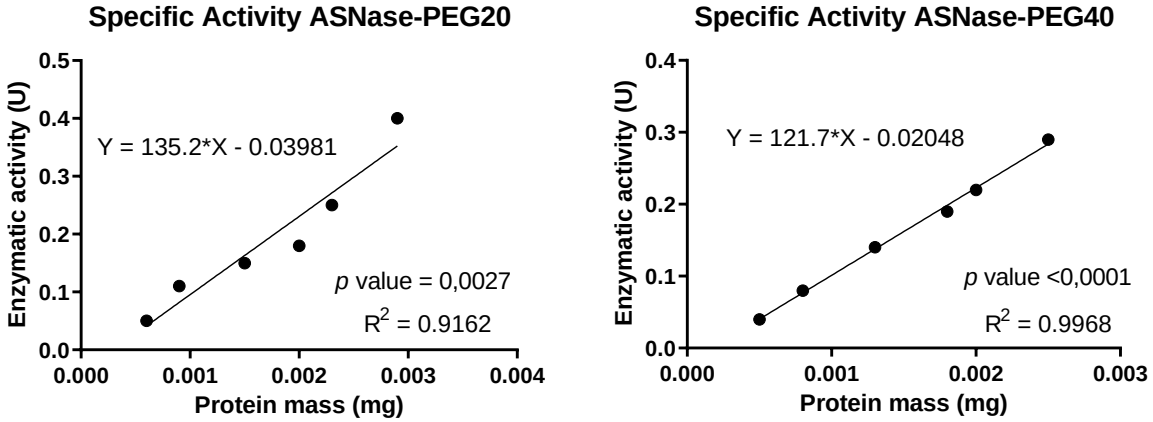

Figure 19. L-asparaginase activity as function of protein mass for PEGylated derivatives of L-asparaginase, with significant *p* values.

Table 3. Specific activity values for each degree of PEGylation and the native L-asparaginase.

Protein	**Speciffic Activity ($U \cdot mg^{-1}$)**
ASNase	269*
ASNase-PEG 5	165
ASNase-PEG10	138
ASNase-PEG20	135
ASNase-PEG40	122

*Value obtained from the ASNase marketed by Prospec and Tany®.

According to Table 3, PEGylation led to a reduction in enzyme activity, as a result of the conformational restriction imposed by the PEG chains attached. Nonetheless, the degree of PEGylation had a minor influence on the specific activity of ASNase. For all the bioconjugates, the number of PEG chains is similar and since L-Asn is a small substrate and can diffuse through the PEG corona, steric hindrance is not playing a major role. On the other hand, polyPEGylated Oncaspar® holds 69 to 82 chains of PEG, resulting in a reduced specific activity (85 $U \cdot mL^{-1}$) (Enzon Pharmaceuticals, 2005).

5.3. Kinetic studies

In order to investigate the suitability of an industrial process involving enzymes, some considerations must be taken into account, such as i) the quantity of protein necessary for the reaction to occur; ii) the reaction time; iii) the concentration of the substrate to initiate the reaction; iv) the reaction conditions; v) the costs involved (Marangoni, 2013). At the criterion of establishing a contribution to a later industrial process, the study of enzyme kinetics helps to introduce the viability of these processes. Therefore, to comprehend the mechanism of action of enzymes, it is necessary to evaluate the reaction velocity and how it changes with the experimental parameters (Nelson and Cox, 2011). An enzyme-substrate (ES) complex is needed to form a product (P) as depicted in Equation 10:

$$E + S \underset{k_2}{\overset{k_1}{\rightleftarrows}} ES \xrightarrow{k_3} E + P \qquad \text{(Eq. 10)}$$

where E is the enzyme, S is the substrate, ES is the Enzyme-Substrate complex, P is the product, k_1 is the first-order rate constant (t^{-1}), k_2 is the second-order rate constant ($M^{-1} \cdot t^{-1}$), and k_3 is the first-order rate constant (t^{-1}).

This equation assists in determining the number of reaction steps and identifying speed-limiting steps. At saturation, k_3 is useful to determine the first-order constant of velocity (k_{cat}). k_{cat} is equivalent to the number of substrate molecules converted into product per unit time by a single enzyme molecule (Nelson and Cox, 2011).

The relationship between substrate concentration [S] and reaction velocity can be quantitatively expressed. Michaelis and Menten represented mathematically that the speed limiting step in an enzymatic reaction is the breakdown of the ES complex into product and free enzyme, given by the following Equation 11:

$$V_0 = \frac{V_{max}[S]}{K_M + [S]} \qquad \text{(Eq. 11)}$$

where K_m is the Michaelis-Menten constant, defined as being equivalent to the concentration of the substrate in which the initial velocity (V_0) is half of the maximum velocity (V_{max}). For comparison between different enzymes, the catalytic efficiency is observed. This parameter is calculated by the relationship k_{cat}/K_m, being the constant of velocity to the conversion of E + S in E + P (Eisenthal, Danson and Hough, 2007). The kinetics for native ASNase and the PEGylated forms are presented in Figure 20.

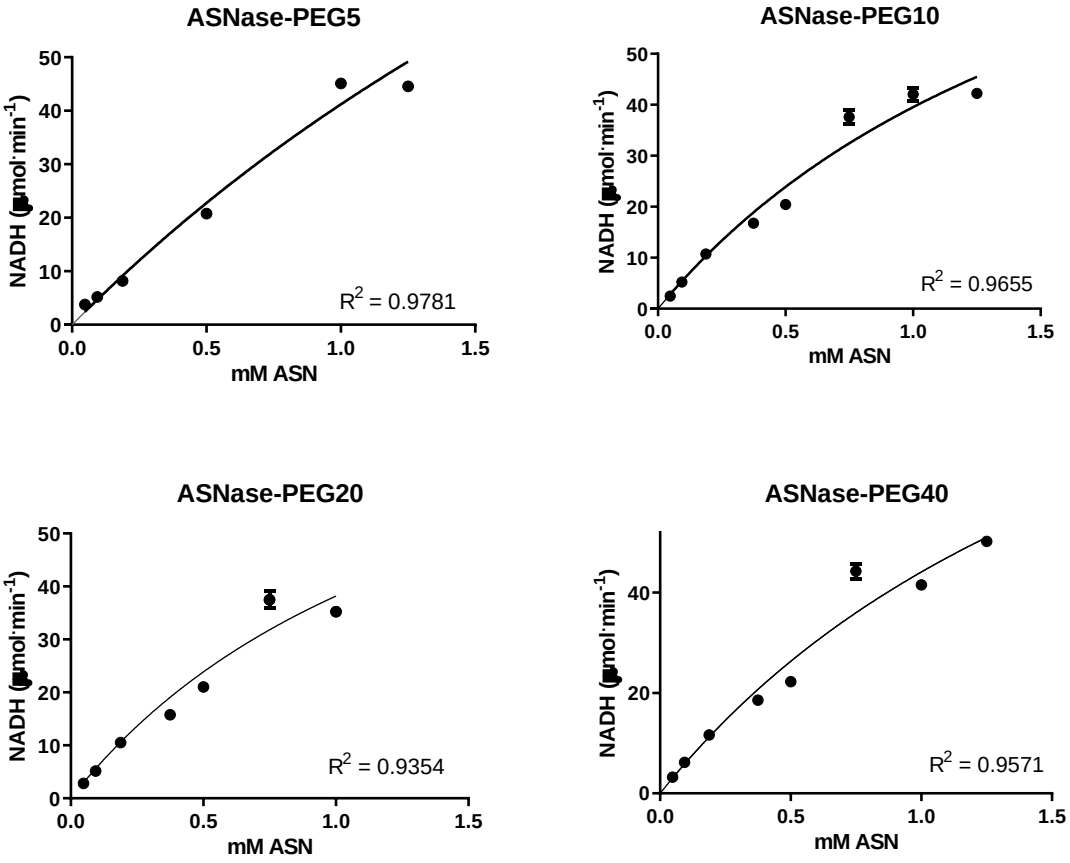

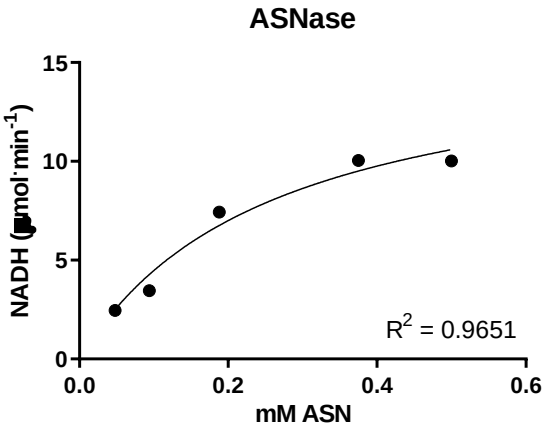

Figure 20. Enzymatic kinetics of native ASNase and PEGylated ASNase with PEG of different molecular weights. Data analysis and statistical analysis (F test) were performed using the GraphPad Prism 5 program.

Native and PEGylated ASNases demonstrated a Michaelis-Menten behavior (all with $R^2 \geq 0.9$), following the literature (Derst, Henseling and Röhm, 2000). However, the steady-state is not apparent for all the enzymes. The steady-state is important to properly define the kinetic parameters, especially V_{max}, therefore the experiments should be repeated to confirm the values obtained. Nonetheless, we estimated the kinetic parameters of the modified and unmodified ASNase and, as observed in Table 4, the native protein presented a significantly higher value of K_m, approximately 13-fold higher than previously reported (19.58 ± 0.003 µM) (Meneguetti et al., 2019). Comparing the kinetic effects for the same molecule can be a difficult task because it could depend on the values of [S]/K_m (Eisenthal, Danson and Hough, 2007). It can also vary depending upon the strain used. For instance, Dias, Santos Aguilar and Sato (2019) obtained the value of K_m (1.41 mM) for L-asparaginase produced by *Aspergillus niger*, the result is similar to what we observed for the PEGylated forms. Lubkowski et al., (2020) obtained a significantly lower K_m for ASNase (0.035 mM), indicating a higher affinity to the substrate. Nonetheless, we should repeat the kinetics study to confirm our results.

As expected, the PEGylated forms presented higher values of K_m (8-15 times higher) when compared to the native protein, owing to the conformational restriction imposed by the polymer conjugation. Nonetheless, the PEG molecular weight did not play a significant role in K_m and or activity. Regarding V_{max}, we did not discuss this parameter since enzyme concentration was not the same for the different ASNases investigated (native and PEGylated forms).

Table 4. Kinetic parameters of native L-asparaginase, and the conjugated ASNases. All of the tests were made in triplicates and calculated by non-linear regression analysis with standard error, using the GraphPad Prism 5 program.

Sample	K_m **(mM)**	k_{cat} **(s^{-1})**	k_{cat}/K_m **($s^{-1} \cdot M^{-1}$)**
ASNase	0.259 ± 0.05	17.86 ± 0.10	6.1×10^{-4}
ASNase-PEG5	3.849 ± 2.97	241.9 ± 8221	6.2×10^{-4}
ASNase-PEG10	1.89 ± 0.65	127.25 ± 1802	6.7×10^{-4}
ASNase-PEG20	1.97 ± 0.69	106.15 ± 1941	5.3×10^{-4}
ASNase-PEG40	2.09 ± 0.85	151.5 ± 2597	7.2×10^{-4}

Concerning the turnover constant, k_{cat}, the value for native ASNase was analogous to the literature (Lubkowski et al., 2020; Meneguetti, 2017). Also, this parameter did follow the same trend of K_m for the PEGylated forms, *i.e.*, higher values were observed. The k_{cat}/K_m, known as catalytic efficiency, was equivalent for all ASNases. Therefore, PEGylation at the *N*-terminal with four PEG moieties did not result in a drastic effect on enzyme activity.

5.4. Circular Dichroism

Circular dichroism was performed to obtain data on protein conformation during the denaturation and renaturation processes for native ASNase and all PEGylated conjugates. The far-UV CD spectra of modified and unmodified ASNase were combined (Figure 21) and, as can be seen, all PEGylated forms preserved the conformation in comparison to the native form. These data were obtained from the normalization of concentration and agree with data available in the literature (Swain et al., 1993). PEGylated ASNase and native ASNase presented similar CD spectra (Figure 21), comprising negative bands at 222 nm and 208 nm and positive bands at 195 to 200 nm, characteristic of a predominance of α-helical structure.

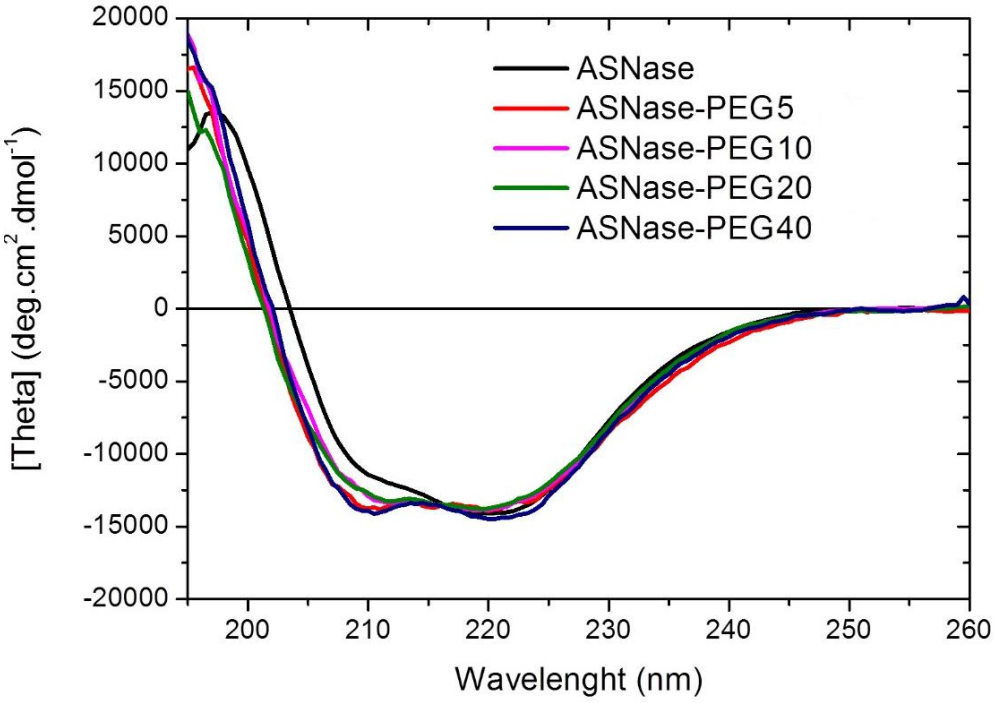

Figure 21. Far-UV spectra of the PEGylated and native L-asparaginase.

CD spectra did not display significant differences between the native (Figure 22) and PEGylated forms (Figures 23 to 26), which is also demonstrated by Pasta et al. (1988). They performed random PEGylation of subtilisin and evaluated the structure conformation by CD. Both spectra (subtilisin and PEG-subtilisin) were almost coincident, implying that they have a

similar secondary structure. This indicates that PEGylation generally does not alter the conformation of proteins.

CD is a common strategy to investigate the thermostability of proteins. Unfolding and refolding processes were studied by monitoring the molar ellipticity at 222 nm while heating the samples from 30 to 90 °C and cooling them back to 30 °C at a rate of 1 °C min^{-1}. Far-UV CD spectra were obtained at 30 °C before and after the temperature scan (30 to 90 °C) to comprehend undergoing conformational changes.

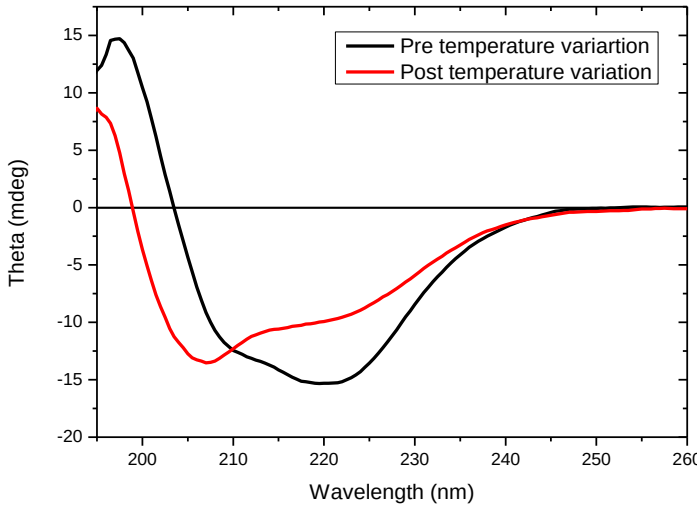

(A)

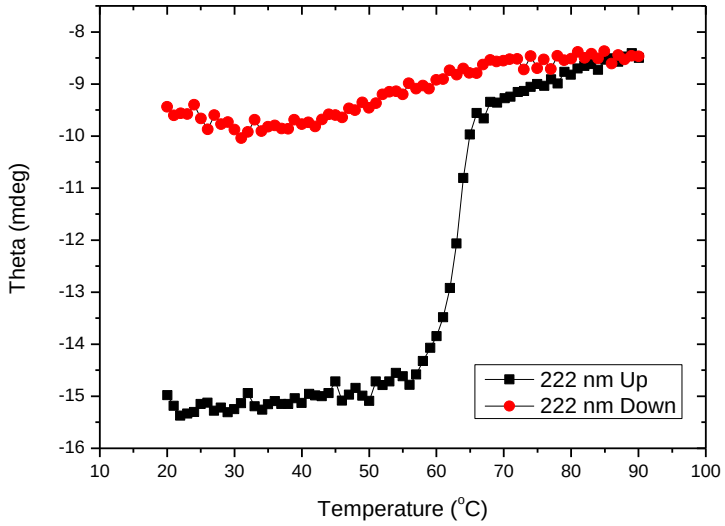

(B)

Figure 22. (A) Circular dichroism (CD) spectrum and variable temperature CD data ASNase at 20 °C (black line) and after heating and cooling (red line). **(B)** Thermostability curves of unfolding (black dots) and refolding (red dots) processes of ASNase. Unfolding curves were fitted to the data using the Hill equation (black line).

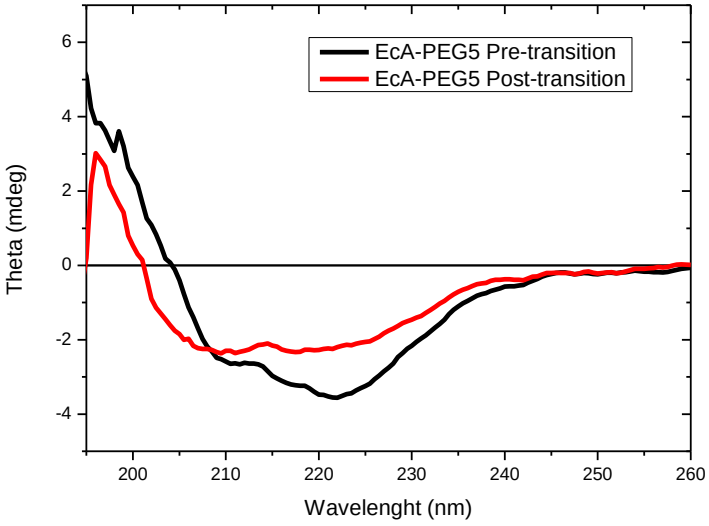

(A)

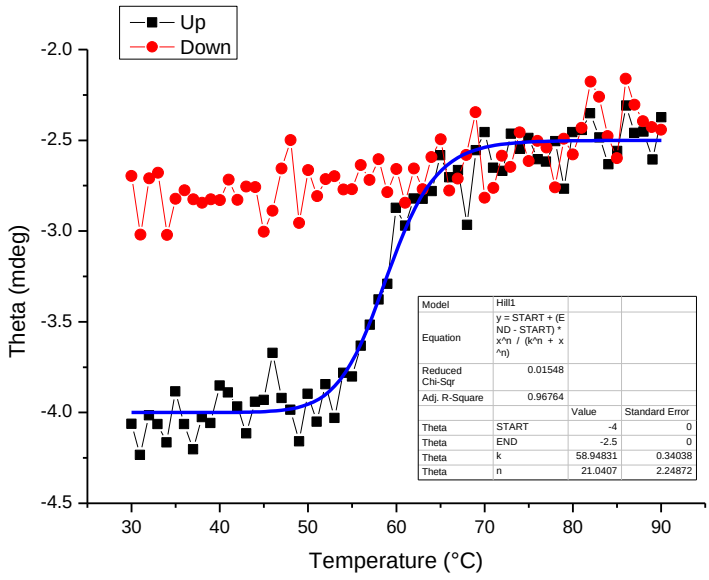

(B)

Figure 23. (A) Circular dichroism (CD) spectrum and variable temperature CD data ASNase-PEG5 at 20 °C (black line) and after heating and cooling (red line). **(B)** Thermostability curves of unfolding (black dots) and refolding (red dots) processes of ASNase-PEG5. Unfolding curves were fitted to the data using the Hill equation (blue line).

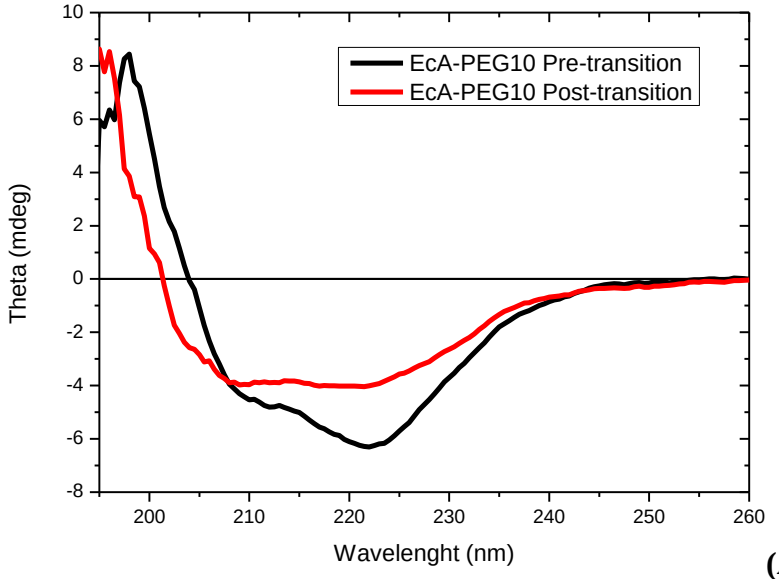

(A)

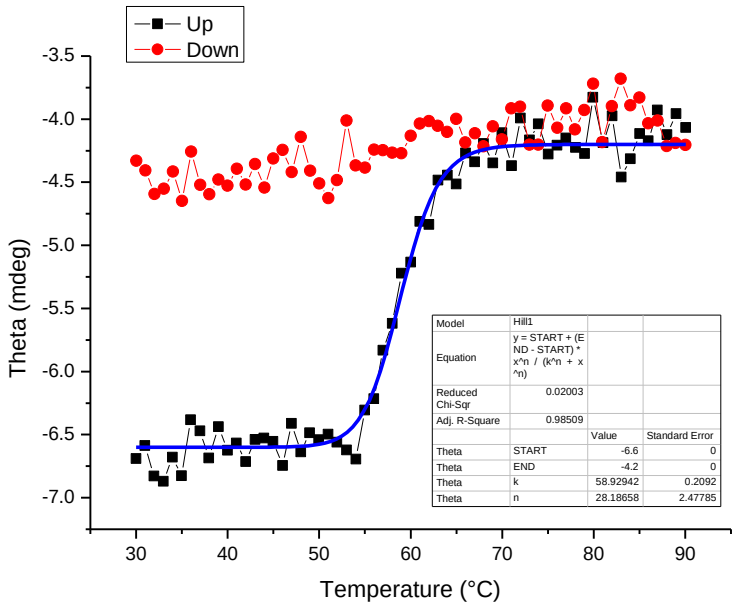

(B)

Figure 24. (A) Circular dichroism (CD) spectrum and variable temperature CD data ASNase-PEG10 at 20 °C (black line) and after heating and cooling (red line). **(B)** Thermostability curves of unfolding (black dots) and refolding (red dots) processes of ASNase-PEG10. Unfolding curves were fitted to the data using the Hill equation (blue line).

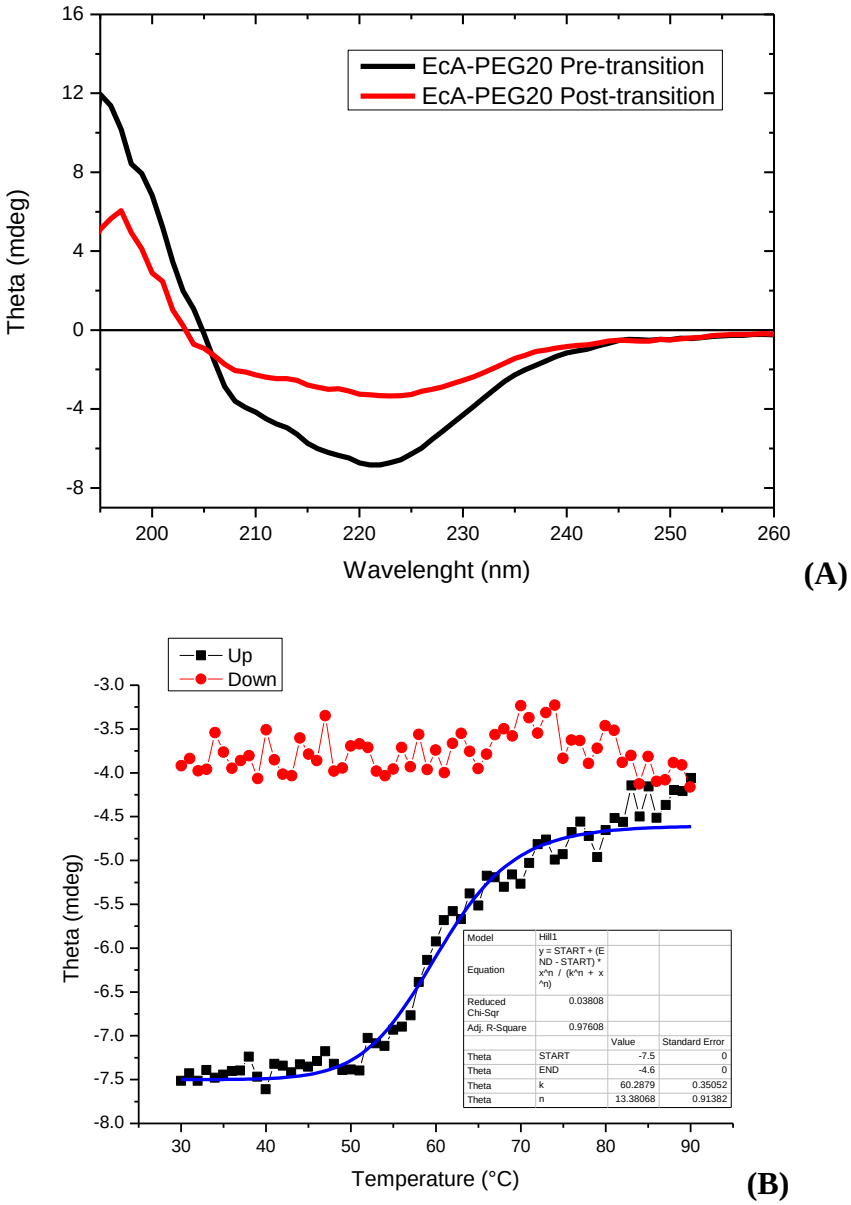

Figure 25. (A) Circular dichroism (CD) spectrum and variable temperature CD data ASNase-PEG20 at 20 °C (black line) and after heating and cooling (red line). **(B)** Thermostability curves of unfolding (black dots) and refolding (red dots) processes of ASNase-PEG20. Unfolding curves were fitted to the data using the Hill equation (blue line).

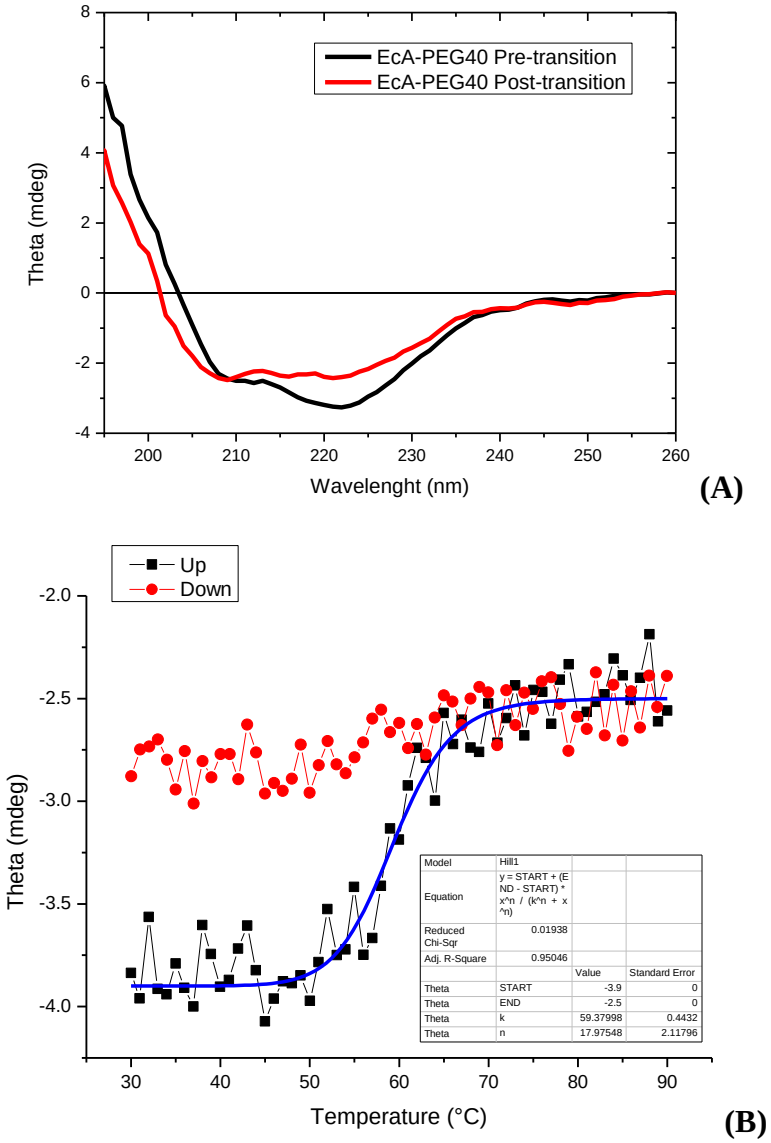

Figure 26. (A) Circular dichroism (CD) spectrum and variable temperature CD data ASNase-PEG40 at 20 °C (black line) and after heating and cooling (red line). **(B)** Thermostability curves of unfolding (black dots) and refolding (red dots) processes of ASNase-PEG40. Unfolding curves were fitted to the data using the Hill equation (blue line).

The unfolding process was slightly different for each PEGylated protein; however, all PEGylation degrees exhibited no refolding as demonstrated by the constant values of ellipticity at 222 nm during sample cooling. As expected, neither PEGylated forms nor native recovered to the folded state after heating. It is also notable that the PEGylated molecules were structurally stable, with melting temperatures similar to native ASNase (T_m of 62.6 ± 0.2 °C); calculated T_m were 58.9 °C, 58.9 °C, 60.3 °C, and 59.4 °C for ASNase-PEG5, ASNase-PEG10, ASNase-

PEG20, and ASNase-PEG40 respectively. The measured melting temperature is in agreement with data from the literature (García-Arellano et al., 2002b; Verma et al., 2014). Around 60 °C, ASNase structures (modified and unmodified) entered in the process of denaturation, therefore, conformational changes are observed (Figure 22). The transition state (folded to unfolded) is characterized by an increase in the system's state of order ($\Delta S^{\ddagger} < 0$) (Santos et al., 2019). The phenomena of aggregation seem to be less accentuated in the modified forms of ASNase compared to the native protein due to minor structural variations.

CD spectra results of the enzymes (native and PEGylated forms) were deconvoluted to calculate the secondary structure content of each ASNase form and the results are in agreement with those of the high-resolution structure found in the PDB, code 3ECA (https://www.rcsb.org/structure/3ECA). These observations indicate that the measurements and analysis of the structure by CD are correct (comparing the reference of the 3D structure with the native form). In general, during denaturation, the native and PEGylated enzymes presented a loss of secondary structure (α-helix and β-sheet) and an increase in fold-type (turn) and unstructured segments (random coil) (Table 5).

Correlating the results for ASNase and PEG-ASNases, we conclude that PEGylation did not significantly alter the secondary structure of ASNase (Table 5). Based on the structure-function relationship and activity, the results corroborate that despite PEG does not alter the structure of the proteins, it somehow creates a steric hindrance at the active site, decreasing the enzymatic activity in the PEGylated forms as verified.

Table 5. Secondary structure content percentage calculated from CD spectra for ASNase, ASNase-PEG5, ASNase-PEG10, ASNase-PEG20, and ASNase-PEG40 Reference structure of *E. coli* ASNase. PDB entry: 3ECA.

Protein	α-helix (%)	β-sheet (%)	Turn (%)	Random coil (%)
ASNase PDB Reference	32	23	45	
ASNase	32	28	5	35
ASNase-PEG5 Pre T	29	24	8	39
ASNase-PEG10 Pre T	32	28	9	31
ASNase-PEG20 Pre T	35	19	5	41
ASNase-PEG40 Pre T	28	16	12	44
ASNase Post T	35	5	12	48
ASNase-PEG5 Post T	33	0	10	57
ASNase-PEG10 Post T	18	12	13	57
ASNase-PEG20 Post T	22	8	13	57
ASNase-PEG40 Post T	27	0	13	60

5.5. Thermodynamic study: PEGylation effect in L-asparaginase at the optimal temperature

PEGylation usually results in differences in protein activity, as well as resistance to temperature variations. The rigidity and flexibility of the protein are important data regarding activity and thermostability. The folded structure is maintained by its rigidity, and certain flexibility is needed for the activity of the molecule (Porto et al., 2006; Yu et al., 2017). The activity of native and PEGylated ASNase was investigated at different temperatures ranging from 20 °C to 80 °C and the optimal temperature (T_{opt}) for ASNase was found to be around 40 °C, equivalent to the value previously described in the literature (Shakambari et al., 2019).

The semi-log plots of $\ln v_0$ vs. $1/T$ ($10^{3} \cdot K^{-1}$) presented in Figures 27 (ASNase) and 28 (PEGylated ASNase) show two tendencies (above and below T_{opt}), but only for native ASNase (Figure 27), the typical Arrhenius behavior was observed. Below optimal temperature, the unfolding equilibrium (measured by the standard enthalpy variation of enzyme unfolding – $\Delta H°_U$) is shifted to the left. However, the increase in temperature shifts the equilibrium to the right. According to the Arrhenius-type plot for native ASNase, the activation energy (E^* = 13.74 kJ) and $\Delta H°_U$ (23.35 kJ/mol) were estimated with good correlation (R^2 = 0.9959 and 0.9724 respectively).

For PEGylated conjugates, it was not possible to calculate the energy of activation based on Arrhenius-type plots since a lack of correlation of the presented data was observed, the linear regression was not significant (*p* values ranging from 0.6887 to 0.9964) to compare the results between the modified and unmodified ASNase. However, the PEGylated conjugates demonstrated similar fluctuations of relative activity during the tests, indicating that irrespectively of the differences between the MWs of PEGs, the relative activity presented comparable behavior.

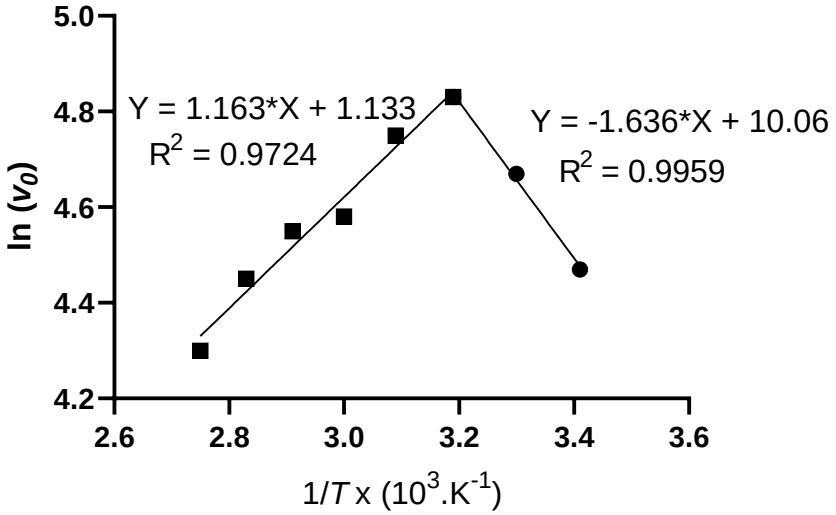

Figure 27. Arrhenius-type plot of initial activity (reversible unfolding) of native L-asparaginase, using L-asparagine as a substrate. The black circles represent the activation energy (E*) and the black squares represent the standard enthalpy variation of the inactivation equilibrium ($\Delta H°_U$).

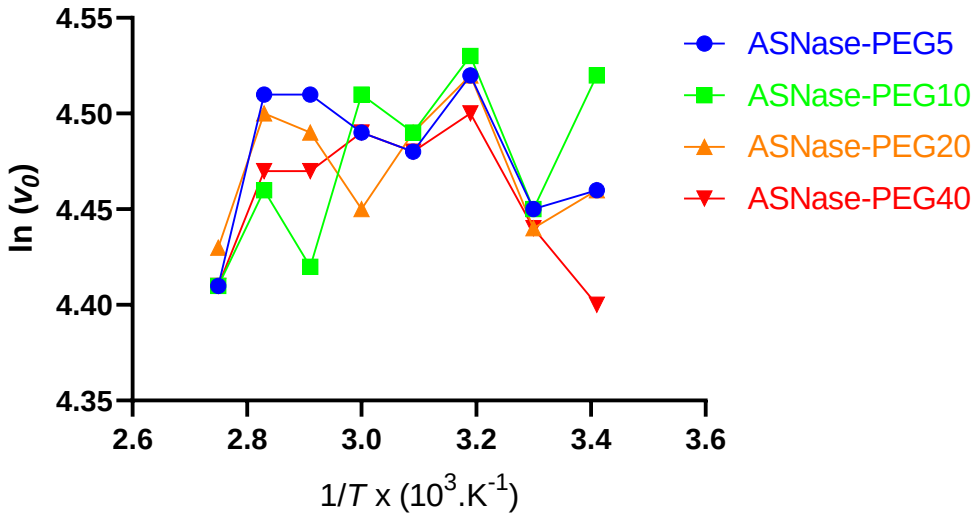

Figure 28. Arrhenius-type plot of initial activity of PEGylated ASNase, using L-asparagine as a substrate.

5.6. Effect of PEGylation in thermoinactivation and irreversible denaturation of L-asparaginase

Thermodynamics studies are relevant to determine the stability of enzymes at different temperatures. These studies provide information on the viability of production, use, and

maintenance of enzymatic activity for longer periods in industrial processes (El-Loly, Awad and Mansour, 2007). In order to determine if the process is economically viable, the enzyme needs to undergo a first-order deactivation reaction, so the main factors to predict the thermostability (Gibbs free energy, enthalpy, entropy) are evaluated. If the thermodynamic parameters indicate higher thermostability, the process is economically advantageous, reducing costs of production of the biological drug (Souza et al., 2015b).

Temperature is an important factor that can influence the kinetics of enzymatic reactions and lead to partially unfolded protein conformations. Very high temperatures can cause irreversible loss of proteins' structural conformation. The temperature rise can lead a protein to the transition state from folded to completely unfolded state; this process is called thermoinactivation. Considering biological drugs, the temperature can increase the speed of a chemical reaction until it reaches the optimal temperature, as observed in Figure 27. The slow increase in temperature revealed the optimal temperature of native ASNase, but at the same time, the increase in temperature also led the enzyme to denaturation, as observed for higher temperatures.

Thermoinactivation of native and PEGylated ASNase was investigated by activity tests in a temperature range from 60 °C to 80 °C. Although the optimal temperature is approximately 40 ^{o}C, we did not include an activity test at 50 ^{o}C since ASNase maintained good stability overtime at this temperature. Therefore, we selected temperatures above 60 °C, where the denaturation process is predominantly irreversible (Figure 29).

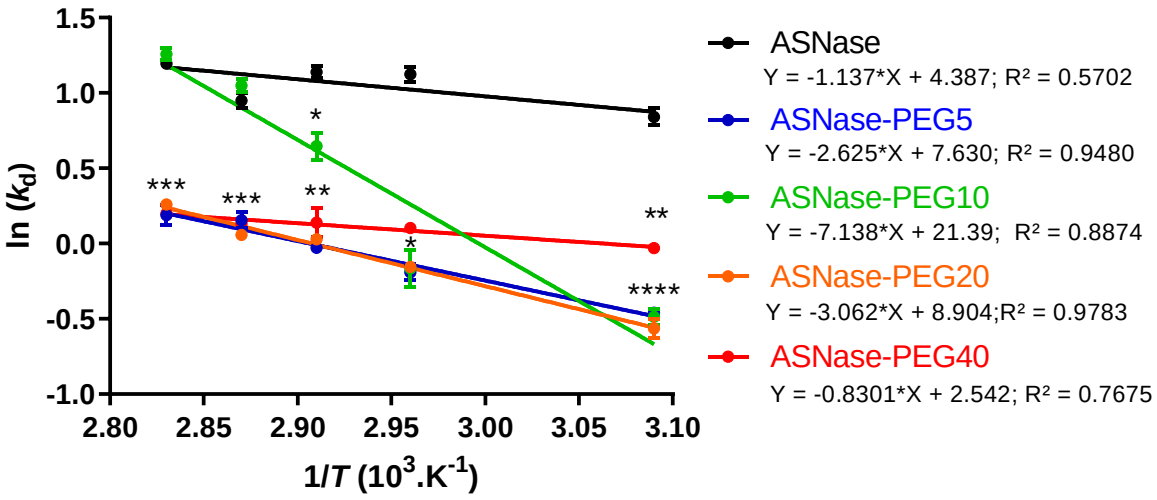

Figure 29. Arrhenius-type semi-log plots of the first-order denaturation constant (k_d) vs. the reciprocal temperature [$1/T(10^3.K^{-1})$]. The slopes of the resulting straight lines were used to estimate the denaturation energies (E^*_d) of irreversible inactivation (denaturation) of native ASNase, ASNase-PEG 5 kDa, ASNase-PEG 10 kDa, ASNase-PEG 20 kDa, and ASNase-PEG 40 kDa. *p<0.05, **p<0.01, ***p<0.001, ****p<0.0001 compared to native ASNase in the respective [$1/T(10^3.K^{-1})$] (Dunnett's *pos-hoc*).

For the thermodynamic characterization of enzyme denaturation, the first-order rate constant (k_d) should be assessed. The enzyme activity of ASNase with and without PEG was monitored as a function of time at several temperatures in which activity loss is observed. As depicted in Figure 29, the first-order rate constant (k_d) gradually increased for the native and PEGylated forms, with a good correlation ($R^2 > 0.9$). Similar plots were observed for the PEGylated forms, presenting linearity on the decay of enzyme activity. However, native ASNase presented a sharper increase compared to the PEGylated forms (except ASNase-PEG10), which implied a less stable enzyme. Hence, PEGylated ASNases, in general, presented higher thermostability, demonstrating long-term stability owing to the polymer conjugation.

We performed a two-way ANOVA (GraphPad Prism 5) which indicated a significative effect for temperature and size of PEG interaction [$F(16,38) = 99.16$; $p<0.0001$)]. Pairwise

comparisons (Dunnett's *pos-hoc* test) relative to native ASNase were depicted in Figure 29. The size of the PEG influenced the log k_d depending on the temperature, results for all sizes of PEG are different from native ASNase from the temperature 70 to 80 °C (2.91 to 3.09 x 10^3.K^{-1}). At initial temperatures 60 to 65 °C (2.83 and 2.87 x 10^3.K^{-1}), only ASNase-PEG10 is similar to the native ASNase.

The irreversible denaturation of ASNase and ASNase conjugates was investigated to determine the effect of PEGylation on the energy of denaturation (E^*_d), half-life ($t_{1/2}$), and other thermodynamic and kinetic parameters (Table 6).

For denaturation to occur, an energy barrier must be overcome, known as the activation energy of denaturation (E^*_d). This amount energy represents the irreversible point of denaturation of enzymes, establishing how much of energy is necessary for the enzyme not to refold to its native form and can be calculated based on the Arrhenius equation. As shown in Table 6, it is easier to overcome the barrier of denaturation for the native form (E^*_d of 11.52 kJ.mol^{-1}) than for PEGylated forms. A higher value was observed for ASNase-PEG10 (E^*_d of 48.85 kJ.mol^{-1}) corresponding to a 4.24-fold increase. Nonetheless, this should be confirmed since considering the other ASNase-PEG conjugates, E^*_d was inversely proportional to the PEG MW, i.e., the higher the polymeric branch attached, the lower was E^*_d. Therefore, it seems we have competing effects. An initial effect of PEG thermo-protection that results in higher E^*_d values for PEGylated proteins; and a PEG MW effect according to which higher MW PEGs usually result in less thermo-protection against irreversible denaturation. This might be related to the van der Waals interactions among PEG moieties owing to dehydration upon temperature increase. The effect is more pronounced for higher MW PEGs. Therefore, the thermostability of PEGylated ASNase depends on the amount of PEG attached to the protein, *i.e.* on the polymer molecular weight and the number of polymeric chains attached.

Table 6. Energy of activation during irreversible denaturation of native and PEGylated forms of L-asparaginase in the range of T = 60 °C to 80 °C.

Protein	E^*_d (kJ/mol)
ASNase	11.52
ASNase-PEG5	29.32
ASNase-PEG10	48.85
ASNase-PEG20	27.61
ASNase-PEG40	21.61

In general, the PEGylated ASNases demonstrated a similar behavior upon denaturation (Table 7). Initially (from temperatures of 60 to 70 °C), all PEG conjugates presented homogeneity of k_d values, ranging from 0.588 h^{-1} to 0.795 h^{-1}. However, at 75 °C, ASNase-PEG10 showed a lack of control over the maintenance of k_d, which was inversely observed for E^*_d. Upon temperature increase, ASNase-PEG10 resulted in a sample with lower thermostability. At 80 °C, ASNase-PEG10 presented k_d = 3.34 h^{-1}, similar to ASNase (k_d = 3.879 h^{-1}); the larger the first-order rate constant during denaturation, the less stable the enzyme (Marangoni, 2003). As mentioned before, this sample should be re-evaluated for more comprehensive results.

Half-life ($t_{1/2}$) is the time required for the enzyme activity to drop down to 50% of the initial value at a given temperature. This is a highly relevant factor concerning the economic viability of a biological product since it usually suffers from certain instability (Souza et al., 2015b). PEGylated forms exhibited higher $t_{1/2}$ values (ranging from 0.87 to 1.17 h at 60 °C) in comparison to the native ASNase (0.21 h at 60 °C). Also, k_d and $t_{1/2}$ are inversely correlated, since the higher values of $t_{1/2}$ and lower values of k_d represent a thermostable molecule. No differences related to the size of MWs were observed since the values of $t_{1/2}$ for all the PEGylated forms were similar.

The thermodynamic parameters ($\Delta H^{\ddagger}$, $\Delta G^{\ddagger}$, and $\Delta S^{\ddagger}$) were calculated based on Eqs. (4-6) and are presented in Table 7. Altogether, they allow to estimate of folded and unfolded states

of ASNase; thus, when the folded state predominates to the unfolded state, the protein is more stable (Matthews, 2013). However, if the unfolded (or partially folded) state predominates, the protein has low conformational stability, which could be caused by proteolysis or aggregation.

Associated to E^*_d, the activation enthalpy of denaturation ($\Delta H^‡$) represents the amount of energy required to denature an enzyme, indicating cleavage of non-covalent linkage that maintains its stability (i.e., hydrogen bonds, electrostatic interactions), mainly the interactions between the hydrophobic linkages of the subunits of L-asparaginase (Sanches et al., 2003). An increase of 2 to 7 times was observed for $\Delta H^‡$ at 80 °C upon PEGylation, reinforcing the effect of the conjugation on protein thermostability. The higher values of $\Delta H^‡$ were observed for ASNase-PEG10, while for the other PEG sizes, the increase in $\Delta H^‡$ was inversely proportional to the PEG chain MW. Further experiments should be performed to confirm that PEGylation with 10 kDa polymer results in a unique behavior owing to the balance of the effects that the ethylene oxide groups can cause in a protein, namely resistance due to conformational restriction and sensibility owing to the possible dehydration of PEG moieties at higher temperatures.

The entropy of inactivation $\Delta S^‡$ is associated with how the amount of energy is distributed *per* temperature during denaturation. At thermal denaturation, there is an opening up of enzyme structure; therefore, at higher temperatures, $\Delta S^‡$ increases. Table 7 presents negative values for $\Delta S^‡$ in the transition to the irreversible denatured state indicating that the structure of the enzyme-substrate complex was stable during denaturation (Silva et al., 2018). The higher values for this parameter were again observed for ASNase-PEG10 (- 0.042 J/mol·K at 80 °C). ASNase, as expected, presented the lowest value of $\Delta S^‡$, - 0.147 J/mol·K at 80 °C. The higher values of entropy mean that higher energy is needed to denature the PEGylated conjugates, reinforcing the increase in thermostability. PEGylation probably decreased

aggregation and protected ASNase, stabilizing intra and/or inter-molecular forces, increasing thermostability (Oliveira et al., 2018).

As for $\Delta G^{\ddagger}$, it is related to the spontaneity of the process; therefore, more adequate to predict the stability of enzymes (Souza et al., 2015a). Positive values ($\Delta S^{\ddagger} < 0$, and $\Delta H^{\ddagger} > 0$) of $\Delta G^{\ddagger}$ indicate that the denaturation process is not spontaneous (Almeida et al., 2020). Negative values of $\Delta G^{\ddagger}$ represent a spontaneous process of denaturation, revealing a thermosensitive protein (Santos et al., 2019), which was not the case for ASNase. Although ASNase-PEG10 presented higher values for a considerable number of parameters ($\Delta H^{\ddagger}$, k_d, and E^*_d), it did not show better control over time than ASNase under different temperatures. ASNase-PEG10 presented $\Delta G^{\ddagger}$ = 60.71 kJ·mol^{-1} at 75 °C, whereas ASNase presented a similar value at the same temperature ($\Delta G^{\ddagger}$ = 60.34 kJ·mol^{-1}). Nonetheless, all other PEG molecular weights resulted in values corresponding to thermo-protection over time and different temperatures. Thus, all modifications (except ASNase-PEG10) presented greater regulation over the temperature in comparison to the native ASNase.

Table 7. Thermodynamic and kinetic parameters of the irreversible thermal deactivation of the native and PEGylated forms of L-asparaginase.

Thermodynamic and kinetic parameters						
	T **(ºC)**	***k*d** **(h^{-1})**	$t_{1/2}$ **(h)**	$\Delta H^{\ddagger}$ **(kJ.mol^{-1})**	$\Delta G^{\ddagger}$ **(kJ.mol^{-1})**	$\Delta S^{\ddagger}$ **(J/mol.K)**
ASNase	60	3.222	0.21	8.75	57.82	-0.147
	65	2.754	0.25	8.70	59.09	-0.149
	70	3.607	0.19	8.66	59.15	-0.147
	75	3.178	0.21	8.62	60.34	-0.149
	80	3.879	0.17	8.58	60.58	-0.147
ASNase-PEG5	60	0.588	1.17	26.55	62.54	-0.108
	65	0.956	0.72	26.51	62.06	-0.105
	70	1.169	0.59	26.46	62.37	-0.105
	75	1.221	0.56	26.42	63.11	-0.105
	80	1.505	0.46	26.38	63.36	-0.105
ASNase-PEG10	60	0.789	0.87	46.08	61.72	-0.047
	65	1.03	0.67	46.04	61.86	-0.047
	70	1.93	0.36	45.99	60.94	-0.044
	75	2.795	0.24	45.95	60.71	-0.043
	80	3.34	0.20	45.91	61.02	-0.042
ASNase-PEG20	60	0.65	1.06	24.84	62.26	-0.112
	65	1.103	0.62	24.80	61.66	-0.109
	70	1.382	0.50	24.76	61.89	-0.108
	75	1.461	0.47	24.72	62.59	-0.109
	80	1.461	0.47	24.68	63.45	-0.110
ASNase-PEG40	60	0.795	0.87	18.84	61.70	-0.129
	65	1.266	0.54	18.80	61.28	-0.126
	70	1.33	0.52	18.76	62.00	-0.126
	75	1.474	0.47	18.72	62.57	-0.126
	80	1.56	0.44	18.67	63.25	-0.126

5.7. Stability of PEGylated and native L-asparaginase over the time

To assess the stability over time, native and PEGylated forms of ASNase were submitted to storage at 37 °C (optimal activity temperature) and 4 °C (at refrigerator), and activity was determined every three days for 21 days. At 37 °C (Figure 30), higher stability was observed for ASNase-PEG5, especially up to 12 days, corresponding to 57% of residual activity.

Nonetheless, all PEGylated forms presented similar activity values after 21 days of storage at 37 °C, corresponding to approximately 26% of residual activity. A two-way ANOVA for the residual activity at 37 °C revealed a significant effect only for the days of measurements [$F(2.36, 17.93) = 104.6$], that is samples presented reduced residual activity throughout the days of measurement. The Dunnett's *post hoc* test yielded no significant differences between PEG sizes, except at day 5, where ASNase-PEG5 presented increased residual activity relative to ASNase-PEG20 and ASNase-PEG40 ($p < 0.05$) (Figure 30). As we can see, even the PEGylated forms of ASNase did not resist at this temperature for long periods. This information is very important in terms of the industrial potential of the enzyme because it demonstrates the best way to store the enzyme. As we mentioned before, ASNase can be used in the food industry to remove acrylamide from thermally processed products, so this study can also be useful for the food industry. The results for native ASNase were not presented in Figure 30 due to the lack of stability over all the studied periods (21 days). Nonetheless, Sindhu and collaborators (2019) already demonstrated the instability of the enzyme at this temperature, with a 50% decrease in activity after 48 hours.

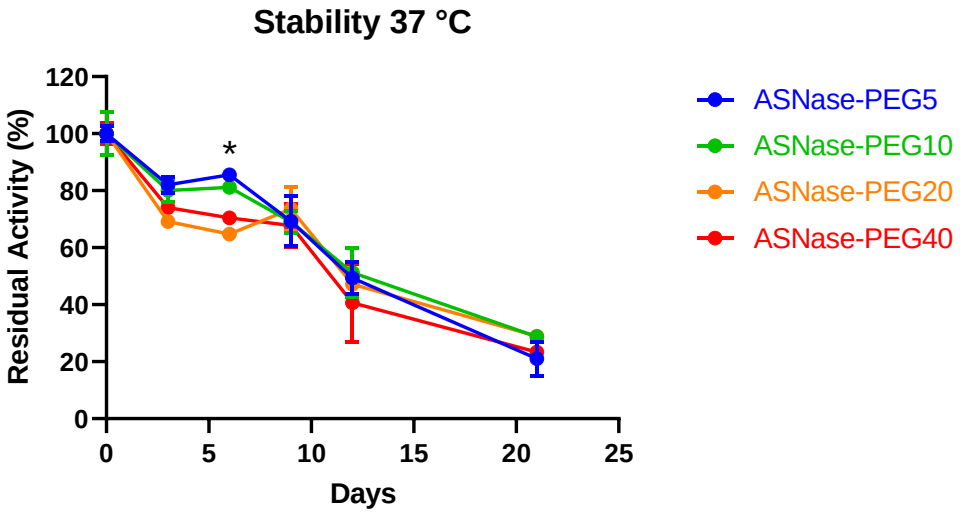

Figure 30. Residual activity of PEGylated L-asparaginase with different PEG molecular weights at 37 °C. The standard errors were calculated with GraphPad Prism 5 program. *p<0.05.

As expected, ASNase was more stable at 4 °C (Figure 31), the PEGylated forms retained at least 50% of the activity even after 21 days. The highest residual activity values were observed for ASNase-PEG5 and ASNase-PEG10. After 9 days, ASNase-PEG5 still presented 89% of residual activity. At the end of the 21 days, ASNase-PEG5 presented 55% of residual activity and ASNase-PEG10 65%. According to the Committee for Medicinal Products for Human Use (CHMP) - EMA (European Medicines Agency) (2001), the polyPEGylated ASNase Oncaspar® is alleged (after dilution) to maintain its physicochemical characteristics and stability of activity for 48 hours. After this period, they claim that the biological drug could be valid until 8 months, but the impact on the activity should be assessed for more information.

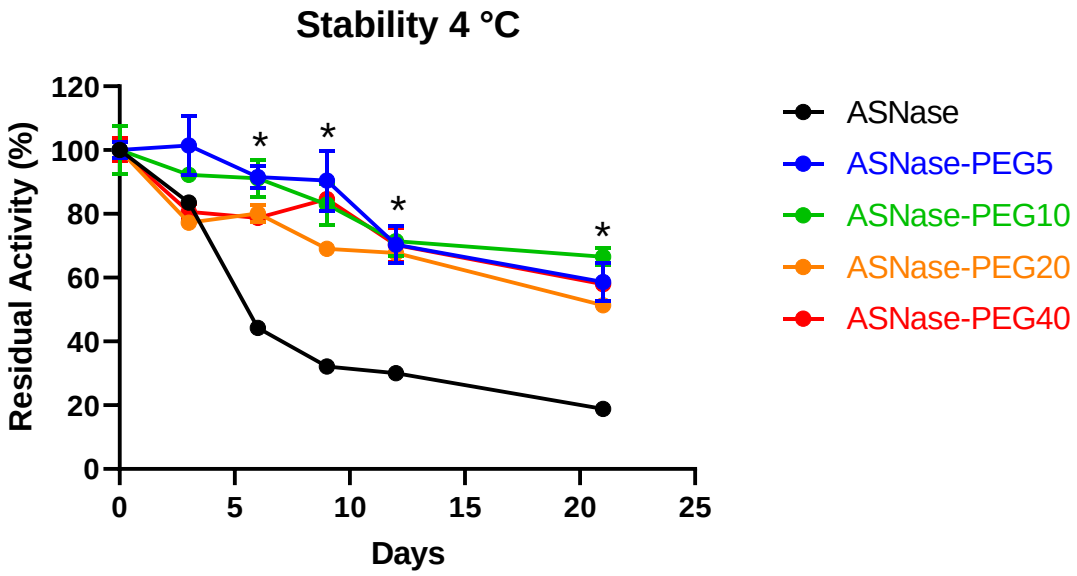

Figure 31. Residual activity of PEGylated L-asparaginase with different PEG molecular weights at 4 °C, compared to the native enzyme. The standard errors were calculated with GraphPad Prism 5 program.

The native ASNase presented 50% of decay on the 6th day, as reported by Meneguetti et al (2019). The two-way ANOVA analysis indicated a significative effect for PEG size and days interaction [$F(20, 47) = 6.774$; $p < 0.0001$]. Dunnett's *post hoc* test highlighted that all PEG sizes preserved ASNase residual activity at 4 ºC relative to the native enzyme, starting at the 6th day ($p < 0.05$).

6 CONCLUSIONS

In this work, we investigated the effect of *N*-terminal PEGylation on ASNase thermostability and thermodynamics. We PEGylated the enzyme with 5, 10, 20, and 40 kDa PEG and yields in the range of 45 to 52% were obtained for 5, 10, and 20 kDa of PEG, and 29% for 40 kDa PEG owing to steric hindrance. PEGylated ASNase variants were successfully purified by ion-exchange chromatography. The conformational structure was evaluated by circular dichroism and no significant changes were observed for the PEGylated forms in comparison to the native protein.

We demonstrated that *N*-terminal monoPEGylation preserved enzyme activity over time (in all of the thermodynamic criteria studied), compared to the native form. Also, stability over time was investigated at different storage temperatures and residual activity was higher for the PEGylated forms. Nonetheless, PEGylation resulted in conformational restriction and higher values of the kinetic parameters K_m and k_{cat}.

For all the studied thermodynamic parameters, the degree of PEGylation (number of PEG chains) presented a homogeneous result for all sizes of PEG. That is, the MW of the PEGs did not matter in the thermodynamic parameters. The protective role of all MW PEGs was demonstrated mainly when the temperature increased, aligned with decreased aggregation (higher $\Delta S^{\ddagger}$ values for the PEGylated ASNases). Therefore, PEGylation was successful to promote ASNase increased thermostability and is suitable to be exploited for future applications in the biotechnological field.

7 FUTURE STEPS

As a future step, it would be interesting to visualize the molecular dynamics of the ASNase-PEG conjugates and understand how bioconjugation is promoting thermostability to ASNase and also influencing activity. Mass spectrometry should also be performed to confirm that PEGylation occurred at the *N*-terminal site. In addition, it would be interesting to study if the PEG molecular weight influences immunogenicity.

REFERENCES

ABUCHOWSKI, A.; MCCOY, J. R. .; PAULCZUK, N. C. .; ES, T. VAN; DAVIS, F. F. Effect of covalent attachment of polyethylene glycol on immunogenicity and circulating life of bovine liver catalase. **Journal of Biological Chemistry**, v. 252, n. 11, p. 3582–3586, 1977.

AKBARZADEHLALEH, P.; MIRZAEI, M.; MASHAHDI-KESHTIBAN, M.; SHAMSASENJAN, K.; HEYDARI, H. **PEGylated human serum albumin: Review of PEGylation, purification and characterization methodsAdvanced Pharmaceutical Bulletin**Tabriz University of Medical Sciences, , 2016. Disponível em: <https://pubmed.ncbi.nlm.nih.gov/27766215/>. Acesso em: 20 jul. 2020

ALMEIDA, GABRIEL MORETTI; MENDONÇA, C. M. N.; CONVERTI, A.; OLIVEIRA, R. P. DE S. Kinetic and thermodynamic parameters of nisin thermoinactivation. **Journal of Food Engineering**, v. 280, 1 set. 2020.

ANANDAKRISHNAN, R.; AGUILAR, B.; ONUFRIEV, A. V. H++ 3.0: Automating pK prediction and the preparation of biomolecular structures for atomistic molecular modeling and simulations. **Nucleic Acids Research**, v. 40, n. W1, p. W537, jul. 2012.

ANGIOLILLO, A. L. *et al.* Pharmacokinetic and pharmacodynamic properties of calaspargase pegol Escherichia coli L-asparaginase in the treatment of patients with acute lymphoblastic leukemia: Results from children's oncology group study AALL07P4. **Journal of Clinical Oncology**, v. 32, n. 34, p. 3874–3882, 1 dez. 2014.

ARMSTRONG, J. K.; HEMPEL, G.; KOLING, S.; CHAN, L. S.; FISHER, T.; MEISELMAN, H. J.; GARRATTY, G. Antibody against poly(ethylene glycol) adversely affects PEG-asparaginase therapy in acute lymphoblastic leukemia patients. **Cancer**, v. 110, n. 1, p. 103–111, 1 jul. 2007.

ARNDT, C.; KORISTKA, S.; BARTSCH, H.; BACHMANN, M. Native polyacrylamide gels. **Methods in Molecular Biology**, v. 869, p. 49–53, 2012.

BAILON, P. *et al.* Rational design of a potent, long-lasting form of interferon: A 40 kDa branched polyethylene glycol-conjugated interferon α-2a for the treatment of hepatitis C. **Bioconjugate Chemistry**, v. 12, n. 2, p. 195–202, 2001.

BALCÃO, V. M.; MATEO, C.; FERNÁNDEZ-LAFUENTE, R.; XAVIER MALCATA, F.; GUISÁN, J. M. Structural and functional stabilization of L-asparaginase via multisubunit immobilization onto highly activated supports. **Biotechnology Progress**, v. 17, n.

3, p. 537–542, 1 jan. 2001.

BARBOSA, M. D. F. S. **Immunogenicity of biotherapeutics in the context of developing biosimilars and biobettersDrug Discovery Today**Drug Discov Today, , abr. 2011. Disponível em: <https://pubmed.ncbi.nlm.nih.gov/21300174/>. Acesso em: 28 dez. 2020

BARBOSA, M. D. F. S.; KUMAR, S.; LOUGHREY, H.; SINGH, S. K. **Biosimilars and biobetters as tools for understanding and mitigating the immunogenicity of biotherapeuticsDrug Discovery Today**Drug Discov Today, , dez. 2012. Disponível em: <https://pubmed.ncbi.nlm.nih.gov/22796124/>. Acesso em: 28 dez. 2020

BLUM, H.; BEIER, H.; GROSS, H. J. Improved silver staining of plant proteins, RNA and DNA in polyacrylamide gels. **Electrophoresis**, v. 8, n. 2, p. 93–99, 1 jan. 1987.

BROCCHINI, S.; BALAN, S.; GODWIN, A.; CHOI, J. W.; ZLOH, M.; SHAUNAK, S. PEGylation of native disulfide bonds in proteins. **Nature Protocols**, v. 1, n. 5, p. 2241–2252, dez. 2006.

BROOME, J. D. Evidence that the L-asparaginase activity of guinea pig serum is responsible for its antilymphoma effects. **Nature**, v. 191, n. 4793, p. 1114–1115, 1961.

BRUMANO, L. P.; SILVA, F. V. S. DA; COSTA-SILVA, T. A.; APOLINÁRIO, A. C.; SANTOS, J. H. P. M.; KLEINGESINDS, E. K.; MONTEIRO, G.; RANGEL-YAGUI, C. DE O.; BENYAHIA, B.; JUNIOR, A. P. **Development of L-asparaginase biobetters: Current research status and review of the desirable quality profilesFrontiers in Bioengineering and Biotechnology**Frontiers Media S.A., , 10 jan. 2019. Disponível em: <www.frontiersin.org>. Acesso em: 13 out. 2020

CACHUMBA, J. J. M.; ANTUNES, F. A. F.; PERES, G. F. D.; BRUMANO, L. P.; SANTOS, J. C. DOS; SILVA, S. S. DA. Current applications and different approaches for microbial L-asparaginase production. **Brazilian Journal of Microbiology**, v. 47, p. 77–85, 2016.

CALO-FERNÁNDEZ, B.; MARTÍNEZ-HURTADO, J. L. Biosimilars: Company strategies to capture value from the biologics market. **Pharmaceuticals**, v. 5, n. 12, p. 1393–1408, 12 dez. 2012.

CEROFOLINI, L.; GIUNTINI, S.; CARLON, A.; RAVERA, E.; CALDERONE, V.; FRAGAI, M.; PARIGI, G.; LUCHINAT, C. Characterization of PEGylated Asparaginase: New Opportunities from NMR Analysis of Large PEGylated Therapeutics. **Chemistry - A**

European Journal, v. 25, n. 8, p. 1984–1991, 2019.

COMMITTEE FOR MEDICINAL PRODUCTS FOR HUMAN USE (CHMP) - EMA. **RESUMO DAS CARACTERÍSTICAS DO MEDICAMENTO**. [s.l: s.n.].

CONVERTI, A.; BORGHI, A. DEL; GANDOLFI, R.; LODI, A.; MOLINARI, F.; PALAZZI, E. Reactivity and stability of mycelium-bound carboxylesterase from Aspergillus oryzae. **Biotechnology and Bioengineering**, v. 77, n. 2, p. 232–237, 20 jan. 2002.

DELGADO, C.; MALMSTEN, M.; ALSTINE, J. M. VAN. Analytical partitioning of poly(ethylene glycol)-modified proteins. **Journal of Chromatography B: Biomedical Applications**, v. 692, n. 2, p. 263–272, 9 maio 1997.

DERST, C.; HENSELING, J.; RÖHM, K.-H. Engineering the substrate specificity of Escherichia coli asparaginase II. Selective reduction of glutaminase activity by amino acid replacements at position 248 . **Protein Science**, v. 9, n. 10, p. 2009–2017, 2000.

DIAS, F. F. G.; SANTOS AGUILAR, J. G. DOS; SATO, H. H. l-Asparaginase from Aspergillus spp.: production based on kinetics, thermal stability and biochemical characterization. **3 Biotech**, v. 9, n. 7, p. 1–10, 2019.

DOZIER, J. K.; DISTEFANO, M. D. **Site-specific pegylation of therapeutic proteinsInternational Journal of Molecular Sciences**MDPI AG, , 1 out. 2015. Disponível em: <https://pubmed.ncbi.nlm.nih.gov/26516849/>. Acesso em: 3 ago. 2020

DUARTE, L.; MATTE, C. R.; BIZARRO, C. V.; AYUB, M. A. Z. **Review transglutaminases: part II—industrial applications in food, biotechnology, textiles and leather productsWorld Journal of Microbiology and Biotechnology**Springer, , 1 jan. 2020. Disponível em: <https://pubmed.ncbi.nlm.nih.gov/31879822/>. Acesso em: 24 nov. 2020

EISENTHAL, R.; DANSON, M. J.; HOUGH, D. W. Catalytic efficiency and kcat/KM: a useful comparator? **Trends in Biotechnology**, v. 25, n. 6, p. 247–249, 1 jun. 2007.

EKLADIOUS, I.; COLSON, Y. L.; GRINSTAFF, M. W. **Polymer–drug conjugate therapeutics: advances, insights and prospectsNature Reviews Drug Discovery**Nature Publishing Group, , 1 abr. 2019. Disponível em: <https://pubmed.ncbi.nlm.nih.gov/30542076/>. Acesso em: 23 jun. 2020

EL-LOLY, M. M.; AWAD, A. A.; MANSOUR, A. I. A. Thermal kinetics denaturation of Buffalo milk immunoglobulins. **International Journal of Dairy Science**, v. 2, n. 4, p. 292–

301, 2007.

ENZON PHARMACEUTICALS, I. **Pegaspargase Oncaspar**. [s.l: s.n.]. Disponível em: <http://primedicin.com.br/wp-content/uploads/2011/07/Oncaspar-Bula-Primedicin.pdf>. Acesso em: 3 fev. 2021.

FDA Approved PEGylated Drugs 2020 | Biochempeg. Disponível em: <https://www.biochempeg.com/article/58.html>. Acesso em: 28 dez. 2020.

FEE, C. J. Size comparison between proteins PEGylated with branched and linear poly(ethylene glycol) molecules. **Biotechnology and Bioengineering**, v. 98, n. 4, p. 725–731, 1 nov. 2007.

FEE, C. J.; ALSTINE, J. M. VAN. Purification of PEGylated Proteins. **Protein Purification: Principles, High Resolution Methods, and Applications: Third Edition**, n. 7, p. 339–362, 2011.

FONTANA, A.; SPOLAORE, B.; MERO, A.; VERONESE, F. M. **Site-specific modification and PEGylation of pharmaceutical proteins mediated by transglutaminaseAdvanced Drug Delivery Reviews**Adv Drug Deliv Rev, , 3 jan. 2008. Disponível em: <https://pubmed.ncbi.nlm.nih.gov/17916398/>. Acesso em: 4 ago. 2020

FRANÇA, P. R. L. **DEGRADAÇÃO DE PECTINA EM SUCO DE CAJU POR POLIGALACTURONASE DE Aspergillus aculeatus URM4953 IMOBILIZADA COVALENTEMENTE EM PÉROLAS DE ALGINATO**. [s.l: s.n.]. Disponível em: <https://www.repository.ufrpe.br/bitstream/123456789/1402/1/tcc_pedrorenannlopesdefrança.pdf>. Acesso em: 5 jan. 2021.

FU, C. H.; SAKAMOTO, K. M. PEG-asparaginase. v. 8 (12), p. 1977–1984, 2007.

GANSON, N. J.; KELLY, S. J.; SCARLETT, E.; SUNDY, J. S.; HERSHFIELD, M. S. Control of hyperuricemia in subjects with refractory gout, and induction of antibody against poly(ethylene glycol) (PEG), in a phase I trial of subcutaneous PEGylated urate oxidase. **Arthritis Research and Therapy**, v. 8, n. 1, 2 dez. 2005.

GARCÍA-ARELLANO, H.; VALDERRAMA, B.; SAAB-RINCÓN, G.; VAZQUEZ-DUHALT, R. High temperature biocatalysis by chemically modified cytochrome c. **Bioconjugate Chemistry**, v. 13, n. 6, p. 1336–1344, nov. 2002a.

___. High temperature biocatalysis by chemically modified cytochrome c.

Bioconjugate Chemistry, v. 13, n. 6, p. 1336–1344, nov. 2002b.

GEFEN, T.; VAYA, J.; KHATIB, S.; HARKEVICH, N.; ARTOUL, F.; HELLER, E. D.; PITCOVSKI, J.; AIZENSHTEIN, E. The impact of PEGylation on protein immunogenicity. **International Immunopharmacology**, v. 15, n. 2, p. 254–259, 1 fev. 2013.

GINN, C.; KHALILI, H.; LEVER, R.; BROCCHINI, S. PEGylation and its impact on the design of new protein-based medicines. **Future Medicinal Chemistry**, v. 6, n. 16, p. 1829–1846, 1 out. 2014.

GIORGI, M. E.; AGUSTI, R.; LEDERKREMER, R. M. DE. Carbohydrate PEGylation, an approach to improve pharmacological potency. **Beilstein Journal of Organic Chemistry**, v. 10, p. 1433–1444, 25 jun. 2014.

GOHEL, S. D.; SINGH, S. P. Characteristics and thermodynamics of a thermostable protease from a salt-tolerant alkaliphilic actinomycete. **International Journal of Biological Macromolecules**, v. 56, p. 20–27, 1 maio 2013.

GRAHAM, M. L. Pegaspargase: A review of clinical studies. **Advanced Drug Delivery Reviews**, v. 55, n. 10, p. 1293–1302, 26 set. 2003.

GUPTA, V.; BHAVANASI, S.; QUADIR, M.; SINGH, K.; GHOSH, G.; VASAMREDDY, K.; GHOSH, A.; SIAHAAN, T. J.; BANERJEE, S.; BANERJEE, S. K. **Protein PEGylation for cancer therapy: bench to bedsideJournal of Cell Communication and Signaling**Springer Netherlands, , 1 set. 2019. Disponível em: <https://pubmed.ncbi.nlm.nih.gov/30499020/>. Acesso em: 27 jul. 2020

GUTTMAN, C. **Purify, purify and…purify more: tips for improving your protein purification capabilities – part 4 | Benchwise**. Disponível em: <https://benchwise.wordpress.com/2012/04/11/purify-purify-andpurify-more-tips-for-improving-your-protein-purification-capabilities-part-4-2-2/>. Acesso em: 2 jan. 2021.

HERMANSON, G. **Bioconjugate Chemistry**. 3. ed. [s.l: s.n.]. v. 3

HU, X.; WILDMAN, K. P.; BASU, S.; LIN, P. L.; ROWNTREE, C.; SAHA, V. The cost-effectiveness of pegaspargase versus native asparaginase for first-line treatment of acute lymphoblastic leukaemia: a UK-based cost-utility analysis. **Health economics review**, v. 9, n. 1, p. 40, 29 dez. 2019.

INGRASCIOTTA, Y.; CUTRONEO, P. M.; MARCIANÒ, I.; GIEZEN, T.; ATZENI,

F.; TRIFIRÒ, G. Safety of Biologics, Including Biosimilars: Perspectives on Current Status and Future Direction. **Drug Safety**, v. 41, n. 11, p. 1013–1022, 23 nov. 2018.

IVENS, I. A. *et al.* **PEGylated Biopharmaceuticals: Current Experience and Considerations for Nonclinical DevelopmentToxicologic Pathology**SAGE Publications Inc., , 1 out. 2015. Disponível em: <https://pubmed.ncbi.nlm.nih.gov/26239651/>. Acesso em: 29 jul. 2020

JAISWAL, P.; SHINDE, S. **PEGylated Proteins Market : Allied Market Research**. Disponível em: <https://www.alliedmarketresearch.com/PEGylated-proteins-market>. Acesso em: 28 dez. 2020.

KIDD, J. G. Regression of transplanted lymphomas induced in vivo by means of normal guinea pig serum. I. Course of transplanted cancers of various kinds in mice and rats given guinea pig serum, horse serum, or rabbit serum. **The Journal of experimental medicine**, v. 98, n. 6, p. 565–582, 1 dez. 1953.

KNOTT, S. R. V. *et al.* Asparagine bioavailability governs metastasis in a model of breast cancer. **Nature**, v. 554, n. 7692, p. 378–381, fev. 2018.

KOLATE, A.; BARADIA, D.; PATIL, S.; VHORA, I.; KORE, G.; MISRA, A. **PEG - A versatile conjugating ligand for drugs and drug delivery systemsJournal of Controlled Release**Elsevier, , 28 out. 2014.

LA TORRE, B. G. DE; ALBERICIO, F. The Pharmaceutical Industry in 2017. An Analysis of FDA Drug Approvals from the Perspective of Molecules. **Molecules**, v. 23, n. 553, 2018.

LAEMMLI, U. K. Cleavage of structural proteins during the assembly of the head of bacteriophage T4. **Nature**, v. 227, n. 5259, p. 680–685, 1970.

LAWRENCE, P. B. *et al.* Criteria for selecting PEGylation sites on proteins for higher thermodynamic and proteolytic stability. **Journal of the American Chemical Society**, v. 136, n. 50, p. 17547–17560, 17 dez. 2014.

LEW, G. Space for Calaspargase? A new asparaginase for acute lymphoblastic leukemia. **Clinical Cancer Research**, v. 26, n. 2, p. 325–327, 15 jan. 2020.

LU, X.; ZHANG, K. PEGylation of therapeutic oligonucletides: From linear to highly branched PEG architectures. **Nano Research**, v. 11, n. 10, p. 5519–5534, 2018.

LUBKOWSKI, J.; VANEGAS, J.; CHAN, W.-K.; LORENZI, P. L.; WEINSTEIN, J. N.; SUKHAREV, S.; FUSHMAN, D.; REMPE, S.; ANISHKIN, A.; WLODAWER, A. Mechanism of Catalysis by L-asparaginase. **Biochemistry**, v. 59, p. 1927–1945, 2020.

MARANGONI, A. G. **Enzyme Kinetics Enzyme Kinetics**. [s.l: s.n.]. v. 2

MARANGONI, A. G.; MARANGONI, A. G. Frontmatter. *In*: **Enzyme Kinetics**. [s.l.] John Wiley & Sons, Inc., 2003. p. i–xv.

MATTHEWS, S. S. **Investigation into the Effects of PEGylation on the Thermodynamic Stability of the WW Domain**, 2013a. Disponível em: <https://scholarsarchive.byu.edu/etd>. Acesso em: 15 abr. 2020

___. Investigation into the Effects of PEGylation on the Thermodynamic Stability of the WW Domain. 2013b.

MELIKOGLU, M.; LIN, C. S. K.; WEBB, C. Kinetic studies on the multi-enzyme solution produced via solid state fermentation of waste bread by Aspergillus awamori. **Biochemical Engineering Journal**, v. 80, p. 76–82, 15 nov. 2013.

MENEGUETTI, G. P. *et al.* Novel site-specific PEGylated L-asparaginase. **PLoS ONE**, v. 14, n. 2, p. e0211951, fev. 2019.

MISHRA, P.; NAYAK, B.; DEY, R. K. PEGylation in anti-cancer therapy: An overview. **Asian Journal of Pharmaceutical Sciences**, v. 11, n. 3, p. 337–348, 1 jun. 2016.

MONFARDINI, C.; SCHIAVON, O.; CALICETI, P.; MORPURGO, M.; VERONESE, F. M.; HARRIS, J. M. A Branched Monomethoxypoly(Ethylene Glycol) for Protein Modification. **Bioconjugate Chemistry**, v. 6, n. 1, p. 62–69, 1995.

MORA, J. R.; WHITE, J. T.; DEWALL, S. L. **Immunogenicity Risk Assessment for PEGylated TherapeuticsAAPS Journal**Springer, , 1 mar. 2020. Disponível em: <https://pubmed.ncbi.nlm.nih.gov/31993858/>. Acesso em: 28 dez. 2020

NATALELLO, A.; AMI, D.; COLLINI, M.; D'ALFONSO, L.; CHIRICO, G.; TONON, G.; SCARAMUZZA, S.; SCHREPFER, R.; DOGLIA, S. M. Biophysical characterization of Met-G-CSF: Effects of different site-specific mono-pegylations on protein stability and aggregation. **PLoS ONE**, v. 7, n. 8, 8 ago. 2012.

NGUYEN, N. T. T.; LEE, J. S.; YUN, S.; LEE, E. K. Separation of mono- and di-PEGylate of exenatide and resolution of positional isomers of mono-PEGylates by preparative

ion exchange chromatography. **Journal of Chromatography A**, v. 1457, p. 88–96, 29 jul. 2016.

NYBORG, A. C. *et al.* A Therapeutic Uricase with Reduced Immunogenicity Risk and Improved Development Properties. 2016.

OLIVEIRA, R. L. DE; SILVA, O. S. DA; CONVERTI, A.; PORTO, T. S. Thermodynamic and kinetic studies on pectinase extracted from Aspergillus aculeatus: Free and immobilized enzyme entrapped in alginate beads. **International Journal of Biological Macromolecules**, v. 115, p. 1088–1093, 1 ago. 2018.

PANDEY, B. K.; SMITH, M. S.; TORGERSON, C.; LAWRENCE, P. B.; MATTHEWS, S. S.; WATKINS, E.; GROVES, M. L.; PRIGOZHIN, M. B.; PRICE, J. L. Impact of site-specific PEGylation on the conformational stability and folding rate of the Pin WW domain depends strongly on PEG oligomer length. **Bioconjugate Chemistry**, v. 24, n. 5, p. 796–802, 15 maio 2013.

PARIKH, H.; BAJAJ, P.; TRIPATHY, R.; PANDE, A. Improving Properties of Recombinant SsoPox by Site-Specific Pegylation. **Protein & Peptide Letters**, v. 22, n. 12, p. 1098–1103, 2 nov. 2015.

PASTA, P.; RIVA, S.; CARREA, G. Circular dichroism and fluorescence of polyethylene glycol-subtilisin in organic solvents. **FEBS Letters**, v. 236, n. 2, p. 329–332, 29 ago. 1988.

PASTORE MENEGUETTI, G. *et al.* Novel site-specific PEGylated L-asparaginase. **PLoS ONE**, v. 14, n. 2, p. 1–18, 2019.

PASTORE MENEGUETTI, G.; DRA CARLOTA DE OLIVEIRA RANGEL YAGUI SÃO PAULO, P. Desenvolvimento nanotecnológico da L-asparaginase empregando-se metodologia de peguilação Dissertação para obtenção do Título de MESTRE. 2017.

PASUT, G.; VERONESE, F. M. **State of the art in PEGylation: The great versatility achieved after forty years of researchJournal of Controlled Release**J Control Release, , 20 jul. 2012. Disponível em: <https://pubmed.ncbi.nlm.nih.gov/22094104/>. Acesso em: 10 jul. 2020

PELEGRI-O'DAY, E. M.; MAYNARD, H. D. Controlled Radical Polymerization as an Enabling Approach for the Next Generation of Protein−Polymer Conjugates. 2016.

PFISTER, D.; MORBIDELLI, M. Process for protein PEGylation. **Journal of Controlled Release**, v. 180, n. 1, p. 134–149, 2014a.

___. Process for protein PEGylation. **Journal of Controlled Release**, v. 180, n. 1, p. 134–149, 2014b.

PLESNER, B.; FEE, C. J.; WESTH, P.; NIELSEN, A. D. Effects of PEG size on structure, function and stability of PEGylated BSA. **European Journal of Pharmaceutics and Biopharmaceutics**, v. 79, n. 2, p. 399–405, out. 2011.

POPP, M. W.; DOUGAN, S. K.; CHUANG, T. Y.; SPOONER, E.; PLOEGH, H. L. Sortase-catalyzed transformations that improve the properties of cytokines. **Proceedings of the National Academy of Sciences of the United States of America**, v. 108, n. 8, p. 3169–3174, 22 fev. 2011.

PORTO, T. S.; PORTO, C. S.; CAVALCANTI, M. T. H.; LIMA FILHO, J. L.; PEREGO, P.; PORTO, A. L. F.; CONVERTI, A.; PESSOA, A. Kinetic and Thermodynamic Investigation on Ascorbate Oxidase Activity and Stability of a Cucurbita maxima Extract. 2006.

RAMIREZ-PAZ, J.; SAXENA, M.; DELINOIS, L. J.; JOAQUÍN-OVALLE, F. M.; LIN, S.; CHEN, Z.; ROJAS-NIEVES, V. A.; GRIEBENOW, K. Thiol-maleimide poly(ethylene glycol) crosslinking of L-asparaginase subunits at recombinant cysteine residues introduced by mutagenesis. 2018.

ROBERTS, M. J.; BENTLEY, M. D.; HARRIS, J. M. Chemistry for peptide and protein PEGylation. **Advanced Drug Delivery Reviews**, v. 54, n. 4, p. 459–476, 17 jun. 2002.

RODRIGUES, M. A. D. **Avaliação da atividade e resistência à clivagem proteolítica de L-asparaginases recombinantes obtidas por reação em cadeia da polimerase propensa a erro**. São Paulo: Universidade de São Paulo, 2016.

RODRÍGUEZ-MARTÍNEZ, J. A.; SOLÁ, R. J.; CASTILLO, B.; CINTRÓN-COLÓN, H. R.; RIVERA-RIVERA, I.; BARLETTA, G.; GRIEBENOW, K. Stabilization of α-chymotrypsin upon PEGylation correlates with reduced structural dynamics. **Biotechnology and Bioengineering**, v. 101, n. 6, p. 1142–1149, 15 dez. 2008.

SAIFER, M. G. P.; WILLIAMS, L. D.; SOBCZYK, M. A.; MICHAELS, S. J.; SHERMAN, M. R. Selectivity of binding of PEGs and PEG-like oligomers to anti-PEG antibodies induced by methoxyPEG-proteins. **Molecular Immunology**, v. 57, n. 2, p. 236–246, fev. 2014.

SANCHES, M.; BARBOSA, J. A. R. G.; OLIVEIRA, R. T. DE; NETO, J. A.; POLIKARPOV, I. Structural comparison of Escherichia coli L-asparaginase in two monoclinic space groups. **Acta Crystallographica - Section D Biological Crystallography**, v. 59, n. 3, p. 416–422, 1 mar. 2003.

SANTOS, J. H. P. M.; CARRETERO, G.; VENTURA, S. P. M.; CONVERTI, A.; RANGEL-YAGUI, C. O. PEGylation as an efficient tool to enhance cytochrome c thermostability: a kinetic and thermodynamic study . **Journal of Materials Chemistry B**, 2019.

SANTOS, J. H. P. M.; OLIVEIRA, C. A.; ROCHA, B. M.; CARRETERO, G.; RANGEL-YAGUI, C. O. Pegylated catalase as a potential alternative to treat vitiligo and UV induced skin damage. **Bioorganic and Medicinal Chemistry**, v. 30, p. 115933, 15 jan. 2021.

SANTOS, J. H. P. M.; TORRES-OBREQUE, K. M.; MENEGUETTI, G. P.; AMARO, B. P.; RANGEL-YAGUI, C. O.; SANTOS, J. H. P. M.; TORRES-OBREQUE, K. M.; MENEGUETTI, G. P.; AMARO, B. P.; RANGEL-YAGUI, C. O. Protein PEGylation for the design of biobetters: from reaction to purification processes. **Brazilian Journal of Pharmaceutical Sciences**, v. 54, n. spe, 8 nov. 2018.

SATO, H. Enzymatic procedure for site-specific pegylation of proteins. **Advanced Drug Delivery Reviews**, v. 54, n. 4, p. 487–504, 17 jun. 2002.

SATTERWHITE, C. **Assessing Development Needs for Biobetters and Biosimilars** . Disponível em: <https://www.biopharminternational.com/view/assessing-development-needs-biobetters-and-biosimilars>. Acesso em: 28 dez. 2020.

SCHELLEKENS, H.; HENNINK, W. E.; BRINKS, V. The Immunogenicity of Polyethylene Glycol: Facts and Fiction. **Pharm Res**, v. 30, p. 1729–1734, 2013.

SHAKAMBARI, G.; ASHOKKUMAR, B.; VARALAKSHMI, P. L-asparaginase – A promising biocatalyst for industrial and clinical applications. **Biocatalysis and Agricultural Biotechnology**, v. 17, p. 213–224, 2019.

SIGMA-ALDRICH. BCA assay Technical bulletin. p. 1–6, [s.d.].

SIGMA-TAU. **Oncaspar (pegaspargase) injection Label**. [s.l: s.n.]. Disponível em: <www.fda.gov/safety/medwatch.>. Acesso em: 26 dez. 2020.

SILVA FREITAS, D. DA; MERO, A.; PASUT, G. Chemical and enzymatic site

specific pegylation of hGH. **Bioconjugate Chemistry**, v. 24, n. 3, p. 456–463, 20 mar. 2013.

SILVA, J. DE C.; FRANÇA, P. R. L. DE; CONVERTI, A.; PORTO, T. S. Kinetic and thermodynamic characterization of a novel Aspergillus aculeatus URM4953 polygalacturonase. Comparison of free and calcium alginate-immobilized enzyme. **Process Biochemistry**, v. 74, p. 61–70, 1 nov. 2018.

SINDHU, R.; PRADEEP, H.; MANONMANI, H. K. Polyethylene Glycol Acts as a Mechanistic Stabilizer of L-asparaginase: A Computational Probing. **Medicinal Chemistry**, v. 15, n. 6, p. 705–714, 26 ago. 2019.

SOUSA, S. F.; PERES, J.; COELHO, M.; VIEIRA, T. F. **Analyzing PEGylation through Molecular Dynamics SimulationsChemistrySelect**, 2018.

SOUZA, P. M.; ALIAKBARIAN, B.; FILHO, E. X. F.; MAGALHÃES, P. O.; JUNIOR, A. P.; CONVERTI, A.; PEREGO, P. Kinetic and thermodynamic studies of a novel acid protease from Aspergillus foetidus. **International Journal of Biological Macromolecules**, v. 81, p. 17–21, 2015a.

___. Kinetic and thermodynamic studies of a novel acid protease from Aspergillus foetidus. **International Journal of Biological Macromolecules**, v. 81, p. 17–21, 1 nov. 2015b.

STROHL, W. R. Fusion Proteins for Half-Life Extension of Biologics as a Strategy to Make Biobetters. **Biodrugs**, v. 29, p. 215–239, 2015.

SWAIN, A. L.; JASK6LSKI, M.; HOUSSETT, D.; RAO, J. K. M.; WLODAWERT, A. **Crystal structure of Escherichia coli L-asparaginase, an enzyme used in cancer therapy (amidohydrolase/leukemia/active site/aspartate)Proc. Natl. Acad. Sci. USA**. [s.l: s.n.]. Disponível em: <https://www.pnas.org/content/pnas/90/4/1474.full.pdf>. Acesso em: 10 jul. 2019.

TORBICA, B. **Performance analysis of a PEGylation process**. [s.l: s.n.]. Disponível em: <www.chemeng.lth.se>. Acesso em: 6 ago. 2020.

TORRES-OBREQUE, K. M. **Desenvolvimento de L-asparaginase peguilada de E. chrysanthemi para o tratamento de leucemias** . São Paulo: [s.n.]. Disponível em: <https://teses.usp.br/teses/disponiveis/9/9135/tde-10082017-114052/publico/Karin_Mariana_Torres_Obreque_ME_Original.pdf>. Acesso em: 13 out. 2020.

TORRES-OBREQUE, K.; MENEGUETTI, G. P.; CUSTÓDIO, D.; MONTEIRO, G.; PESSOA-JUNIOR, A.; OLIVEIRA RANGEL-YAGUI, C. DE. Production of a novel N-terminal PEGylated crisantaspase. **Biotechnology and Applied Biochemistry**, v. 66, n. 3, p. 281–289, maio 2019.

TURECEK, P. L.; BOSSARD, M. J.; SCHOETENS, F.; IVENS, I. A. PEGylation of Biopharmaceuticals: A Review of Chemistry and Nonclinical Safety Information of Approved Drugs. **Journal of Pharmaceutical Sciences**, v. 105, n. 2, p. 460–475, fev. 2016.

VERHOEF, J. J. F.; CARPENTER, J. F.; ANCHORDOQUY, T. J.; SCHELLEKENS, H. Potential induction of anti-PEG antibodies and complement activation toward PEGylated therapeutics. **Drug Discovery Today**, v. 19, n. 12, p. 1945–1952, 17 dez. 2014.

VERMA, S.; MEHTA, R. K.; MAITI, P.; RÖHM, K. H.; SONAWANE, A. Improvement of stability and enzymatic activity by site-directed mutagenesis of E. coli asparaginase II. **Biochimica et Biophysica Acta - Proteins and Proteomics**, v. 1844, n. 7, p. 1219–1230, 2014.

VERONESE, F. M.; PASUT, G. **PEGylation, successful approach to drug deliveryDrug Discovery Today**Drug Discov Today, , 1 nov. 2005. Disponível em: <https://pubmed.ncbi.nlm.nih.gov/16243265/>. Acesso em: 10 jul. 2020

___. **PEGylation: Posttranslational bioengineering of protein biotherapeuticsDrug Discovery Today: Technologies**Elsevier Ltd, , 1 set. 2008.

VOLKIN, D. B. .; KLIBANOV, A. M. **Protein Function: A Practical Approach (Practical Approach Series)**. 1. ed. [s.l: s.n.].

WRÓBLEWSKA, B.; JĘDRYCHOWSKI, L. Effect of conjugation of cow milk whey protein with polyethylene glycol on changes in their immunoreactive and allergic properties. **Food and Agricultural Immunology**, v. 14, n. 2, p. 155–162, 2002.

WU, L. *et al.* Precise and combinatorial PEGylation generates a low-immunogenic and stable form of human growth hormone. **Journal of Controlled Release**, v. 249, p. 84–93, 10 mar. 2017.

XU, B.; LI, A.; HAO, X.; GUO, R.; SHI, X.; CAO, X. PEGylated dendrimer-entrapped gold nanoparticles with low immunogenicity for targeted gene delivery. **RSC Advances**, v. 8, n. 3, p. 1265–1273, 2018.

YADAV, D.; DEWANGAN, H. K. PEGYLATION: an important approach for novel drug delivery system. **Journal of Biomaterials Science, Polymer Edition**, v. 0, n. 0, p. 000, 2020.

YAMASAKI, N.; MATSUO, A.; HATAKEYAMA, T.; FUNATSU, G. Some properties of ricin d modified with a methoxypolyethylene glycol derivative. **Agricultural and Biological Chemistry**, v. 54, n. 10, p. 2635–2640, 1990.

YU, H.; YAN, Y.; ZHANG, C.; DALBY, P. A. Two strategies to engineer flexible loops for improved enzyme thermostability. **Scientific Reports**, v. 7, n. November 2016, p. 1–15, 2017.

ZALIPSKY, S. **Chemistry of polyethylene glycol conjugates with biologically active moleculesAdvanced Drug Delivery Reviews**. [s.l: s.n.].

___. Functionalized Poly(Ethylene Glycols) for Preparation of Biologically Relevant Conjugates. **Bioconjugate Chemistry**, v. 6, n. 2, p. 150–165, 1995b.

ZHANG, C.; YANG, X. L.; YUAN, Y. H.; PU, J.; LIAO, F. Site-specific PEGylation of therapeutic proteins via optimization of both accessible reactive amino acid residues and PEG derivatives. **BioDrugs**, v. 26, n. 4, p. 209–215, 2012.

ZHANG, F.; LIU, M.-R.; WAN, H.-T. **Discussion about Several Potential Drawbacks of PEGylated Therapeutic ProteinsBiol. Pharm. Bull**. [s.l: s.n.].

ZHANG, P.; SUN, F.; LIU, S.; JIANG, S. Anti-PEG antibodies in the clinic: Current issues and beyond PEGylation. **Journal of Controlled Release**, v. 244, p. 184–193, 28 dez. 2016.

ZHANG, Z.; ZHANG, Y.; SONG, S.; YIN, L.; SUN, D.; GU, J. Recent advances in the bioanalytical methods of polyethylene glycols and PEGylated pharmaceuticals. **Journal of Separation Science**, v. 43, n. 9–10, p. 1978–1997, 11 maio 2020.

ZHENG, C. Y.; MA, G.; SU, Z. Native PAGE eliminates the problem of PEG-SDS interaction in SDS-PAGE and provides an alternative to HPLC in characterization of protein PEGylation. **Electrophoresis**, v. 28, n. 16, p. 2801–2807, ago. 2007.

8 APENDIX

CERTIFICADO

A Srta Jheniffer Rabelo Cunha

Em nome do Programa de Pós-Graduação em Tecnologia Bioquímico-Farmacêutica, a CCP parabeniza você e sua orientadora Profa. Dra. Carlota de Oliveira Rangel-Yagui, pela menção honrosa no Prêmio Vídeo de Pós-Graduação USP - TV Cultura 2020, área Ciências da Saúde II.

Desejamos sucesso em sua carreira e agradecemos sua valiosa contribuição.

PROFA. DRA GISELE MONTEIRO
Coordenadora do Programa de Pós-Graduação em Tecnologia Bioquímico-Farmacêutica
Faculdade de Ciências Farmacêuticas – FCF, Universidade de São Paulo - USP

Universidade de São Paulo
Brasil

Declaração de Participação nº 831

Declaro para os devidos fins que **Mileyde Araujo** apresentou o trabalho **Efeito da peguilação na atividade e estabilidade térmica da enzima lisozima** na área de **Biotecnologia** no **28º** Simpósio Internacional de Iniciação Científica e Tecnológica da USP - SIICUSP, sob a orientação de **Carlota de Oliveira Rangel Yagui**, com a colaboração de **João Henrique Picado Madalena Santos** e **Jheniffer Rabelo Cunha**, em 2020.

Prof. Dr. Sylvio Roberto Accioly Canuto
Pró Reitor de Pesquisa
Universidade de São Paulo

Documento emitido às **15:33:03** horas do dia **14/12/2020** (hora e data de Brasilia).
Código de controle: **GAVM-1KSC-1JT5-VEAZ**
A autenticidade deste documento pode ser verificada na página da Universidade de São Paulo
http://uspdigital.usp.br/webdoc

CERTIFICADO

Certificamos que **JHENIFFER RABELO** participou do **I Congresso Digital de Nanobiotecnologia e Bioengenharia** (I CDNB), durante o período de 01/06/2020 a 04/06/2020, com carga horária de 40 horas.

Luciano Paulino da Silva
Coordenador do I CDNB
Pesquisador Embrapa

Cínthia Caetano Bonatto
Vice Coordenadora do I CDNB
Pesquisadora NanoDiversity

Embrapa Laboratório de Nanobiotecnologia NANODIVERSITY TECSINAPSE

Evento: **I Congresso Digital de Nanobiotecnologia e Bioengenharia** Local: **Evento online**

Participante: **Jheniffer Rabelo** Data: **01/06/2020 - 04/06/2020**

Programação:

01/06/2020 - 10:00 - Nanobiofabricação	01/06/2020 - 11:00 - Biomanufatura
01/06/2020 - 11:45 - Nanotecnologia para todos	01/06/2020 - 14:00 - Computação Gráfica 3D Aplicada à Bioengenharia
01/06/2020 - 14:45 - Propriedade Intelectual e Nanotecnologia	02/06/2020 - 10:00 - Células-tronco pluripotentes e engenharia de tecidos
02/06/2020 - 11:00 - Nanotecnologia em Alimentos	02/06/2020 - 11:45 - Aplicações de Materiais Biomiméticos
02/06/2020 - 14:00 - Nanotecnologia Farmacêutica	02/06/2020 - 14:45 - Técnicas de Biofabricação e Prototipagem de Equipamentos
03/06/2020 - 10:00 - Nanomedicina	03/06/2020 - 11:00 - Biotintas
03/06/2020 - 11:45 - Consolidação da nanotecnologia no país	03/06/2020 - 13:00 - Fundos de investimento e o seu olhar para a Nanobiotecnologia e Bioengenharia
03/06/2020 - 14:00 - Perspectivas futuras para fabricação de tecidos e órgãos	03/06/2020 - 14:45 - Nanotoxicologia
04/06/2020 - 10:00 - Cultura 3D Magnética	04/06/2020 - 11:00 - Aplicações de nanotecnologia para saúde e produção animal
04/06/2020 - 11:45 - Biomiméticos: Pele Artificial	04/06/2020 - 14:00 - Nanotoxicologia: Ciência para Inovação e Regulação
04/06/2020 - 14:45 - Perspectivas para o Empreendedorismo em Bioengenharia	

CERTIFICADO

Certificamos que **Jheniffer Rabelo** apresentou o trabalho intitulado de **EFEITO DA TERMOESTABILIDADE E TERMODINÂMICA DA PEGUILAÇÃO SÍTIO-DIRIGIDA EM L-ASPARAGINASE** de autoria de Jheniffer Rabelo; João Henrique Picado Madalena Santos; Karin Mariana Torres Obreque; Gustavo Penteado Battesini Carretero: Adalberto Pessoa-Junior; Attilio Converti; Carlota de Oliveira Rangel Yagui., na forma de *e-Pôster* no I Congresso Digital de Nanobiotecnologia e Bioengenharia (I CDNB) organizado pela Embrapa Recursos Genéticos e Biotecnologia e pela *startup* NanoDiversity no período de 01 a 04 de junho de 2020.

Luciano Paulino da Silva
Coordenador do I CDNB
Pesquisador Embrapa

Cínthia Caetano Bonatto
Vice Coordenadora do I CDNB
Pesquisadora NanoDiversity

Embrapa Laboratório de Nanobiotecnologia NANODIVERSITY TECSINAPSE

PDA Parenteral Drug Association Brazil Chapter

Semana Internacional de Biotecnologia, Biossimilares, Terapias Avançadas, Vacinas e RDCs de produtos estéreis

Webinar - 19 á 23 de Outubro de 2020 – São Paulo

CERTIFICADO

Certificamos que

Jheniffer Rabelo

Participou nas Palestras na Semana de Biotecnologia, Biossimilares, Terapias Avançadas, e RDCs de produtos estéreis realizado de 19 á 23 de Outubro de 2020 em São Paulo e organizado pela PDA BRAZIL – Parenteral Drug Association com carga horaria de 25 horas

Richard Johnson
Presidente PDA

Leonidas Orjuela
Presidente Brazil Chapter PDA

PDA Parenteral Drug Association Brazil Chapter

Semana internacional de Biotecnologia, Biossimilares, Terapias avançadas, Vacinas e RDC de produtos estéreis

Webinar - Outubro 19-23, 2020 - Time: 13:00 -18:00

Tradução simultânea Inglês, Português e Espanhol

100 Industrias
15 países
33 palestrantes
300 participantes

Segunda feira, outubro 19 Moderador: Carollna Camargo			
13:00	Introdução	Leonidas Orjuela	PDA BRAZIL
13:10	O desenvolvimento de biossimilares e o mercado mundial	Martin Schiestl	Sandoz
14:00	Expectativas Anvisa desenvolvimento farmacêutico (Fase 1) em linha com a RDC 301/2020 e IN 47/2020	Ronaldo Gomes	Anvisa
15:05	Filtração viral e estratégias para a prevenção da contaminação por partículas virais	Kathy Remington	Merck
16:05	Transferência de tecnologia e comparabilidade para Terapias Celulares e Genicas	Luciana Mansolelli Diluiks da Silva	Novartis
17:05	Eficiência da purificação de mAb através de cromatografia de proteína A baseada em fibra de ciclo rápido	Aledo Pimenta	Cytiva
Terça feira, outubro 20 Moderador: David Hengeltraub			
13:00	Comercialização de Terapias Genicas: importância das tecnologias de manufatura	Clive Glover Paul Cashen	Pall Biotech
14:00	Simulações de processamento Asséptico para Terapias Celulares e Genicas	Luciana Mansolelli Damien Howlck	Novartis
15:00	A visão do setor privado dos Biossimilares e biológicos no Brasil: mercado, tecnologias e infraestrutura	Thiago Guia	Bionovis
16:00	Panorama do desenvolvimento de vacinas anti COVID no mundo e oportunidade brasileira	Jorge Kalil	FMUSP
16:30	Desenvolvimento de novos Biobetters para o tratamento de Neoplasias	Adalberto Pessoa	USP
17:05	Gerenciamento de Risco da Contaminação Cruzada em instalações multipropósito de insumos biológicos	Roberto Dos Reis	Anvisa
Quarta feira, outubro 21 Moderadora: Bruna Vinco			
13:00	Desafios de manufatura, qualidade e regulatório para Terapias Celulares e Genicas	Damien Howlck Diluiks de Silva	Novartis
14:00	Tendências globais e requerimentos do mercado de PFS seringas pré-enchidas	Nicolas Eon	Terumo
14,30	CDMO para Biossimialares e Terapias Avançadas	Claudia Berdugo	Catalent
15:05	Avanços na purificação Biofarmaceutica	David Chau e Matthew Peters	3M
16:05	A visão do setor publico dos Biossimilares no Brasil: produção, atençao do SUS e tech transfer	Rosane Cuber	Biomanguinhos
17:05	Biossegurança para vacinas e terapias celulares	Maria Dagli	USP/SP
Quinta feira, outubro 22 Moderadora: Tatiana Oliveira			
13:00	Modelo regulatório Brasileiro para produtos de Terapias Avançadas	Joao Batista	Anvisa
13:30	Aspectos da qualidade de terapias avançadas: discussão de dossiê de ensaios clinicos e registro	Renata Parça	Anvisa
14:05	Avanços no design de biorreatores Single-use e seus componentes	Pablo Fernandez	Thermo Fisher
15:00	Soros para Covid-19 e outras aplicações	Fan Hui	Butantan
15:30	Transferência de tecnologia e desafios da Vacina para Covid19	Tiago Rocca	Butantan
16:05	Biossimilares: da caracterização à atividade biológica	luciana Dzik	Sartorius
17:00	Introdução aos conceitos e diretrizes da RDC 301/2019, IN 36/2020 e RDC 69/2014	Andrea Geyer	Anvisa
Sexta feira, outubro 23 Moderadora: Rosane Cuber			
13:00	Plano para validação de limpeça e boas praticas - TR49	Beth Kroger	Steris
14:00	Adaptando métodos microbiológicos rápidos para atender requisitos farmacêuticos	Lori Deane	Biomerieux
15:00	Flexibilidade nos processos de envase e gestao de dados que beneficiam a manufatura	Frank Haeterich	Bausch&Stroebel
15:30	QbD for RQD	Darius Pillsbury	Valsource
16:30	Estratégia de Supply chain para a transição desde testes clinicas até comercialização ATPM	Carla Reed	New Creed
17:00	Processo de desenvolvimento de vacinas com foco em Covid-19	Elena Caride	Biomanguinhos
17:30	Pontos específicos da BPF de produtos de terapias avançadas: perspectivas regulatórias	Francielle Mello	Anvisa

Informação: Cel. 55-11-99390-0887 / 2894-9730 biotec@pdabrazil.org

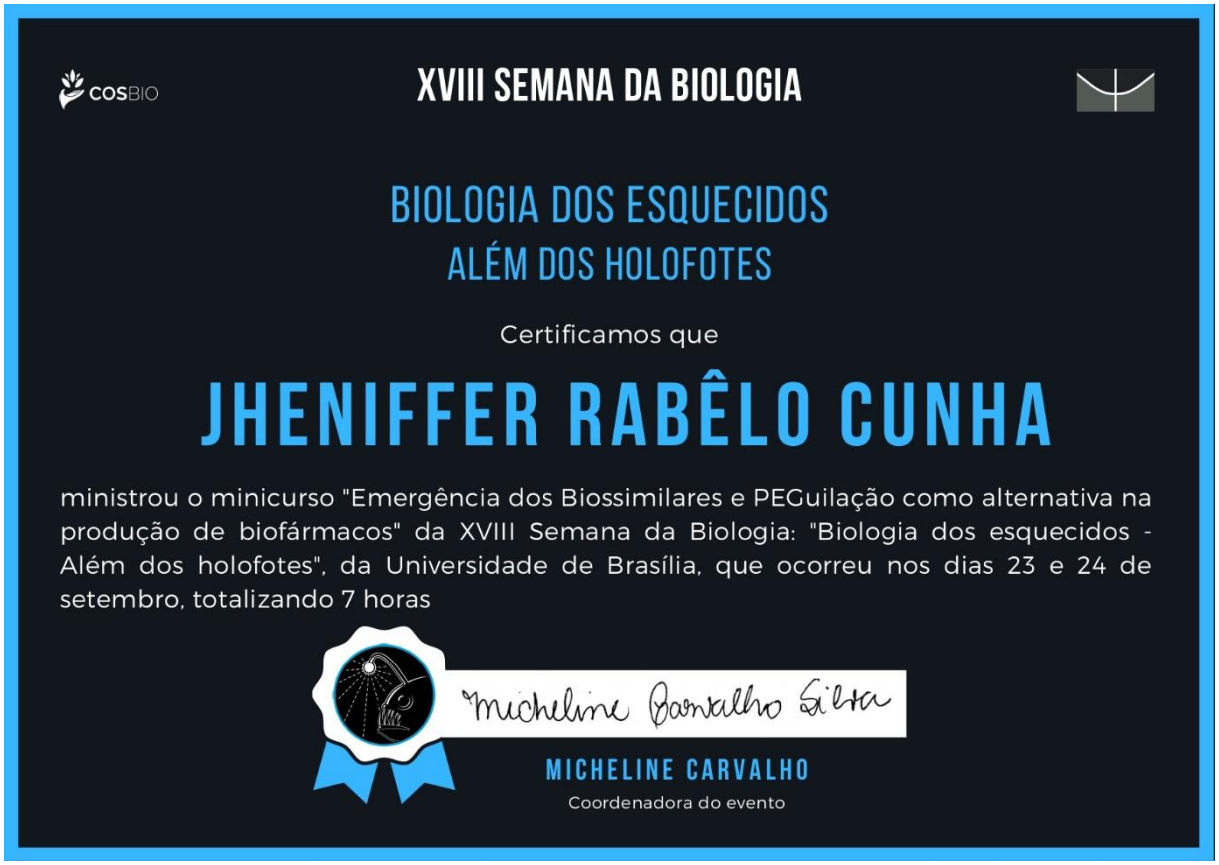

cosBIO

XVIII SEMANA DA BIOLOGIA

BIOLOGIA DOS ESQUECIDOS
ALÉM DOS HOLOFOTES

Certificamos que

JHENIFFER RABÊLO CUNHA

ministrou o minicurso "Emergência dos Biossimilares e PEGuilação como alternativa na produção de biofármacos" da XVIII Semana da Biologia: "Biologia dos esquecidos - Além dos holofotes", da Universidade de Brasília, que ocorreu nos dias 23 e 24 de setembro, totalizando 7 horas

Micheline Carvalho Silva

MICHELINE CARVALHO
Coordenadora do evento

BPP2019 BIOPARTITIONING & PURIFICATION CONFERENCE
GUARUJÁ·SP - BRAZIL

Certificate

We certify that JHENIFFER RABELO CUNHA has presented the POSTER (PAINEL) presentation entitled EFFECT OF PEGYLATION ON THE ACTIVITY AND THERMAL STABILITY OF ENZYMES, authored by JHENIFFER CUNHA, GUSTAVO CARRETERO, BEATRIZ ROCHA, JOÃO SANTOS, CARLOTA RANGEL-YAGUI, during the Biopartitioning & Purification Conference 2019 (BPP 2019), which was held in Casa Grande Hotel Resort & Spa, Guarujá, SP, Brazil from November 11th to 13th, 2019.

Guarujá, 13th November, 2019

Prof. Dr. Jorge Fernando Brandão Pereira
Co-Chair – BBP 2019

Prof. Dr. Adalberto Pessoa Junior
Co-Chair – BBP 2019

Organization and Realization

unesp UNIVERSIDADE ESTADUAL PAULISTA "JÚLIO DE MESQUITA FILHO"
SBM Sociedade Brasileira de Microbiologia

Support

FAPESP
CAPES
CNPq Conselho Nacional de Desenvolvimento Científico e Tecnológico

BPP2019 BIOPARTITIONING & PURIFICATION CONFERENCE
GUARUJÁ·SP - BRAZIL

Certificate

We certify that JHENIFFER RABELO CUNHA has participated in the Biopartitioning & Purification Conference 2019 (BPP 2019), which was held in Casa Grande Hotel Resort & Spa, Guarujá, SP, Brazil from November 11th to 13th, 2019.

Guarujá, 13th November, 2019

Prof. Dr. Jorge Fernando Brandão Pereira
Co-Chair – BBP 2019

Prof. Dr. Adalberto Pessoa Junior
Co-Chair – BBP 2019

Organization and Realization

unesp UNIVERSIDADE ESTADUAL PAULISTA "JÚLIO DE MESQUITA FILHO"
SBM Sociedade Brasileira de Microbiologia

Support

FAPESP
CAPES
CNPq Conselho Nacional de Desenvolvimento Científico e Tecnológico

Journal of chemical & engineering data

pubs.acs.org/jced

Article

Imidazolium-based Ionic Liquids as Adjuvants to Form Polyethylene Glycol with Salt Buffer Aqueous Biphasic Systems

João H. P. M. Santos, Margarida Martins, Amanda R. P. Silva, Jheniffer R. Cunha, Carlota O. Rangel-Yagui, and Sónia P. M. Ventura*

Cite This: J. Chem. Eng. Data 2020, 65, 3794−3801

Read Online

ACCESS | Metrics & More | Article Recommendations | Supporting Information

ABSTRACT: Aqueous biphasic systems (ABS) are biocompatible systems applied in the extraction of biomolecules. Despite the biocompatibility of polymers and, particularly polyethylene glycol (PEG), to form ABS, their limitation in terms of phase separation is recognized. A new approach was recently proposed based on the use of ionic liquids (ILs) as adjuvants in ABS, enlarging the polarity range of these systems. Up to now, the effects of ILs in PEG-salt ABS have been poorly described. To overcome this limitation, the phase diagrams of imidazolium-based ILs acting as adjuvants in ABS based in PEG with potassium salt buffers (pH = 7), that is potassium citrate ($C_6H_5K_3O_7/C_6H_8O_7$) and potassium phosphate (K_2HPO_4/KH_2PO_4) buffers, are herein addressed. Imidazolium-based ILs were focused in this work, since they have been applied on the purification of several biomolecules with success, even as adjuvants or electrolytes. The phase diagrams were mapped out for PEG/salt ABS without adjuvants. In this work, systems composed of PEG (1000, 1500, 2000, 3350, 4000, 6000, and 8000) with potassium phosphate buffer and PEG (2000, 6000, 10 000, and 20 000) with potassium citrate buffer were tested. Moreover, the presence of 5 wt % of imidazolium-based ILs (varying the anion moiety) for the system PEG 1500 with potassium phosphate buffer was also investigated. Imidazolium-based ILs with different anions were tested to investigate a large range of polarities attributed to the adjuvant. Moreover, the effect of the adjuvant content (5, 10, and 20 wt %) in the PEG 2000 with potassium citrate buffer system was studied for two distinct ILs, namely $[C_4mim][CF_3SO_3]$ and $[C_4mim][(CH_3O)_2PO_2]$, with lower and higher energy of intramolecular hydrogen bond, E_{HB}, respectively, a parameter representing the ions' hydration. A correlation between the anion moiety of imidazolium-based IL and the ability to form two phases was observed, being this related to the ILs' anion E_{HB} value. The concentration of the adjuvant confirmed the effects of enhancing or decreasing the ability to form two phases for ILs with lower and higher E_{HB} value, respectively.

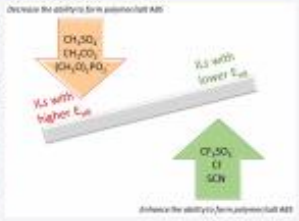

1. INTRODUCTION

Aqueous biphasic systems (ABS) are formed by the dissolution of two polymers, a polymer and a salt, or two salts in water. These systems allow liquid−liquid extraction processes originally proposed by Albertsson in 1958.[1] ABS composed of polymers (namely polymer−polymer or polymer−salt) were recognized as biocompatible systems to cells, organelles, and biologically active substances, turning them as suitable systems to be applied on the recovery and purification of biomolecules.[2,3] Conventionally, from the polymers applied to form the two-phase systems polyethylene glycol (PEG) takes the lead as the most used as phase forming in combination with other polymers or salts.[4,5] The PEG/salt ABS offer plenty of advantages, such as their low interfacial tension, biocompatibility, fast and high phase separation rates, and low cost.[6,7] However, their performance is significantly affected by the limited range of polarity of the coexisting phases, which affect the extraction and purification performance of the biomolecules. To overcome this drawback, the use of small amounts of ionic liquids (ILs) has been proposed to extend the hydrophilicity/hydrophobicity range between the two aqueous phases.[8,9] Contrary to the common polymer/salt-based ABS, in general ILs do not suffer from high viscosity[10] or the formation of opaque aqueous solutions and display a much broader range of polarity.[11] One of the main advantages of ILs for ABS formulation is related to the designer solvents inner characteristics tuning the physicochemical properties[12] by the proper combination/manipulation of the ILs' cation, anion, and alkyl chains.[13] Due to their advantages, ILs have been extensively studied as adjuvants in PEG/salt ABS[14−16] and applied in the extraction of a wide variety of compounds such

Received: December 27, 2019
Accepted: March 30, 2020
Published: April 13, 2020

https://dx.doi.org/10.1021/acs.jced.9b01199
J. Chem. Eng. Data 2020, 65, 3794−3801

Jheniffer Rabêlo Cunha

Endereço para acessar este CV: http://lattes.cnpq.br/4164832357562734
ID Lattes: **4164832357562734**
Última atualização do currículo em 09/10/2020

Mestranda no Departamento de Tecnologia Bioquímica-Farmacêutica na FCF-USP. Atualmente desenvolve pesquisa na área de nanobiotecnologia, realizando PEGuilação para o melhoramento de biofármaco antileucêmico nos parâmetros de termoestabilidade, termodinâmica e meia-vida do biofármaco. Bacharelada e Licenciada no curso de Ciências Biológicas na Universidade de Brasília. Tem experiência com Bioquímica e Fisiologia Comparada, no Laboratório de Radicais Livres, focando na atuação de antioxidantes em período de stress oxidativo de espécies animais. Trabalhou como estagiária na Embrapa Agroenergia, na área de Microbiologia, com ênfase em fungos filamentosos advindos de plantas, com objetivo de seleção enzimática desses microrganismos, contando também com a caracterização genética e molecular dos mesmos fungo para a produção de biodiesel. **(Texto informado pelo autor)**

Identificação

Nome Jheniffer Rabêlo Cunha
Nome em citações bibliográficas CUNHA, J. R.;CUNHA, JHENIFFER R.
Lattes iD http://lattes.cnpq.br/4164832357562734

Endereço

Endereço Profissional Universidade de São Paulo, Faculdade de Ciências Farmacêuticas.
Rua do Lago 250 (prédio Semi-Industrial)
Butantã
05508080 - São Paulo, SP - Brasil
Telefone: (61) 998802586

Formação acadêmica/titulação

2018 Mestrado em andamento em Tecnologia Bioquímico-Farmacêutica (Conceito CAPES 5).
Universidade de São Paulo, USP, Brasil.
Título: Estudo do efeito da peguilação na atividade e estabilidade térmica de enzimas,Orientador: Carlota de Oliveira Rangel Yagui.
Bolsista do(a): Coordenação de Aperfeiçoamento de Pessoal de Nível Superior, CAPES, Brasil.
Palavras-chave: Peguilação; Termoestabilidade; Termodinâmica; Biossimilares; Biobetters.
Grande área: Ciências da Saúde
Grande Área: Ciências da Saúde / Área: Farmácia / Subárea: Biotecnologia.

2012 - 2016 Graduação em Ciências Biológicas.
Universidade de Brasília, UnB, Brasil.

2010 - 2012 Ensino Médio (2º grau).
Centro de Ensino Tecnológico de Brasília, CETEB, Brasil.

Formação Complementar

2019 - 2019 8th International School of Production of Biologicals. (Carga horária: 40h).
Universidade Federal do Rio de Janeiro, UFRJ, Brasil.

2017 - 2017 FlexFactory Operator Training. (Carga horária: 80h).
GE Healthcare, GE, Estados Unidos.

2016 - 2016 Extensão universitária em XV Curso de Inverno de Bioquímica e Biologia Molecular 2016. (Carga horária: 80h).
Faculdade de Medicina de Ribeirão Preto, FMRP, Brasil.

2016 - 2016 Curso de Extensão - Biologia e Genética Forense. (Carga horária: 10h).
Instituto LG Cursos e Treinamentos, LG, Brasil.

2014 - 2014 Redação Científica. (Carga horária: 6h).
Universidade de Brasília, UnB, Brasil.

2014 - 2014 Modelos Animais para o Estudo de Dependência. (Carga horária: 6h).
Universidade de Brasília, UnB, Brasil.

2013 - 2013 Análises Clínicas. (Carga horária: 6h).
Universidade de Brasília, UnB, Brasil.

2013 - 2013 Entomologia de campo. (Carga horária: 6h).
Universidade de Brasília, UnB, Brasil.

Atuação Profissional

Universidade de São Paulo, USP, Brasil.

Vínculo institucional
2017 - Atual Vínculo: , Enquadramento Funcional:

BTHEK Biotecnologia, BTHEK, Brasil.

Vínculo institucional
2017 - 2018 Vínculo: Celetista, Enquadramento Funcional: Técnica de Produção, Carga horária: 44, Regime: Dedicação exclusiva.

Outras informações Trabalhei majoritariamente no desenvolvimento de processos para produção de biofármacos (a partir de dados de transferência de tecnologia) e produção de biopesticidas. Atuei na realização de cultivo microbiano em biorreatores, purificação de proteínas (por meio de FPLC com auxílio do Unicorn Software), testes enzimáticos, transformação bacteriana, entre outros testes de qualificação de pureza de proteínas. Também elaborei Protocolos Operacionais Padrão (POPs) seguindo Boas Práticas de Fabricação (BPF), acompanhamento de instalação e manutenção de equipamentos single-use em ambiente produtivo.

Empresa Brasileira de Pesquisa Agropecuária, EMBRAPA, Brasil.

Vínculo institucional
2013 - 2016 Vínculo: Bolsista, Enquadramento Funcional: Estagiária, Carga horária: 20
Atividades
03/2013 - 12/2016 Estágios , Embrapa Agroenergia, .
Estágio realizado
Novas lipases para a síntese de biodiesel: prospecção de fungos a partir da biodiversidade e seleção de linhagens produtoras de lipases.

Projetos de pesquisa

2017 - Atual Peguilação N-terminal de proteínas e purificação por sistemas aquosos bifásicos
Descrição: Os medicamentos biológicos representam um grande avanço realizado pela indústria farmacêutica, que gerou receitas consideráveis para as companhias detentoras das patentes das moléculas inovadoras inseridas recentemente no mercado. Entretanto, a necessidade econômica de permanecer competitivo no mercado e de solucionar os problemas intrínsecos de biofármacos proteicos como imunogenicidade e instabilidade biológica levou ao aprimoramento de fármacos biotecnológicos existentes, surgindo então os biobetters. Nesse contexto, uma das técnicas mais empregadas atualmente para obtenção de biofármacos, incluindo biobetters, consiste na ligação covalente de cadeias de poli(etileno glicol) (PEG). Essa técnica, também conhecida como peguilação, permite o aprimoramento tanto farmacocinético quanto farmacodinâmico de biofármacos, em especial aqueles de natureza proteica. Nesse projeto, pretendemos estudar a peguliação sítio específica N-terminal de diversas proteínas (BSA, catalase, L-asparaginase e lisozima), bem como a utilização de sistemas de duas fases aquosas para purificação das proteínas peguiladas das moléculas de proteína que não reagirem. Inicialmente, será estudada a reação com a proteína BSA, de maneira a definir as melhores condições de monopeguilação. Será estudada a influência da força iônica variando-se a molaridade do tampão PBS (0,01, 0,1 ou 0,2 M), a influência da proporção PEG:Proteína (25:1 ou 50:1) e a influência do pH (6,0, 6,5, 7,0, 7,5 ou 8,0) no rendimento da reação e estabilidade proteica. Definidas as condições acima, investigaremos o tempo reacional que forneça a menor taxa de polidispersão (por ligação do PEG em sítios inespecíficos). Em seguida, as proteínas peguiladas serão purificadas por cromatografia de troca iônica e exclusão molecular. A partição das proteínas monopeguiladas em sistemas de duas fases aquosas PEG/fosfato de potássio será investigada, empregando-se PEG de diferentes massas moleculares e diferentes composições de tampão fosfato de potássio. Será investigada também a

possibilidade de se utilizar a própria proteína peguilada como agente polimérico formador de fase em sistema PEG-proteína/fosfato de potássio. As melhores condições obtidas serão testadas com o meio reacional contendo a proteína peguilada, sem purificação prévia. Para as proteínas que forem enzimas (catalase, L-asparaginase e lisozima), estudaremos também a termodinâmica de desnaturação térmica da enzima peguilada em comparação com a forma não peguilada, assim como a termodinâmica da reação catalisada para as formas peguilada e não peguilada..
Situação: Em andamento; Natureza: Pesquisa.

Integrantes: Jheniffer Rabêlo Cunha - Integrante / Carlota de Oliveira Rangel Yagui - Coordenador / Attilio Converti - Integrante / João Henrique Picado Madalena Santos - Integrante / Adalberto Pessoa Junior - Integrante.

2013 - 2015

Plano de Ação (BIOENZI) - Novas lipases para a síntese de biodiesel: prospecção de microrganismos a partir da biodiversidade microbiana e seleção de linhagens hipersecretoras de lipases
Descrição: A descoberta de microrganismos hipersecretores de lipases com características bioquímicas de interesse para a síntese de biodiesel constitui o principal objetivo deste Plano de Ação. A estratégia consiste na bioprospecção (qualitativa e quantitativa) direcionada para a atividade fim, ou seja, uma estratégia que simule as condições encontradas durante as etapas do bioprocesso. Para tanto, será realizado o isolamento de microrganismos a partir de diferentes ambientes e substratos ricos em lipídios, microrganismos estes que sejam capazes de secretar elevadas quantidades de lipases estáveis nas condições do bioprocesso (lipases ativas sobre óleo de dendê e tolerantes a etanol). Além da capacidade de secretar altos níveis de lipases em comparação com linhagens industriais, as linhagens serão analisadas quanto à taxa de crescimento e colonização de substrato, maximizando as chances de seleção de cepas adaptadas às condições do bioprocesso, bem como quanto às características bioquímicas do extrato lipolítico. As linhagens selecionadas serão identificadas. Este Plano de Ação prevê a construção de uma coleção de trabalho de microrganismos caracterizada fenotipicamente e genotipicamente, com base em diretrizes institucionais de qualidade de coleções microbianas. Neste Plano de Ação serão obtidos insumos para produção de biodiesel que poderão futuramente ser inseridos em programas de melhoramento genético de microrganismos e de enzimas...
Situação: Concluído; Natureza: Pesquisa.

Integrantes: Jheniffer Rabêlo Cunha - Integrante / Léia Cecília de Lima Fávaro - Coordenador / Paula Fernandes Franco - Integrante / Carolina Madalozzo Poletto - Integrante.
Financiador(es): Empresa Brasileira de Pesquisa Agropecuária - Auxílio financeiro.

Idiomas

Inglês Compreende Bem, Fala Bem, Lê Bem, Escreve Razoavelmente.
Espanhol Compreende Razoavelmente, Fala Razoavelmente, Lê Razoavelmente, Escreve Pouco.

Produções

Produção bibliográfica

Artigos completos publicados em periódicos

Ordenar por

Ordem Cronológica

1. SANTOS, JOÃO H. P. M. ; MARTINS, MARGARIDA ; SILVA, AMANDA R. P. ; **CUNHA, JHENIFFER R.** ; RANGEL-YAGUI, CARLOTA O. ; VENTURA, SÓNIA P. M. . Imidazolium-based Ionic Liquids as Adjuvants to Form Polyethylene Glycol with Salt Buffer Aqueous Biphasic Systems. JOURNAL OF CHEMICAL AND ENGINEERING DATA JCR, v. 65, p. 3794-3801, 2020.

Apresentações de Trabalho

1. **CUNHA, J. R.**; SANTOS, J. H. P. M. ; TORRES-OBREQUE, K. ; CARRETERO, G. ; PESSOA JUNIOR, A. ; YAGUI, C. O. R. . EFEITO DA TERMOESTABILIDADE E TERMODINÂMICA DA PEGUILAÇÃO SÍTIO-DIRIGIDA EM LASPARAGINASE. 2020. (Apresentação de Trabalho/Congresso).
2. **CUNHA, J. R.**. Emergência dos Biossimilares e PEGuilação como alternativa na produção de biofármacos. 2019. (Apresentação de Trabalho/Conferência ou palestra).
3. **CUNHA, J. R.**; TORRES-OBREQUE, K. ; SANTOS, J. H. P. M. ; CONVERTI, A. ; PESSOA JUNIOR, A. ; CARRETERO, G. ; YAGUI, C. O. R. . EFFECT OF PEGYLATION ON THE ACTIVITY AND THERMAL STABILITY OF ENZYMES,. 2019. (Apresentação

de Trabalho/Congresso).

4. **CUNHA, J. R.**; LEITE, L. S. ; POLETTO, C. M. ; FRANCO, P. F. ; SANTOS, J. A. ; FAVARO, L. C. L. . POTENCIAL BIOTECNOLÓGICO DE FUNGOS ASSOCIADOS AOS FRUTOS DE DENDÊ PARA PRODUÇÃO DE LIPASES. 2014. (Apresentação de Trabalho/Congresso).
5. **CUNHA, J. R.**; LEITE, L. S. ; POLETTO, C. M. ; FRANCO, P. F. ; SANTOS, J. A. ; SALUM, T. F. C. ; FAVARO, L. C. L. . Fungos associados aos frutos da palma de óleo (Elaeis guineensis) e seu potencial para produção de lipases. 2014. (Apresentação de Trabalho/Outra).
6. FAVARO, L. C. L. ; LEITE, L. S. ; **CUNHA, J. R.** ; MAGALHAES, L. C. R. ; POLETTO, C. M. ; FRANCO, P. F. ; SANTOS, J. A. ; SALUM, T. F. C. . Novas lipases para a síntese de biodiesel: microrganismos associados à palma de óleo (Elaeis guineensis) e seu potencial biotecnológico. 2014. (Apresentação de Trabalho/Congresso).

Eventos

Participação em eventos, congressos, exposições e feiras

1. 28º Congresso Brasileiro de Microbiologia. MICROORGANISMS ASSOCIATED WITH ELAEIS GUINEENSIS JACQ. FRUITS AND THEIR POTENTIAL TO PRODUCE LIPASE. 2015. (Congresso).
2. II Encontro de Pesquisa e Inovação. Bacteria and fungi associated with Elaeis guineensis Jacq. and their potential to produce lipase. 2015. (Encontro).
3. I Encontro de Pesquisa e Inovação. POTENCIAL BIOTECNOLÓGICO DE FUNGOS ASSOCIADOS AOS FRUTOS DE DENDÊ PARA PRODUÇÃO DE LIPASES. 2014. (Encontro).
4. III Congresso Brasileiro de Recursos Genéticos. Potencial biotecnológico de fungos associados aos frutos de dendê para produção de lipases. 2014. (Congresso).
5. VII Congresso Brasileiro de Micologia. FUNGOS ASSOCIADOS À PLANTAS DE INTERESSE PARA AGROENERGIA E SEU POTENCIAL BIOTECNOLÓGICO PARA PRODUÇÃO DE LIPASES. 2013. (Congresso).

Organização de eventos, congressos, exposições e feiras

1. **CUNHA, J. R.**; YAGUI, C. O. R. . 1º Simpósio de Cooperação entre as Universidades de Aveiro e São Paulo. 2019. (Congresso).

USP Universidade de São Paulo Brasil

FICHA DO ALUNO

Janus

9135 - 10971420 / 1 - Jheniffer Rabelo Cunha

Email:	rabelo.jheniffer@usp.br
Data de Nascimento:	05/12/1994
Cédula de Identidade:	RG - 2.674.229 - DF
Local de Nascimento:	Distrito Federal
Nacionalidade:	Brasileira
Graduação:	Bacharela em Ciências Biológicas - Universidade de Brasília - Brasil - 2017

Curso:	Mestrado
Programa:	Tecnologia Bioquímico-Farmacêutica
Área:	Tecnologia Químico-Farmacêutica
Data de Matrícula:	07/08/2018
Início da Contagem de Prazo:	07/08/2018
Data Limite para o Depósito:	07/06/2021
Orientador:	Prof(a). Dr(a). Carlota de Oliveira Rangel Yagui - 07/08/2018 até o presente Email: corangel@usp.br

Proficiência em Línguas:

Inglês, Aprovado em 07/08/2018

Data de Aprovação no Exame de Qualificação:	Aprovado em 05/09/2019

USP Universidade de São Paulo Brasil

FICHA DO ALUNO

Janus

Data do Depósito do Trabalho:

Título do Trabalho:

Data Máxima para Aprovação da Banca:

Data de Aprovação da Banca:

Data Máxima para Defesa:

Data da Defesa:

Resultado da Defesa:

Histórico de Ocorrências: Primeira Matrícula em 07/08/2018
Aluno matriculado no Regimento da Pós-Graduação USP (Resolução nº 6542 em vigor de 20/04/2013 até 28/03/2018).

Última ocorrência: Matrícula de Acompanhamento em 28/07/2020

Sigla	Nome da Disciplina	Início	Término	Carga Horária	Cred.	Freq.	Conc.	Exc.	Situação
PQI5870-2/3	Proteínas Recombinantes: Aspectos Moleculares e Desenvolvimento de Processos (Escola Politécnica - Universidade de São Paulo)	10/09/2018	21/12/2018	120	8	90	A	N	Concluída
FBT5776-5/9	Tópicos Especiais de Tecnologia Bioquímico-Farmacêutica II	15/10/2018	28/10/2018	30	2	100	A	N	Concluída
FBT5773-8/3	Tópicos Especiais em Tecnologia Bioquímico-Farmacêutica	11/03/2019	19/05/2019	30	2	90	A	N	Concluída
FBF5833-1/1	Qualidade por Design Analítica (AQbD) Aplicado às Análises Farmacêuticas	19/03/2019	27/05/2019	90	6	100	A	N	Concluída
FBT5728-1/1	Inglês Científico - Pronúncia e Apresentação Oral	01/04/2019	14/04/2019	30	2	100	A	N	Concluída
FBA5728-4/8	Aprimoramento Pedagógico	02/04/2019	30/04/2019	60	4	100	A	N	Concluída
BTC5782-2/3	Enzimologia Básica e Aplicações em Processos Industriais (Curso Interunidades: Biotecnologia - Universidade de São Paulo)	03/06/2019	16/06/2019	60	4	85	A	N	Concluída
FBT5700-4/1	Preparo de Artigos Científicos na Área de Tecnologia Bioquímico-Farmacêutica	03/02/2020	05/04/2020	90	6	90	A	S	Concluída

Universidade de São Paulo

FICHA DO ALUNO

Janus

	Créditos mínimos exigidos		Créditos obtidos
	Para exame de qualificação	Para depósito da dissertação	
Disciplinas:	0	25	28
Estágios:			
Total:	0	25	28

Créditos Atribuídos à Dissertação: 71

Conceito a partir de 02/01/1997:

A - Excelente, com direito a crédito; B - Bom, com direito a crédito; C - Regular, com direito a crédito; R - Reprovado; T - Transferência.

Um(1) crédito equivale a 15 horas de atividade programada.

Este documento eletrônico dispensa carimbo e assinatura. Sua autenticidade pode ser comprovada fornecendo-se o código de controle na seguinte página da Universidade de São Paulo: https://uspdigital.usp.br/iddigital

Documento emitido às 16:54:39 horas do dia 28/02/2021 (hora e data de Brasília)

Código de controle: 77X1-62TG-W2ET-TBEI

Código de controle válido até: 28/03/2021